โครงการ: กลัยโคไซด์จากสมุนไพรและอนุพันธ์อะมิโนไซคลิทอลที่มีฤทธิ์ยับยั้งเอนไซม์อัลฟากลูโคซิเดส

โดย ผู้ช่วยศาสตราจารย์ ดร.ปรีชา ภูวไพรศิริศาล และคณะ
ภาควิชาเคมี คณะวิทยาศาสตร์ จุฬาลงกรณ์มหาวิทยาลัย

30 พฤษภาคม 2556

สัญญาเลขที่ (DBG5380037)

รายงานวิจัยฉบับสมบูรณ์

โครงการ: กลัยโคไซด์จากสมุนไพรและอนุพันธ์อะมิโนไซคลิทอลที่มีฤทธิ์ยับยั้งเอนไซม์อัลฟากลูโคซิเดส

คณะผู้วิจัย
ผู้ช่วยศาสตราจารย์ ดร. ปรีชา ภูวไพรศิริศาล
ผู้ช่วยศาสตราจารย์ ดร.สัมฤทธิ์ วัชรสินธุ์
นางสาววิศุษฏญา วรวะลัย
นายเอกพล รัตนางกูร

ภาควิชาเคมี คณะวิทยาศาสตร์ จุฬาลงกรณ์มหาวิทยาลัย

สนับสนุนโดย สำนักงานกองทุนสนับสนุนการวิจัย (สกว.) และ
จุฬาลงกรณ์มหาวิทยาลัย

บทคัดย่อ

อัลฟากลูโคซิเดสเป็นเอนไซม์ในกลุ่มไฮโดรเลส ซึ่งช่วยเร่งปฏิกิริยาไฮโดรไลซิสของโอลิโกแซคคาไรด์ให้กลายเป็นน้ำตาลกลูโคส การมีปริมาณน้ำตาลในเลือดสูงเป็นเวลานาน ทำให้การเป็นโรคเบาหวาน ในผู้ป่วยที่มีหลายร้อยล้านคนทั่วโลกมีความรุนแรงมากขึ้น เพื่อที่จะหยุดยั้งอุบัติการณ์โรคเบาหวานและโรคแทรกซ้อน การยับยั้งการทำงานของอนไซม์อัลฟากลูโคซิเดสจึงเป็นแนวทางหนึ่งในการแก้ปัญหาดังกล่าว สำหรับโครงการวิจัยนี้มีวัตถุประสงค์เพื่อค้นหาสารที่ออกฤทธิ์ยับยั้งเอนไซม์อัลฟากลูโคซิเดสจากพืชที่รับประทานได้ และจากการสังเคราะห์ คณะผู้วิจัยประสบความสำเร็จในการค้นพบและพิสูจน์สารยับยั้งอัลฟากลูโคซิเดส ได้แก่ quercetin-3-*O*-glucoside จากมะรุมและกระเจี๊ยบเขียว, (+)-pinoresinol จากงา และ chaplupyrrolidone B จากชะพลู นอกจากนี้ยังพบว่าสารดังกล่าว มีกลไกการออกฤทธิ์แบบผสม โดยสามารถยับยั้งการทำงานของเอนไซม์ได้ ทั้งแบบ competitive และ noncompetitive ซึ่งข้อมูลดังกล่าวสามารถระบุเบื้องต้นได้ว่าพืชเหล่านี้สามารถใช้ร่วมกับยารักษาโรคเบาหวาน โดยออกฤทธิ์เสริมกัน หรือใช้เป็นยาเดี่ยว ในขณะเดียวกัน คณะผู้วิจัยได้สังเคราะห์อนุพันธ์ที่มี quercitol เป็นพื้นฐาน โดยปรับเปลี่ยนโครงสร้าง 3 แนวทาง คือ การเกิดปฏิกิริยาดีไฮเดรชันของหมู่ไฮดรอกซีกลายเป็นพันธะคู่, การแทนที่หมู่ไฮดรอกซีด้วยหมู่ *N*-alkyl และ *N*-acyl และการสังเคราะห์อนุพันธ์เอสเทอร์ด้วยการทำปฏิกิริยากับ cinnamic acid หลายชนิด สิ่งที่น่าสนใจคือ สารส่วนใหญ่ที่สังเคราะห์ได้มีฤทธิ์ยับยั้งดีกว่าสารตั้งต้น ซึ่งรวมถึงอนุพันธ์ *N*-hexyl ซึ่งออกฤทธิ์เทียบเท่ากับยารักษาโรคเบาหวาน acarbose แต่มีการจับกับเอนไซม์ได้ดีกว่า นอกจากนี้ยังพบว่า quercityl caffeate ซึ่งสังเคราะห์จาก quercitol กับ caffeic acid เป็นสารในกลุ่มอนุพันธ์เอสเทอร์ที่ออกฤทธิ์ดีที่สุด อีกทั้งยังสามารถคงสมบัติต้านการเกิดออกซิเดชันได้เช่นเดียวกับ caffeic acid ซึ่งสมบัติดังกล่าวมีส่วนสำคัญในการป้องกันการเกิดโรคแทรกซ้อน

Abstract

α-Glucosidase is a key hydrolase that catalyzes hydrolysis of oligosaccharide into glucose. The prolonged elevated glucose level in blood stream leads to the development of diabetes mellitus, accounting for hundreds million people worldwide. To hamper the outbreak of diabetes mellitus and its related complications, inhibition of α-glucosidase is an approach of choice to address this problem. In this project, we aim to search for α-glucosidase inhibitors from edible plants and synthetic compounds. We succeeded in identifying active compounds quercetin-3-*O*-glucoside from *Molinga oleifera* and *Abelmoschus esculentus*, (+)-pinoresinol from *Sesamum indicum* and chaplupyrrolidone B from *Piper sarmentosum*. The mechanisms underlying inhibition were proved to be a mixed type manners of competitive and noncompetitive inhibitions. The results imply the use of these plants as single drug or combination with other antidiabetic drugs. Meanwhile, we also synthesized quercitol-based analogues by 3 different pathways: dehydration of hydroxyl and forming double bond, replacing one hydroxyl group with *N*-alkyl and *N*-acyl moieties and ester formation with cinnamic acids. Interestingly, most synthesized analogues showed improved inhibition over their parent compounds. The *N*-hexyl analogue was the most potential α-glucosidase inhibitor because of its equipotency to antidiabetic drug acaarbose and more tightly binding to the enzyme. In addition, quercityl caffeate, the bioconjugate generated from quercitol and caffeic acid, was the most potent inhibitor among 15 related synthesized analogues, in addition to the retained antioxidant property associated with complications prevention.

Keyword: diabetes mellitus; α-glucosidase; glycoside; quercitol-based analogue

1) การสังเคราะห์ conduritol F และอนุพันธ์ inositol จาก (+)-*proto*-quercitol และฤทธิ์ยับยั้งเอนไซม์อัลฟากลูโคซิเดส

Conduritol F เป็นสารในกลุ่ม cyclohexene ที่มีหมู่ไฮดรอกซี เรียงติดกัน 4 หมู่ สารดังกล่าวเคยมีรายงานว่าสามารถยับยั้งเอนไซม์อัลฟากลูโคซิเดสได้ ในงานวิจัยนี้ได้ศึกษาการสังเคราะห์ conduritol F โดยตั้งต้นจาก (+)-*proto*-quercitol ซึ่งเป็นวิธีใหม่ โดยมีขั้นตอนการสังเคราะห์เพียง 3 ขั้นตอนเท่านั้น (แผนภาพที่ 1) โดยมีขั้นตอนที่สำคัญคือการเปลี่ยนหมู่ไฮดรอกซีให้อยู่ในรูป Trifate (-OTf) แล้วเกิดปฏิกิริยาการกำจัดออก (elimination reaction) ในสภาวะเบส เกิดเป็น conduritol F ที่ต้องการ นอกจากนี้ผู้วิจัยยังพบว่า หากนำ conduritol-F มาทำปฏิกิริยากับ OsO_4 แล้วจะเกิดปฏิกิริยา dihydroxylation เกิดเป็นผลิตภัณฑ์ inositols นอกจากนี้ยังได้ทดสอบฤทธิ์การยับยั้งยับยั้งเอนไซม์อัลฟากลูโคซิเดส ได้ผลดังแสดงในตารางที่ 1 งานวิจัยนี้ได้รับการตีพิมพ์ใน Bioorganic & Medicinal Chemistry Letters 2012, 22, 1538-1540

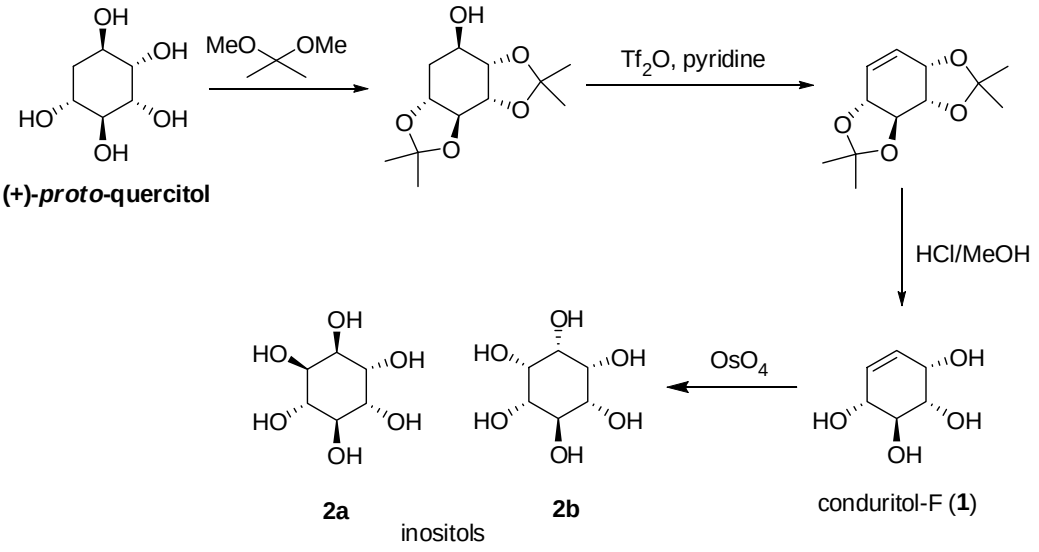

แผนภาพที่ 1 การสังเคราะห์ conduritol F และอนุพันธ์ inositol

ตารางที่ 1 ฤทธิ์การยับยั้งเอนไซม์อัลฟากลูโคซิเดสของ conduritol F (**1**) และอนุพันธ์ inositol (**2a** และ **2b**)

	IC_{50} (μM)		
Cyclitol	Baker's yeast	Maltase	Sucrase
1	86.1±0.5	NI	NI
2a	1256.1±1.7	NI	NI
2b	475.7±0.9	NI	NI

NI, No inhibition, ออกฤทธิ์ยับยั้งเอนไซม์ α-glucosidase น้อยกว่า 30% ที่ความเข้มข้น 10 mg/mL.

2) การสังเคราะห์อนุพันธ์อะมิโนเคอร์ซิทอล (*N*-substituted aminoquercitol) และฤทธิ์ยับยั้งเอนไซม์อัลฟากลูโคซิเดส

ในงานวิจัยนี้ได้สังเคราะห์อนุพันธ์อะมิโนเคอร์ซิทอล 2 กลุ่ม คือ *N*-acyl aminoquercitol (**4-13**, แผนภาพที่ 2) และ *N*-alkyl aminoquercitol (**29-43**, แผนภาพที่ 3) รวมทั้งหมด 25 ชนิด เมื่อนำสารที่แยกได้ไปทดสอบออกฤทธิ์ยับยั้งเอนไซม์อัลฟากลูโคซิเดส (ตารางที่ 2) พบความสัมพันธ์ระหว่างโครงสร้างกับการออกฤทธิ์ซึ่งสามารถสรุปได้ดังนี้

1) *N*-acyl aminoquercitol และ *N*-alkly aminoquercitol มีแนวโน้มการยับยั้งเอนไซม์มอลเทสได้ดีกว่า เอนไซม์ซูเครส แต่กลับไม่ค่อยมีฤทธิ์ยับยั้งเอนไซม์อัลฟากลูโคซิเดสจากยีสต์

2) โดยทั่วไป *N*-alkly aminoquercitol มักมีฤทธิ์ยับยั้งเอนไซม์มอลเทสดีกว่า *N*-acyl aminoquercitol

3) จำนวน methylene (n) ในสายโซ่ไฮโดรคาร์บอน ที่ทำให้ *N*-acyl aminoquercitol และ *N*-alkly aminoquercitol มีฤทธิ์การยับยั้งดีที่สุด เมื่อ n = 4 หรือ 8

4) คอนฟิกูเรชันของคาร์บอนที่ต่อกับไนโตรเจน หรือตำแหน่ง C-1 ไม่ค่อยมีผลต่อการออกฤทธิ์ยับยั้ง

จากแนวโน้มดังกล่าวผู้วิจัยได้เลือกสาร **7**, **35** และ **41** ซึ่งเป็นสารที่มีฤทธิ์ดีที่สุดและเป็นตัวแทนของสารในกลุ่ม *N*-acyl aminoquercitol, *N*-alkyl aminoquercitol และ *N*,*N*-dialkyl aminoquercitol ตามลำดับมาศึกษากลไกการออกฤทธิ์ (รูปที่ 1) และพบว่าสารทั้ง 3 ชนิดมีกลไกการยับยั้งเอนไซม์มอลเทส เป็นแบบแข่งขัน (competitive inhibition) เหมือนกันหมด ที่น่าสนใจยิ่งกว่านั้นคือ สาร **35** มีฤทธิ์การยับยั้งที่ดีกว่ายารักษาเบาหวาน acarbose นอกจากนี้เมื่อสาร **35** สามารถจับกับเอนไซม์แล้วจะมีค่าคงที่ของการสลายตัวน้อยกว่า acarbose (ตารางที่ 3) ทำให้สาร **35** มีแนวโน้มในการออกฤทธิ์ที่นานกว่า acarbose ด้วยเช่นกัน ผลงานวิจัยดังกล่าวได้ตีพิมพ์เผยแพร่ใน Medicinal Chemical Communications 2012, 3, 1466-1470.

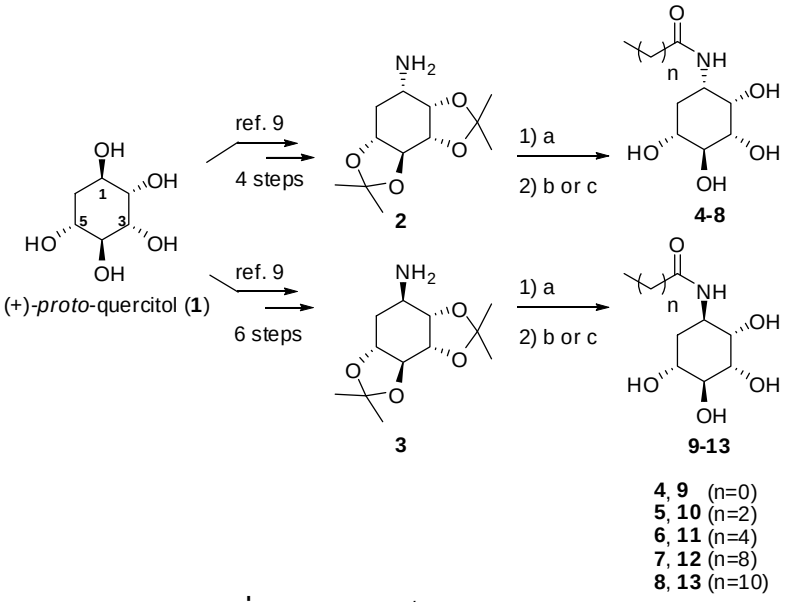

แผนภาพที่ 2 การสังเคราะห์ *N*-acyl aminoquercitol

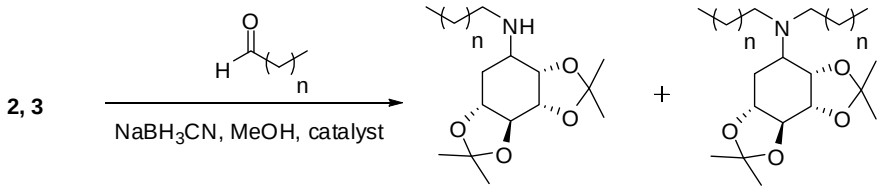

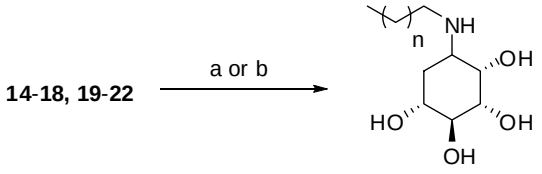

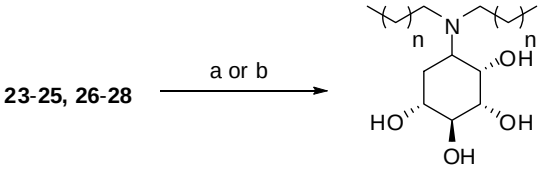

29, **38**, **41** (n=0)
30, **34**, **39**, **42** (n=2)
31, **35**, **40**, **43** (n=4)
32, **36** (n=8)
33, **37** (n=10)

แผนภาพที่ 3 การสังเคราะห์ *N*-alkyl aminoquercitol

ตารางที่ 2 ฤทธิ์การยับยั้งเอนไซม์อัลฟากลูโคซิเดสของ *N*-acyl aminoquercitol และ *N*-alkyl aminoquercitol

	IC_{50} (μM)				IC_{50} (μM)		
Compound	Baker's yeast	Maltase	Sucrase	Compound	Baker's yeast	Maltase	Sucrase
4	270	180	NI	**32**	NI	2.0	410
5	NI	38	NI	**33**	NI	1.9	NI
6	NI	4.2	NI	**34**	1200	57	NI
7	NI	2.0	NI	**35**	400	0.24	NI
8	NI	10	NI	**36**	NI	0.41	NI
9	150	5.3	5.3	**37**	NI	1.5	NI
10	1200	19	4.7	**38**	1600	21	360
11	1700	3.8	6.1	**39**	2300	24	36
12	NI	3.5	NI	**40**	NI	32	120
13	NI	7.4	NI	**41**	1600	5.0	NI
29	NI	NI	NI	**42**	1800	7.6	NI
30	NI	290	NI	**43**	NI	48	NI
31	NI	2.5	NI	**Acarbose**®	480	1.5	2.3

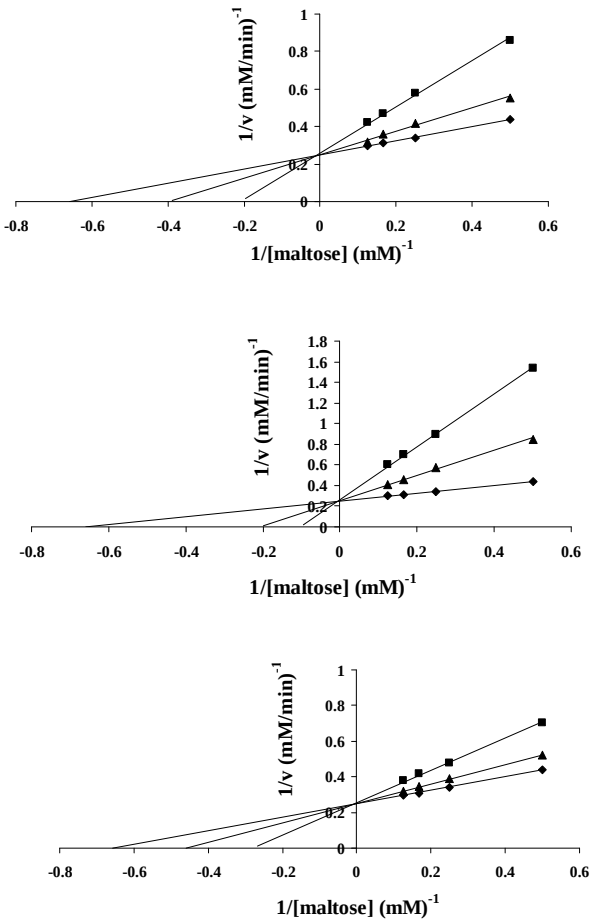

รูปที่ 1 Lineweaver-Burk plot ของ *N*-substituted aminoquercitols **7** (บน), **35** (กลาง) และ **41** (ล่าง)

ตารางที่ 3 การยับยั้งเอนไซม์มอลเทส ค่าคงที่การสลายตัวของเอนไซม์และตัวยับยั้งและชนิดของการยับยั้ง

Compound	IC_{50} (μM)	K_i (μM)	Inhibition type
7	2.0	1.5	Competitive
35	0.24	0.73	Competitive
41	5.0	3.5	Competitive
Acarbose	1.5	0.99	Competitive

3) การสังเคราะห์อนุพันธ์เคอร์ซิติวซินนาเมต (quercityl cinnamates) ที่ออกฤทธิ์ยับยั้งเอนไซม์อัลฟากลูโคซิเดสและฤทธิ์ต้านอนุมูลอิสระ

โครงการนี้ได้สังเคราะห์อนุพันธ์ที่ประกอบด้วย 2 ส่วน โดยส่วนแรกมาจาก quercitol และอีกส่วนหลังมาจาก cinnamic acid และอนุพันธ์ โดยคาดว่าอนุพันธ์ที่ได้จากการสังเคราะห์นี้จะออกฤทธิ์ทั้ง 2 อย่าง คือ ยับยั้งอัลฟากลูโคซิเดสและต้านอนุมูลอิสระพร้อมกัน ซึ่งจะส่งผลดีในการละระดับน้ำตาลในเลือดอีกทั้งช่วยป้องกันโรคที่เกี่ยวข้องซึ่งเกิดจากอนุมูลอิสระ เนื่องจากการมีระดับน้ำตาลสูงต่อเนื่องเป็นเวลานาน ในงานวิจัยนี้สามารถสังเคราะห์อนุพันธ์เคอร์ซิติวซินนาเมต ได้ทั้งหมด 15 ชนิด (**1a**-**8b**) ดังแผนภาพที่ 4 และ 5

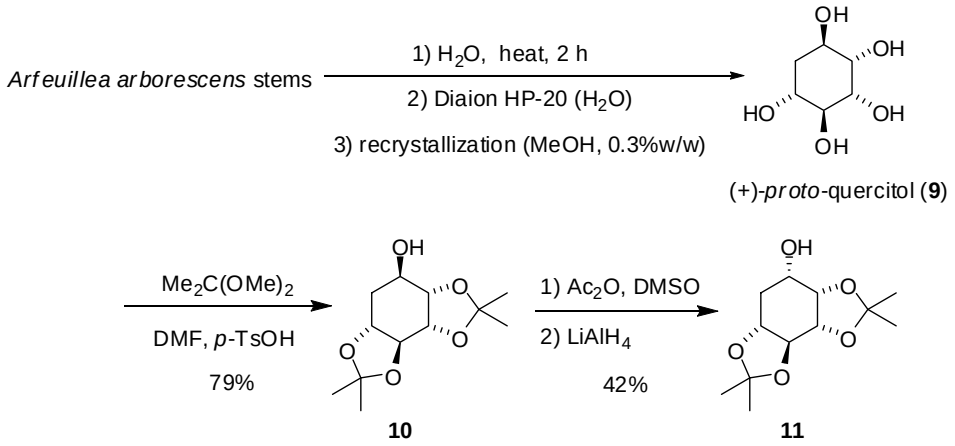

แผนภาพที่ 4 การสังเคราะห์อนุพันธ์ quercitol ก่อนทำปฏิกิริยากับ cinnamic acid และอนุพันธ์

เมื่อนำ quercityl cinnamate ทั้งหมดที่สังเคราะห์ไปทดสอบฤทธิ์ยับยั้งเอนไซม์อัลฟากลูโคซิเดสจากยีสต์ เอนไซม์มอลเทส และเอนไซม์ซูเครส (ตารางที่ 1) พบว่า สารทั้งหมดไม่มีฤทธิ์ยับยั้งเอนไซม์อัลฟากลูโคซิเดสจากยีสต์ ในขณะที่ quercityl cinnamate ที่มีหมู่ phenolic อย่างน้อย 1 หมู่ (**6a- 8b**) ที่มีฤทธิ์ยับยั้งเอนไซม์มอลเทส และซูเครส ในบรรดา quercityl cinnamate ทั้งหมดที่ทดสอบ พบว่า สาร **6a** ซึ่งมีส่วนของ caffeic acid มีฤทธิ์ยับยั้งเอนไซม์มอลเทส และซูเครสดีที่สุด โดยมีค่า IC_{50} 5.31 และ 43.65 μM ตามลำดับ นอกจากนี้ ยังเป็นสารเพียงชนิดเดียวที่มีฤทธิ์ดักจับอนุมูลอิสระ โดยมีค่า SC_{50} .0.11 mM ซึ่งใกล้เคียงกับ BHA ซึ่งเป็นสารต้านอนุมูลอิสระ ดังนั้นสาร **6a** จึงมีศักยภาพทั้งในแง่ของการลดระดับน้ำตาลโดยการยับยั้งเอนไซม์มอลเทสและยังต้านอนุมูลอิสระ ซึ่งมักเกิดขึ้นในสภาวะที่ผู้ป่วยเบาหวานมีภาวะน้ำตาลในเลือดสูงต่อเนื่องกันเป็นเวลานาน

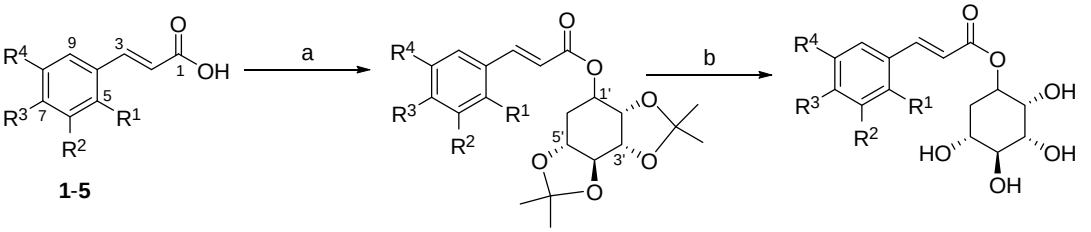

R^1 = OMe, R^2 = R^3 = R^4 = H; **1**
R^1 = R^3 = R^4 = H, R^2 = OMe; **2**
R^1 = R^2 = R^4 = H, R^3 = OMe; **3**
R^1 = R^4 = H, R^2 = R^3 = OMe; **4**
R^1 = H, R^2 = R^3 = R^4 = OMe; **5**

R^1 = OMe, R^2 = R^3 = R^4 = H, 1'*R*; **1R**
R^1 = OMe, R^2 = R^3 = R^4 = H, 1'*S*; **1S**
R^1 = R^3 = R^4 = H, R^2 = OMe, 1'*R*; **2R**
R^1 = R^3 = R^4 = H, R^2 = OMe, 1'*S*; **2S**
R^1 = R^2 = R^4 = H, R^3 = OMe, 1'*R*; **3R**
R^1 = R^2 = R^4 = H, R^3 = OMe, 1'*S*; **3S**
R^1 = R^4 = H, R^2 = R^3 = OMe, 1'*R*; **4R**
R^1 = R^4 = H, R^2 = R^3 = OMe, 1'*S*; **4S**
R^1 = H, R^2 = R^3 = R^4 = OMe, 1'*R*; **5R**

R^1 = OMe, R^2 = R^3 = R^4 = H, 1'*R*; **1a**
R^1 = OMe, R^2 = R^3 = R^4 = H, 1'*S*; **1b**
R^1 = R^3 = R^4 = H, R^2 = OMe, 1'*R*; **2a**
R^1 = R^3 = R^4 = H, R^2 = OMe, 1'*S*; **2b**
R^1 = R^2 = R^4 = H, R^3 = OMe, 1'*R*; **3a**
R^1 = R^2 = R^4 = H, R^3 = OMe, 1'*S*; **3b**
R^1 = R^4 = H, R^2 = R^3 = OMe, 1'*R*; **4a**
R^1 = R^4 = H, R^2 = R^3 = OMe, 1'*S*; **4b**
R^1 = H, R^2 = R^3 = R^4 = OMe, 1'*R*; **5a**

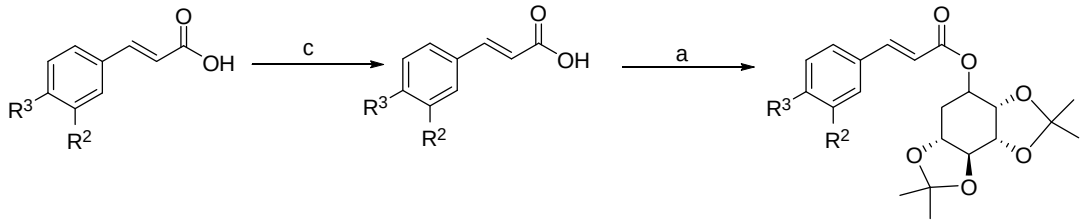

R^2 = R^3 = OH; **6**
R^2 = OMe, R^3 = OH; **7**
R^2 = OH, R^3 = OMe; **8**

R^2 = R^3 = $OSi(CH_3)_3$; **6Si**
R^2 = OMe, R^3 = $OSi(CH_3)_3$; **7Si**
R^2 = $OSi(CH_3)_3$, R^3 = OMe; **8Si**

R^2 = R^3 = $OSi(CH_3)_3$, 1'*R*; **6R**
R^2 = R^3 = $OSi(CH_3)_3$, 1'*S*; **6S**
R^2 = OMe, R^3 = $OSi(CH_3)_3$, 1'*R*; **7R**
R^2 = OMe, R^3 = $OSi(CH_3)_3$, 1'*S*; **7S**
R^2 = $OSi(CH_3)_3$, R^3 = OMe, 1'*R*; **8R**
R^2 = $OSi(CH_3)_3$, R^3 = OMe, 1'*S*; **8S**

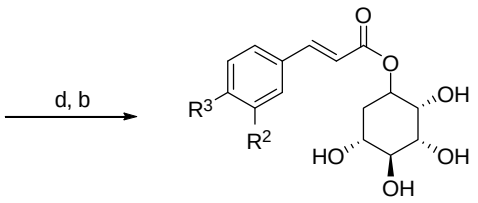

R^2 = R^3 = OH, 1'*R*; **6a**
R^2 = R^3 = OH, 1'*S*; **6b**
R^2 = OMe, R^3 = OH, 1'*R*; **7a**
R^2 = OMe, R^3 = OH, 1'*S*; **7b**
R^2 = OH, R^3 = OMe, 1'*R*; **8a**
R^2 = OH, R^3 = OMe, 1'*S*; **8b**

Reagents and conditions: (a) 10 or 11, DCC, DMAP, CH2Cl2, 0 C to rt; (b) Amberlyst-15, MeOH; (c) TBDMSCl, imidazole, DMF, rt; (d) TBAF, THF, rt

แผนภาพที่ 5 การสังเคราะห์ quercityl cinnamate (**1a-8b**) จาก (+)-*proto*-quercitol (**9**) และสารกลุ่ม cinnamic acid (**1-8**)

ตารางที่ 4 ฤทธิ์ยับยั้งเอนไซม์อัลฟากลูโคซิเดสและต้านอนุมูลอิสระของ quercityl cinnamate (**1a-8b**)

Compounds	α-Glucosidase inhibitory effect (IC_{50}, μM)			Radical scavenging (SC_{50}, mM)
	Baker's yeast glucosidase	Maltase	Sucrase	
1a	NI*	NI	NI	NS*
1b	NI	NI	NI	NS
2a	NI	NI	NI	NS
2b	NI	NI	NI	NS
3a	NI	NI	NI	NS
3b	NI	NI	NI	NS
4a	NI	NI	NI	NS
4b	NI	NI	NI	NS
5a	NI	NI	NI	NS
6a	NI	5.31	43.65	0.11
6b	NI	497.48	954.08	NS
7a	NI	51.93	67.21	NS
7b	NI	21.07	171.43	NS
8a	NI	20.81	53.00	NS
8b	NI	367.15	805.48	NS
Acarbose®	??	1.50	2.30	??
BHA	ND	ND	ND	0.10

อนุพันธ์ quercityl cinnamate **6a** มีฤทธิ์ที่ดีในการยับยั้งเอนไซม์มอลเทส และซูเครส จึงได้นำสารดังกล่าวมากลไกการยับยั้ง พบว่ามีกลไกแบบผสม (mixed inhibition) ดังแสดงใน รูปที่ 2 และ 3 รวมทั้งตารางที่ 5 ผลงานวิจัยนี้ได้รับการตอบรับให้ตีพิมพ์ใน European Journal of Medicinal Chemistry (2013) doi: 10.1016/j.ejmech.2013.05.047

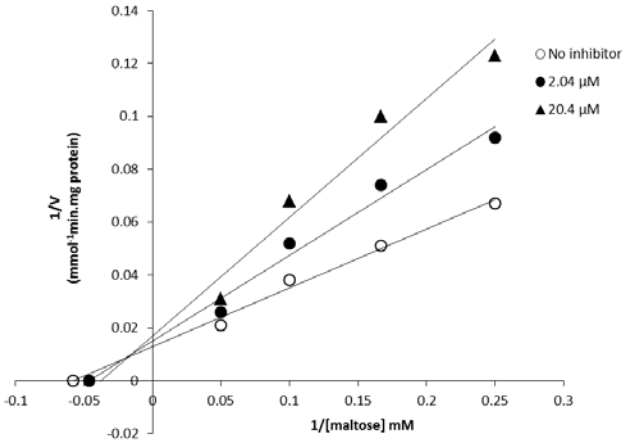

รูปที่ 2 Lineweaver-Burk Plot ของ **6a** ต่อเอนไซม์มอลเทส

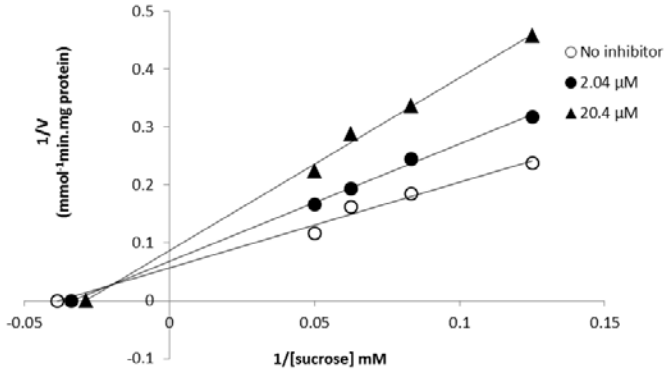

รูปที่ 3 Lineweaver-Burk Plot ของ **6a** ต่อเอนไซม์ซูเครส

ตารางที่ 5 ฤทธิ์ยับยั้งเอนไซม์มอลเทส และซูเครสของ **6a** ค่าคงที่การสลายตัวของเอนไซม์ สารยับยั้งและชนิดการยับยั้ง

α-Glucosidase	Inhibition type	K_i (µM)	K_i' (µM)	K_m (mM)
Maltase	Mixed-inhibition	23.8	64.5	17.3
sucrase	Mixed-inhibition	22.4	47.5	25.9

4) สารยับยั้งเอนไซม์อัลฟากลูโคซิเดสจากกากงา (*Sesamum indicum*)

งาเป็นพืชที่รู้จักและใช้ประโยชน์กันอย่างกว้างขวาง นอกจากนี้ยังมีรายงานว่าสารสกัดน้ำจากกากงามีฤทธิ์ลดระดับน้ำตาลในเลือดของสัตว์ทดลอง ผู้วิจัยจึงได้ศึกษาเพื่อพิสูจน์สารที่ออกฤทธิ์ดังกล่าว โดยใช้ผลการทดสอบฤทธิ์ยับยั้งเอนไซม์อัลฟากลูโคซิเดส ช่วยบ่งชี้การแยกด้วยเทคนิคทางโครมาโตกราฟี สามารถแยกสารกลุ่ม lignin ได้ทั้งหมด 4 ชนิดคือ (+)-pinoresinol, sesamolin, sesamin และ sesaminol monolgucoside จากการทดสอบ (ตารางที่ 6) พบว่าสาร 3 ชนิดแรกออกออกฤทธิ์ยับยั้งเอนไซม์อัลฟากลูโคซิเดสที่ได้จากยีสต์ แต่จะมีเฉพาะ (+)-pinoresinol เท่านั้นที่ออกออกฤทธิ์ยับยั้งเอนไซม์มอลเทส ซึ่งจัดอยู่ในกลุ่ม α-glucosidase ที่ได้จากลำไส้หนู ดังนั้นจึงอาจสรุปได้ว่า (+)-pinoresinol น่าจะออกฤทธิ์ลดระดับน้ำตาลในเลือดของหนูทดลองดังที่เคยมีรายงานมาก่อนหน้านี้

นอกจากนี้ผู้วิจัยยังได้ศึกษากลไกการยับยั้งเอนไซม์มอลเทสของ (+)-pinoresinol (รูปที่ 4) ซึ่งพบว่ามีการยับยั้งแบบผสม (mixed inhibition) โดยประกอบด้วยการยับยั้งแบบแข่งขัน (competitive inhibition) และแบบไม่แข่งขัน (noncompetitive inhibition) แต่เนื่องจากการยับยั้งแบบแข่งขันมีค่าคงที่ของการสลายตัว (k_i = 288 µM) น้อยกว่าการยับยั้งแบบไม่แข่งขัน (k'_i = 1342 µM) จึงทำให้ทราบว่า (+)-pinoresinol มีแนวโน้มในการจับกับเอนไซม์มอลเทสได้ดีกว่าการจับกับสารเชิงซ้อน maltase-maltose นอกจากนี้ความสามารถของ (+)-pinoresinol ในการจับกับเอนไซม์มอลเทสแบบไม่แข่งขัน ทำให้สารดังกล่าวมีแนวโน้มสามารถที่จะนำไปใช้ควบคู่กับยารักษาเบาหวาน เช่น acarbose ได้ ซึ่งจะส่งผลให้สามารถลดปริมาณการใช้ยาลงได้มาก ผลงานวิจัยนี้ตีพิมพ์ในวารสาร Bioorganic & Medicinal Chemistry Letters 2012, 22, 5215-5217

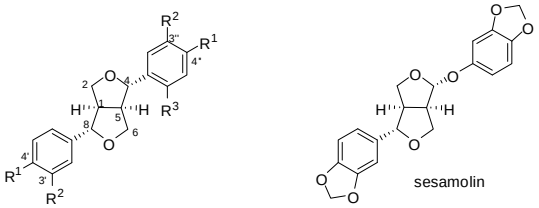

(+)-pinoresinol: R^1 = OH, R^2 = OCH_3, R^3 = H
sesamin: $R^1 + R^2$ = OCH_2O, R^3 = H
sesaminol monoglucoside: $R^1 + R^2$ = OCH_2O, R^3 = O-β-Glc

ตารางที่ 6 ฤทธิ์ยับยั้งเอนไซม์อัลฟากลูโคซิเดสของสารที่แยกได้จากกากงา

	IC_{50} (μM)		
Lignans	Baker's yeast	Maltase	Sucrase
(+)-pinoresinol	492 ± 2.5	34.3 ± 0.8	NI
sesamolin	200 ± 1.2	NI	NI
sesamin	450 ± 1.9	NI	NI
Sesaminol monoglucoside	NI	NI	NI

NI, No inhibition, ออกฤทธิ์ยับยั้งเอนไซม์ α-glucosidase น้อยกว่า 30% ที่ความเข้มข้น 10 mg/mL.

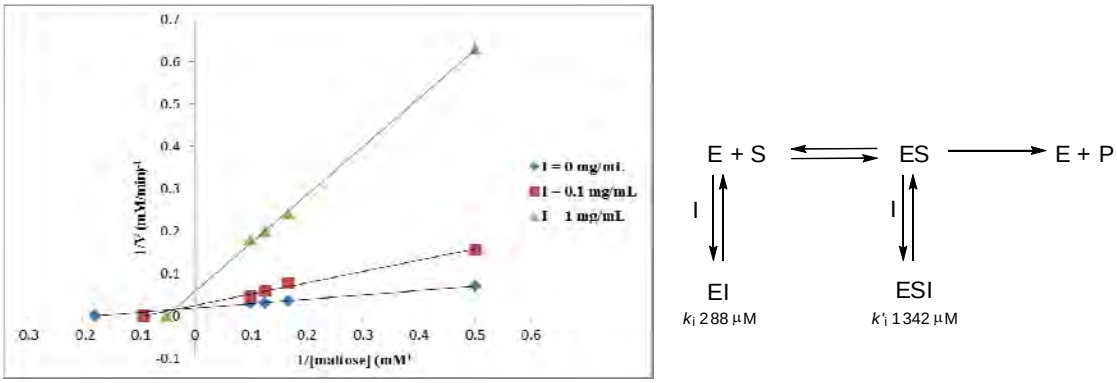

รูปที่ 4 Lineweaver-Burk plot ของ (+)-pinoresinol และกลไกการยับยั้งเอนไซม์มอลเทส แบบผสม (mixed inhibition)

5) สารยับยั้งอัลฟากลูโคซิเดสจากกระเจี๊ยบเขียว (*Abelmoschus esculentus*)

กระเจี๊ยบเขียว (*Abelmoschus esculentus*) เป็นพืชที่คนไทยนิยมบริโภค อีกทั้งมีรายงานว่ากระเจี๊ยบเขียวสามารถลดระดับน้ำตาลในเลือดของหนูทดลองได้ แต่ยังไม่มีรายงานการศึกษา และพิสูจน์สารที่ออกฤทธิ์ดังกล่าว ในงานวิจัยนี้ ได้ศึกษาฤทธิ์ยับยั้งเอนไซม์อัลฟากลูโคซิเดสจากเมล็ดกระเจี๊ยบเขียว พบว่า

มีสารออกฤทธิ์หลัก 2 ชนิด คือ quercetin-3-*O*-glucoside และ quercetin-3-*O*-glucosyl (1‴⟶6″) glucoside โดยมีแผนภาพการสกัดแยกสารดังกล่าว ในรูปที่ 3

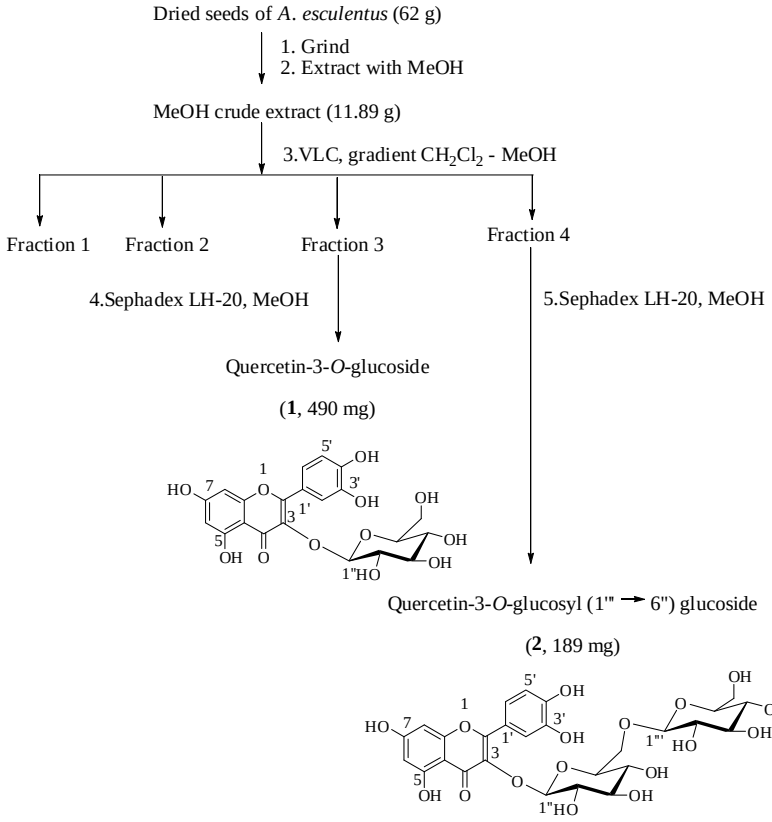

รูปที่ 5 ขั้นตอนการสกัดแยกสารออกฤทธิ์ยับยั้งเอนไซม์อัลฟากลูโคซิเดสจากเมล็ดกระเจี๊ยบเขียว

เมื่อทดสอบฤทธิ์ยับยั้งเอนไซม์อัลฟากลูโคซิเดสของสารที่แยกได้ พบว่า quercetin-3-*O*-glucoside ให้ฤทธิ์ยับยั้งเอนไซม์มอลเทส และซูเครสได้ดีที่สุด โดยมีค่า IC_{50} 64.1 และ 42.5 μM ตามลำดับ ผู้วิจัยจึงได้ศึกษาฤทธิ์ยับยั้งเอนไซม์อัลฟากลูโคซิเดสของ quercetin ต่อไป เนื่องจากพบแนวโน้มว่า การไม่มีน้ำตาลมาเกาะที่ตำแหน่ง C-3 น่าจะให้ฤทธิ์การยับยั้งที่สูงขึ้น ซึ่งก็พบว่า quercetin มีฤทธิ์ยับยั้งเอนไซม์มอลเทส และซูเครส ด้วยค่า IC_{50} 12.3 และ 31.7 μM ตามลำดับ นอกจากนี้ ยังพบว่า quercetin มีกลไกยับยั้งเอนไซม์มอลเทส และซูเครสแบบผสม (mixed inhibition) และแบบแข่งขัน (competitive inhibition) ตามลำดับ ดังแสดงในรูปที่ 6, 7 และตารางที่ 7

ผลงานวิจัยในส่วนนี้ได้รับการตอบรับให้ตีพิมพ์ในวารสาร Natural Product Communications (Accepted: April 30, 2013)

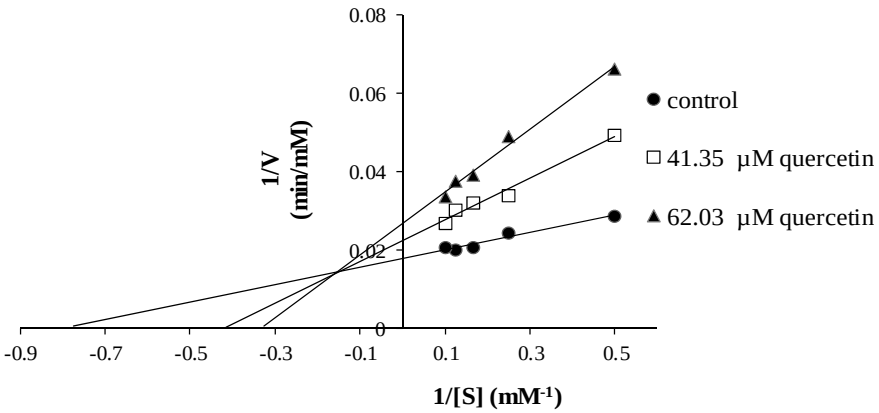

รูปที่ 6 Lineweaver-Burk Plot ของ quercetin ต่อเอนไซม์มอลเทส

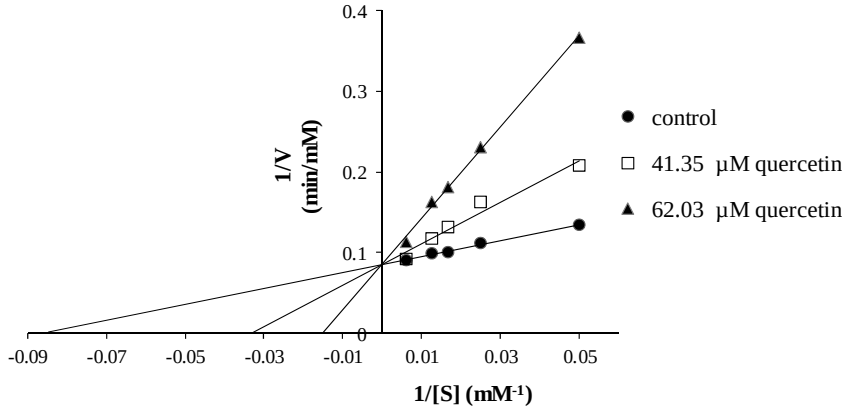

รูปที่ 7 Lineweaver-Burk Plot ของ quercetin ต่อเอนไซม์ซูเครส

ตารางที่ 7 ฤทธิ์ของ quercetin ในการยับยั้งเอนไซม์มอลเทส และซูเครส ค่าคงที่การสลายตัวของเอนไซม์สารยับยั้งและชนิดการยับยั้ง

Compound	Maltase		Sucrase	
	K_i (µM)	Inhibition type	K_i (µM)	Inhibition type
quercetin	462 2153[a]	Mixed	218	Competitive

[a] K_i' value for noncompetitive manner.

6) สารยับยั้งเอนไซม์อัลฟากลูโคซิเดสจากใบชะพลู (*Piper sarmentosum*)

ชะพลู (*Piper sarmentosum*) เป็นพืชที่รู้จักกันเป็นอย่างดีในไทย นอกจากจะใช้ประกอบอาหารแล้ว ยังเป็นสมุนไพรที่มีสรรพคุณที่น่าสนใจหลายอย่าง โดยเฉพาะสรรพคุณในการลดระดับน้ำตาลในเลือด ซึ่งจะส่งผลดีอย่างยิ่งในการควบคุมและรักษาโรคเบาหวาน นอกจากนี้ได้มีการรายงานฤทธิ์ดังกล่าวในสัตว์ทดลองแล้ว แต่ยังไม่มีการพิสูจน์ถึงสารที่ทำหน้าที่ออกฤทธิ์ดังกล่าว ในงานวิจัยนี้ผู้วิจัยได้ศึกษาสารที่น่าจะมีส่วนในการลดระดับน้ำตาลในเลือดโดยทำการแยกสารสกัดจากใบชะพลูและติดตามสารออกฤทธิ์โดยการทดสอบการยับยั้งเอนไซม์อัลฟากลูโคซิเดส (α-glucosidase) ซึ่งเป็นเอนไซม์ที่ย่อยโอลิโกแซคคาไรด์ (oligosaccharide) ให้กลายเป็นน้ำตาลกลูโคส สามารถแยกสารบริสุทธิ์ได้ทั้งหมด 7 ชนิด (รูปที่ 8) ซึ่งในบรรดาสารที่แยกได้ทั้งหมดนี้เป็นสารใหม่ที่ยังไม่เคยมีรายงานมาก่อน 3 ชนิดคือ chaplupyrrolidone A (**1**) chaplupyrrolidone B (**2**) และ deacetylsarmentamide B (**7**) สารใหม่ทั้ง 3 ชนิดจัดเป็นสารในกลุ่มเฟนนิลโพรพาโนอิล เอไมด์ (phenylpropanoyl amide) ซึ่งโครงสร้างสารใหม่พิสูจน์ยืนยันโดยเทคนิคทางสเปกโตรสโคปีรวมทั้ง 2D (รูปที่ 9) โครงสร้างของสาร **1** และ **2** มีส่วนของ 5-oxygenated-Δ^3-2-pyrrolidone ซึ่งเป็นรายงานแรกที่พบโครงสร้างดังกล่าวจากผลิตภัณฑ์ธรรมชาติ นอกจากนี้ผู้วิจัยยังได้พิสูจน์ยืนยัน absolute configuration ของตำแหน่ง C-5 ด้วย วิธีของ Moscher ซึ่งพบว่ามี configuration เป็น *S*

จากการทดสอบฤทธิ์ยับยั้งอัลฟากลูโคซิเดส (ตารางที่ 8) พบว่าสาร **2** ออกฤทธิ์ดีที่สุด โดยมีฤทธิ์ดีกว่าสาร **1** ซึ่งมีโครงสร้างคล้ายกันถึง 18 เท่า นอกจากนี้ยังได้ศึกษากลไกการยับยั้งอัลฟากลูโคซิเดสของสาร **2** พบว่าเป็นแบบ noncompetitive

ผลงานวิจัยนี้ได้รับการตีพิมพ์ในวารสาร Phytochemistry Letters 2013, 6, 350-354.

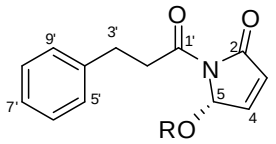

chaplupyrrolidone A (**1**); R = H
chaplupyrrolidone B (**2**); R = CH_3

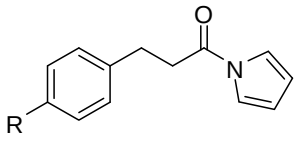

3; R = OCH_3
4; R = H

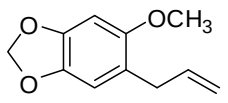

5

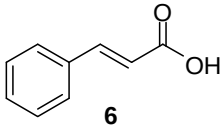

6

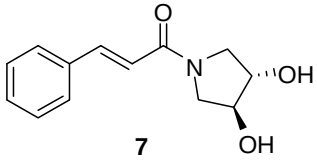

7
deacetylsarmentamide B

รูปที่ 8 โครงสร้างของสารที่แยกได้จากใบชะพลู

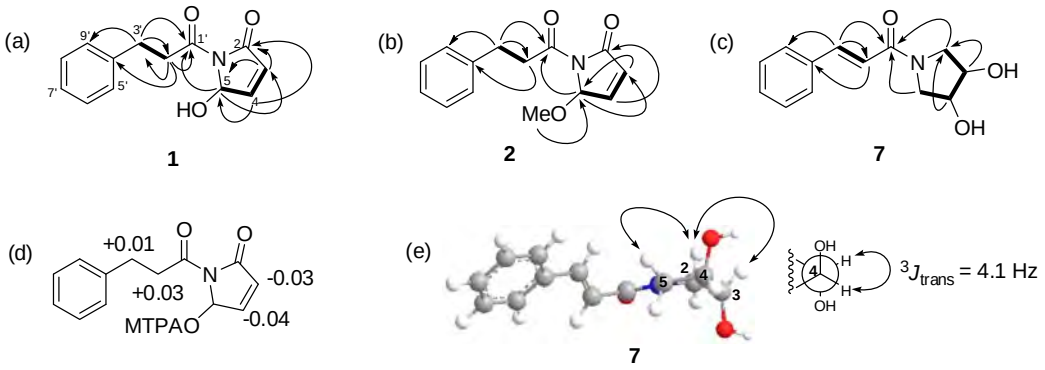

รูปที่ 9 (a), (b) และ (c) โครงสร้างของสาร **1**, **2** และ **7** ที่แสดง COSY (เส้นทึบ) และ HMBC (ลูกศรโค้ง) correlation; (d) การกระจายตัวของ $\Delta\delta H_{SR}$ ของอนุพันธ์ MTPA esters ของสาร **1**; (e) NOESY correlation ของสาร **7** และการวิเคราะห์ค่า coupling constant

ตารางที่ 8 ฤทธิ์ของสารที่แยกได้จากใบชะพลูในการยับยั้งเอนไซม์อัลฟากลูโคซิเดส

Compounds	α-Glucosidase inhibition IC_{50} (μM)
1	7820±6.0
2	430±1.2
3	NI[a]
4	NI
5	NI
6	NI
7	NI
Acarbose	404±0.4

[a]NI, inhibitory effect less than 30% at concentration of 10 mg/mL.

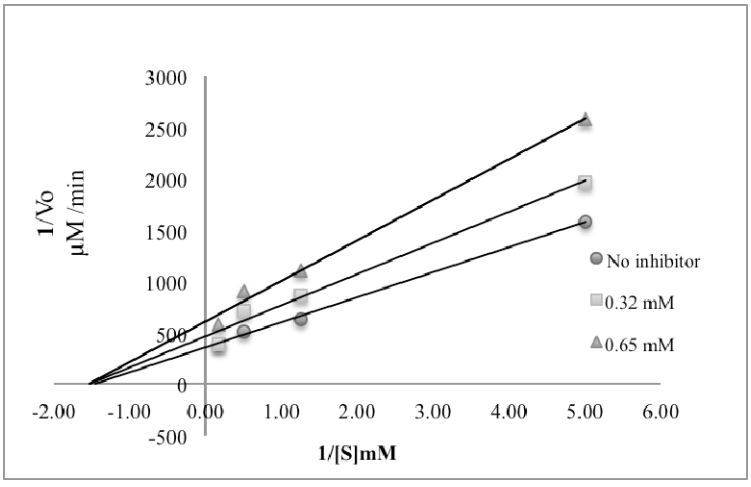

รูปที่ 10 Lineweaver-Burk plot ของ chaplupyrrolidone B (**2**) ต่อเอนไซม์อัลฟากลูโคซิเดส

7) สารยับยั้งเอนไซม์อัลฟากลูโคซิเดสจากใบและเมล็ดมะรุม (*Moringa oleifera*)

มะรุมเป็นสมุนไพรที่มีขายในรูปใบและเมล็ดโดยมีสรรพคุณลดระดับน้ำตาลในเลือด คณะผู้วิจัยจึงได้ศึกษาเปรียบเทียบฤทธิ์ยับยั้งเอนไซม์อัลฟากลูโคซิเดส ของสารสกัดจากทั้งใบและเมล็ด พร้อมทั้งศึกษาสารที่ออกฤทธิ์ดังกล่าว สารออกฤทธิ์ที่พบในใบมะรุมแบ่งออกเป็น 2 กลุ่ม คือ flavonoid และ simple aromatic ประกอบด้วยสาร **1**-**11** ในขณะที่สารออกฤทธิ์ในเมล็ดมะรุมจะพบเพียง 3 ชนิด คือ สาร **3**, **4** และ **8** ซึ่งเหมือนกับที่พบในใบ สารที่ออกฤทธิ์ดีที่สุดคือ quercetin-3-*O*-glucside (**11**) นอกจากนี้ยังพบว่าสาร 5 และ 6 ออกฤทธิ์ยับยั้งเอนไซม์อัลฟากลูโคซิเดสจากยีสต์ ดีที่สุดโดยมีค่า IC_{50} เท่ากับ 27.2 และ 81.7 mg/mL ตามลำดับ ซึ่งเป็นงานวิจัยแรกที่มีการรายงานฤทธิ์ของสารดังกล่าวในการยับยั้งเอนไซม์อัลฟากลูโคซิเดส งานวิจัยนี้อยู่ในระหว่างการเตรียม manuscript เพื่อยื่นตีพิมพ์ในวารสารนานาชาติต่อไป

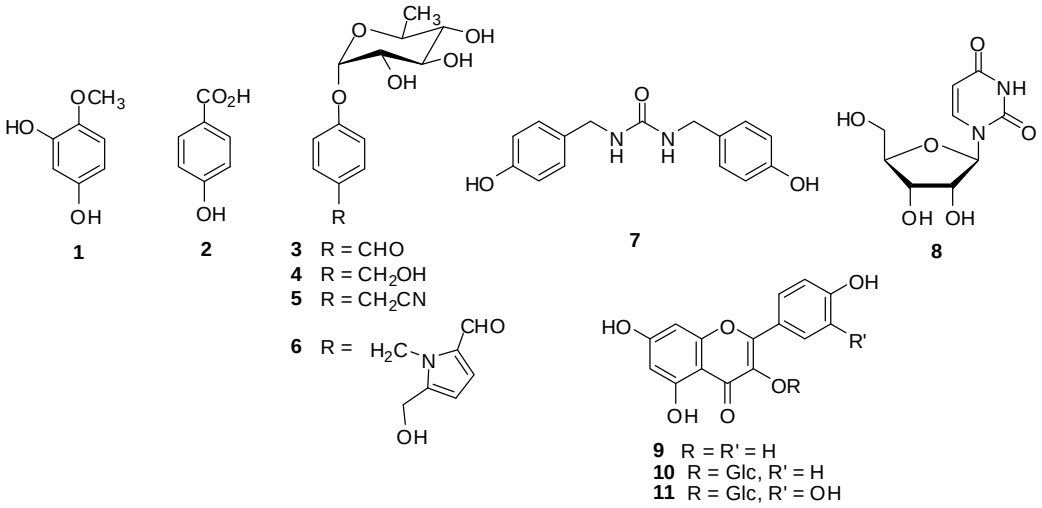

รูปที่ 11 โครงสร้างของสารออกฤทธิ์ที่พบในใบและเมล็ดมะรุม

ผลผลิตที่ได้จากโครงการ

ผลงานตีพิมพ์ในวารสารระดับนานาชาติที่ได้การสนับสนุนจากทุนวิจัยนี้ได้แก่

1) Worawalai W, Rattanangkool E, Vanitcha A, Phuwapraisirisan P, Wacharasindhu S.* Concise synthesis of (+)-conduritol F and inositol analogues from naturally available (+)-*proto*-quercitol and their glucosidase inhibitory activity. *Bioorganic and Medicinal Chemistry Letters* **2012**; 22: 1538-1540.
2) Worawalai W, Wacharasindhu S, Phuwapraisirisan P*. Synthesis of new *N*-substituted aminoquercitols from naturally available (+)-*proto*-quercitol and their α-glucosidase inhibitory activity. *Medical Chemical Communications* **2012**; 3: 1466-1470.
3) Rattanangkool E, Kittikhunnatham P, Damsut T, Wacharasindhu S, Phuwapraisirisan P.* Quercitylcinnamates, a new series of antidiabetic bioconjugates possessing α-glucosidase inhibition and antioxidant. *European Journal of Medicinal Chemistry* (In press, DOI 10.1016/j.ejmech.2013.05.047)
4) Wikul A, Damsud T, Kataoka K, Phuwapraisirisan P*. (+)-Pinoresinol is a putative hypoglycemic agent in defatted sesame (*Sesamum indicum*) seeds though inhibiting α-glucosidase. *Bioorganic and Medicinal Chemistry Letters* **2012**; 22: 5215-5217.
5) Thanakosai W, Phuwapraisirisan P*. First identification of α-glucosidase inhibitors from Okra (*Abelmoschus esculentus*) seeds. *Natural Product Communications* (Accepted, April 30 2013).
6) Damsud T; Adisakwattana S; Phuwapraisirisan P*. Three new phenylpropanoyl amides from the leaves of *Piper sarmentosum* and their α-glucosidase inhibitory activities. *Phytochemistry Letters* **2013**; 6, 350-354.

นอกจากนี้ยังมีงานวิจัยที่เกี่ยวข้องกับการศึกษาสารยับยั้งเอนไซม์อัลฟากลูโคซิเดสจากใบและเมล็ดมะรุม ที่อยู่ในระหว่างการเตรียมต้นฉบับสำหรับการตีพิมพ์ แต่ยังไม่แล้วเสร็จ ซึ่งจะได้แจ้งความคืบหน้าในโอกาสต่อไป

ภาคผนวก

1) บทความที่เกี่ยวข้องกับงานวิจัย สำหรับการเผยแพร่

เบาหวานเป็นโรคที่เกี่ยวข้องกับความผิดปกติของระบบเมตาบอลิซึม (metabolic syndrome) เนื่องจากร่างกายไม่สามารถนำน้ำตาลไปใช้เป็นพลังงานได้ตามปกติ ทำให้ระดับน้ำตาลในเลือดสูงขึ้น ในปัจจุบันพบว่าคนไทยเป็นโรคเบาหวานมากถึง 5% จากประชากรกว่า 60 ล้านคน ในขณะที่แนวโน้มของคนที่เป็นโรคเบาหวานเพิ่มขึ้นทุกปี ยาที่ใช้รักษาโรคเบาหวานมีหลายชนิดแตกต่างกันตามกลไกการทำงาน ยาที่ยับยั้งการทำงานของเอนไซม์อัลฟากลูโคซิเดส เช่น Acarbose® เป็นอีกกลุ่มหนึ่งที่ใช้กันอย่างแพร่หลาย เพราะช่วยลดการดูดซึมน้ำตาลที่ได้จากการย่อยคาร์โบไฮเดรตบริเวณลำไส้เล็กเข้าสู่กระแสเลือด ซึ่งเป็นผลดีในการควบคุมและรักษาโรคเบาหวานรวมทั้งโรคที่เกี่ยวเนื่อง เช่น แผลหายช้า และจอประสาทตาเสื่อม อย่างไรก็ตามเบาหวานเป็นโรคที่ใช้เวลานานในการรักษา ทำให้สิ้นเปลืองค่าใช้จ่ายสูง ดังนั้นหากสามารถเข้าถึงยารักษาโรคเบาหวานได้ในราคาถูก จะส่งผลดีต่อการรักษา จากปัญหาดังกล่าวทำให้ผู้ป่วยหลายคนหันมาใช้สมุนไพรในการรักษาแทนการใช้ยาแผนปัจจุบัน สมุนไพรหลายชนิดมีศักยภาพในการรักษาเบาหวานได้เทียบเท่าหรือดีกว่ายาแผนปัจจุบัน แต่ยังไม่มีการศึกษาอย่างเป็นระบบในการนำมาพัฒนาเป็นยารักษาเบาหวานเนื่องยังขาดข้อมูลของสารที่ออกฤทธิ์ดังกล่าว

เพื่อแก้ปัญหานี้ คณะผู้วิจัยได้ดำเนินโครงการนำร่องซึ่งได้รับการสนับสนุนจาก สกว. เมื่อปี 2551 ในการศึกษาสมุนไพรที่มีสรรพคุณรักษาเบาหวานและมีรายงานว่าสามารถลดระดับน้ำตาลในเลือดของสัตว์ทดลอง (*in vivo*) แต่ยังไม่มีการศึกษาระบุถึงสารออกฤทธิ์ การดำเนินโครงการในครั้งนั้น คณะผู้วิจัยประสบความสำเร็จในการบ่งชี้สารที่ออกฤทธิ์ยับยั้งการทำงานของเอนไซม์ α-glucosidase จากสมุนไพร 2 ชนิดคือ ใบมะตูมและใบปอกระเจา เป็นที่น่าสังเกตว่าสารที่ออกฤทธิ์ยับยั้งการทำงานของเอนไซม์ได้ดี ส่วนใหญ่เป็นสารในกลุ่มกลัยโคไซด์ (glycoside) ซึ่งบางชนิดมีฤทธิ์ดีกว่ายารักษาเบาหวาน เช่น Acarbose® หลายเท่า ผลจากการวิจัยครั้งนั้นทำให้เห็นศักยภาพของสารกลุ่มกลัยโคไซด์จากสมุนไพรในการพัฒนาเป็นยารักษาโรคเบาหวาน การดำเนินงานในโครงการวิจัยนี้สามารถพิสูจน์ทราบสารออกฤทธิ์ยับยั้งเอนไซม์อัลฟากลูโคซิเดส จากสุมนไพร 4 ชนิด คือ มะรุม, กระเจี๊ยบเขียว, งา และชะพลู รวมทั้งศึกษากลไกการทำงานของสารดังกล่าว ข้อมูลนี้เป็นข้อมูลพื้นฐานยืนยันประสิทธิภาพการทำงานของสมุนไพร ที่มีสารออกฤทธิ์ดังกล่าว และยังสามารถเป็นแนวทางในการใช้งานร่วมกับยาที่ใช้รักษาเบาหวานในปัจจุบัน

นอกจากนี้คณะผู้วิจัยยังได้ดำเนินโครงการนำร่อง การสังเคราะห์เลียนแบบยาที่ใช้รักษาเบาหวาน ซึ่งเป็นสารกลุ่มอะมิโนไซคลิทอล ด้วยการปรับเปลี่ยนโครงสร้างสารผลิตภัณฑ์ธรรมชาติที่มีปริมาณมาก แต่มีฤทธิ์น้อยให้มีฤทธิ์สูงขึ้น การดำเนินโครงการในครั้งนั้นได้เลือกใช้เคอร์ซิทอล (quercitol) ซึ่งเป็นสารในกลุ่มไซคลิทอลและมีปริมาณมากในธรรมชาติ มาเปลี่ยนหมู่ฟังก์ชันจากไฮดรอกซี (-OH) ให้เป็นหมู่อะมิโน ($-NH_2$) ได้อะมิโนเคอร์ซิทอล (aminoquercitol) เป็นสารผลิตภัณฑ์ สารดังกล่าวออกฤทธิ์ดีกว่า Acarbose® ซึ่งเป็นยารักษาเบาหวานถึง 45 เท่า นอกจากนี้การเลือกใช้เคอร์ซิทอลเป็นสารตั้งต้น ช่วยลดขั้นตอนการสังเคราะห์และได้สารผลิตภัณฑ์ที่บริสุทธิ์ในปริมาณสูง ซึ่งเป็นข้อดีที่เหนือกว่าวิธีการที่เคยมีรายงานแล้ว นอกจากนี้ยังพบว่าสเตอริโอเคมีของหมู่อะมิโนยังมีผลต่อการออกฤทธิ์ ดังนั้นทำให้เห็นแนวโน้มว่าหากศึกษาในรายละเอียดถึงการปรับเปลี่ยนหมู่อะมิโนและหมู่ฟังก์ชันอื่นที่เกี่ยวข้อง ที่ตำแหน่งต่าง ๆ ของโมเลกุลมีโอกาสในการค้นพบสารที่ออกฤทธิ์ดีขึ้น ซึ่งจะเป็นแนวทางในการสังเคราะห์สารกลุ่มอะมิโนไซคลิทอลชนิดใหม่ที่มีประสิทธิภาพสูง ผลการดำเนินงานในโครงการนี้พบสารออกฤทธิ์ชนิดใหม่ที่มีฤทธิ์ดีเทียบเท่า acarbose ซึ่งเป็นยาที่ใช้รักษาโรคเบาหวานในปัจจุบัน แต่มีฤทธิ์การจับกับเอนไซม์เป้าหมายได้ดีกว่า ซึ่งมีผลทำให้ออกฤทธิ์นานกว่า acarbose

2) การเชื่อมโยงทางวิชาการกับนักวิจัยอื่น ๆ ทั้งในและต่างประเทศ

1. ดร.ชุติวรรณ เดชสกุลวัฒนา สถาบันวิทยาศาสตร์ทางทะเล มหาวิทยาลัยบูรพา ในการศึกษาสารออกฤทธิ์ทางชีวภาพจากแบคทีเรียทะเลที่แยกได้จากฟองน้ำทะเล ปัจจุบันมีนิสิตปริญญาเอก 1 คนและปริญญาโท 1 คน กำลังทำวิจัยในหัวข้อดังกล่าว

2. ผศ.ดร.วิมลพรรณ รุ่งพรหม คณะวิทยาศาสตร์และเทคโนโลยี มหาวิทยาลัยราชภัฏพระนครศรีอยุธยา ในการศึกษาสมุนไพรในท้องถิ่นภาคกลางที่มีสรรพคุณรักษาโรคเบาหวานโครงการดังกล่าวได้รับทุนวิจัยและการสนับสนุนจากสกอ.สำหรับมหาวิทยาลัยในกลุ่มอัตลักษณ์

3. รศ.ดร.พรเทพ สมพรพิสุทธิ์ ภาควิชาเคมี คณะวิทยาศาสตร์ มีความร่วมมือในการศึกษาความสัมพันธ์ระหว่างโครงสร้างของสารที่สังเคราะห์ได้กับการยับยั้งเอนไซม์ α-glucosidase โดยการใช้แบบจำลองทางคอมพิวเตอร์ ซึ่งในขณะนี้อยู่ในขั้นตอนการประมวลผล

4. อ.ดร.ปกรณ์ วินะยานุวัติคุณ. ภาควิชาชีวเคมี คณะวิทยาศาสตร์ มีส่วนช่วยเหลือและให้คำปรึกษาเกี่ยวกับการศึกษากลไกการยับยั้งเอนไซม์ α-glucosidase รวมทั้งให้ความอนุเคราะห์การใช้เครื่องมือบางชนิดในการศึกษาเกี่ยวกับเอนไซม์ และได้รับเป็นอาจารย์ที่ปรึกษาร่วมให้กับนิสิตปริญญาเอก ซึ่งมีส่วนในการผลิตผลงานให้กับโครงการที่กำลังรับทุนนี้

5. รศ.ดร.จันทร์เพ็ญ จันทร์เจ้า ภาควิชาชีววิทยา คณะวิทยาศาสตร์ มีความร่วมมือเกี่ยวกับการศึกษาความเป็นพิษต่อเซลล์ของสารที่สังเคราะห์ เพื่อเป็นข้อมูลพื้นฐานเกี่ยวกับความปลอดภัย หากจะมีการนำสารดังกล่าวไปใช้ประโยชน์ต่อไป

6. รศ.ดร.สิริชัย อดิศักดิ์วัฒนา คณะสหเวชศาสตร์ มีส่วนช่วยเหลือและให้คำปรึกษาเกี่ยวกับการทดสอบการยับยั้งเอนไซม์ α-glucosidase ในช่วงแรกที่ดำเนินโครงการ จนผู้วิจัยสามารถดำเนินการได้เองที่ภาควิชาเคมี คณะวิทยาศาสตร์

7. Professor Emmanuel A. Theodorakis แห่ง University of California at San Diego ที่ให้คำปรึกษาเกี่ยวกับปฏิกิริยาต่าง ๆ ที่คณะผู้วิจัยยังไม่มีประสบการณ์ นอกจากนี้ยังรับเป็นที่ปรึกษาให้กับนิสิตปริญญาเอก เพื่อฝึกประสบการณ์ในต่างประเทศ

3) รางวัลที่ได้รับ

รางวัลนักวิจัยรุ่นกลางดีเด่น สาขาวิทยาศาสตร์กายภาพและคณิตศาสตร์ ประจำปี 2556 คณะวิทยาศาสตร์ จุฬาลงกรณ์มหาวิทยาลัย

Bioorganic & Medicinal Chemistry Letters 22 (2012) 5215–5217

Contents lists available at SciVerse ScienceDirect

Bioorganic & Medicinal Chemistry Letters

journal homepage: www.elsevier.com/locate/bmcl

(+)-Pinoresinol is a putative hypoglycemic agent in defatted sesame (*Sesamum indicum*) seeds though inhibiting α-glucosidase

Arin Wikul [a,b], Thanakorn Damsud [a,b], Keita Kataoka [c], Preecha Phuwapraisirisan [a,*]

[a] Natural Product Research Unit, Department of Chemistry, Faculty of Science, Chulalongkorn University, Bangkok 10330, Thailand
[b] Program of Biotechnology, Faculty of Science, Chulalongkorn University, Bangkok 10330, Thailand
[c] Department of Functional Molecular Science, The Graduate University for Advanced Studies, Myodaiji, Okazaki 444-8787, Japan

ARTICLE INFO

Article history:
Received 24 April 2012
Revised 6 June 2012
Accepted 21 June 2012
Available online 3 July 2012

Keywords:
(+)-Pinoresinol
α-Glucosidase
Sesamum indicum
Maltase
Diabetes mellitus

ABSTRACT

Defatted sesame seeds have been reported for hypoglycemic effect in mice and T2DM women. An attempted to identify active components responsible for this effect was conducted using α-glucosidase-guided fractionation, resulting in the isolation of various lignans. Of compounds isolated, only (+)-pinoresinol showed inhibitory activity against rat intestinal maltase with an IC_{50} value of 34.3 μM. The kinetic study indicated that enzymatic hydrolysis of maltose is inhibited by (+)-pinoresinol through competitive and noncompetitive manners. However, a lower dissociation constant (k_i 288 M) of EI complex suggested that competitive inhibition is predominant over noncompetitive mode (k'_i1342 M).

Type 2 diabetes mellitus (T2DM) ranks a top metabolic disorder effecting people worldwide. Intensive control on blood glucose level is critical not only to halt T2DM development but also alleviated micro- and macrovascular complications.[1] Effective reduction in blood glucose level can be accomplished using antidiabetic drugs possessing α-glucosidase inhibitory effect such as acarbose and volglibose. Due to their unique mechanism of action, they can be given at any stage of T2DM, either as monotherapy or in combination with other agents.[2]

In our project on identification of natural α-glucosidase inhibitors from edible plants and synthesis of glycomimic compounds,[3] we have discovered various novel structural motifs essentially responsible for inhibiting enzyme function. In the present investigation, we are intrigued by sesame or *Sesamum indicum* seeds because of hypoglycemic effect, in addition to various benefits to health such as antioxidation[4] and antihyperlipidemic effect.[5] Hypoglycemic effect was first discovered by Takeuchi[6a] in a hot-water extract of defatted sesame seeds. Significant reduction (33%) in plasma glucose was detected within 2 h in genetically diabetic kk-A^y mice, fed with maltose solution containing 4% hot water extract. Similar results were also observed in ethanol extract of sesame seeds.[6b] Additional investigation in T2DM women proved potent hypoglycemic effect of defatted sesame seeds together with benefit linked to regulation of weight gain.[7] More interestingly, the hypoglycemic effect in the previous studies revealed no connection with serum insulin level, suggesting that α-glucosidase possibly plays a major role in suppressing blood glucose level. An attempt to identify active principles in defatted sesame seeds that inhibit enzyme function as well as inhibition mechanism is first elaborated in this Letter.

The defatted sesame seeds used in this experiment was prepared by soaking the coarsely ground seeds (2.0 Kg) in hexane at room temperature. This step was repeatedly performed until no oil was obtained. The resulting defatted seeds were divided into two equal portions (each 0.4 Kg). The first portion was boiled with water using identical method described by Takeuchi, [6a] and another was extracted with methanol, which is a common method applied in previous reports.[8] The hot water extract was first loaded onto Diaion HP-20, which was successively eluted with water and methanol. The combined fractions eluted with methanol were further chromatographed using silica gel CC eluted with 20:80 EtOAc/hexane, EtOAc and MeOH/EtOAc (10:90 and 50:50), yielding (+)-pinoresinol (**1**, 60 mg)[9] (Fig. 1) after recrystallization in hot hexane, as a single active principle. On the other hands, the methanol extract was chromatographed on silica gel CC eluted with CH_2Cl_2, MeOH-CH_2Cl_2 (10:90, 20:80, 30:70 and 40:60) to afford five major fractions. The second fraction was further purified on silica gel CC eluted with CH_2Cl_2 and 5:95 MeOH-CH_2Cl_2 to yield sesamolin (**2**, 6 mg) and sesamin (**3**, 17 mg). The third fraction was repeatedly purified on silica gel CC eluted with CH_2Cl_2 and MeOH-CH_2Cl_2

* Corresponding author.
E-mail address: preecha.p@chula.ac.th (P. Phuwapraisirisan).

0960-894X/$ - see front matter © 2012 Elsevier Ltd. All rights reserved.
http://dx.doi.org/10.1016/j.bmcl.2012.06.068

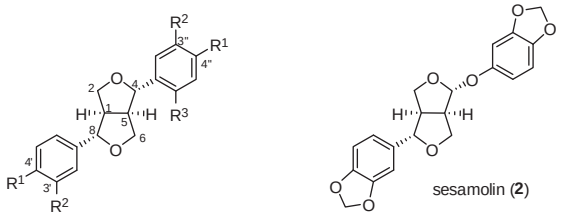

(+)-pinoresinol (**1**): R^1 = OH, R^2 = OCH_3, R^3 = H
sesamin (**3**): $R^1 + R^2$ = OCH_2O, R^3 = H
sesaminol monoglucoside (**4**): $R^1 + R^2$ = OCH_2O, R^3 = O-β-Glc

Figure 1. Structures of isolated compounds from defatted sesame seeds.

Table 1
α-Glucosidase inhibitory effect of isolated lignans (**1**–**4**)

		IC_{50} (μM)	
Lignans	Baker's yeast	Maltase[a]	Sucrase[b]
1	492 ± 2.5	34.3 ± 0.8	NI
2	200 ± 1.2	NI	NI
3	450 ± 1.9	NI	NI
4	NI	NI	NI

[a] α-Glucosidase was obtained from rat small intestine.
[b] NI, No inhibition, inhibitory effect less than 30% at 10 mg/mL.

(5:95 and 10:90) to obtained (+)-pinoresinol (**1**, 8 mg) and sesaminol monoglucoside (**4**, 52 mg).[10]

All isolated lignans, except for sesaminol monoglucoside (**4**), inhibited α-glucosidase from baker's yeast[11] with IC_{50} values in range of 200–492 μM (Table 1), indicating that lignan aglycone is a core bioactive motif, whereas increased hydrophilicity by a sugar moiety in **4** revealed no improved inhibition. Interestingly, (+)-pinoresinol (**1**) is the only lignan inhibiting rat intestinal maltase[12] with IC_{50} value of 34.3 μM. Since α-glucosidases in human brush border and rat intestine are categorized into the same group (α-glucosidase I),[13] we thus conclude that (+)-pinoresinol is possibly responsible for hypoglycemic effect found in defatted sesame seeds.

To gain insight into inhibition mechanism of (+)-pinoresinol against maltase, the kinetic study was carried out.[14] Lineweaver–Burk plots of the initial velocity versus enzyme concentrations in the presence of different concentrations of **1** gave a series of straight lines; all of which intersect to the second quadrant (Fig. 2). The analysis demonstrated that V_{max} decreased with elevated K_m in the presence of increasing concentrations of **1**. This behavior indicated that **1** inhibits maltase by two distinct ways; forming competitively enzyme-inhibitor (EI) complex and interrupting enzyme-substrate (ES) intermediate through forming enzyme-substrate-inhibitor (ESI) complex in noncompetitive manner.[15]

To elucidate binding affinities of EI and ESI complexes, a Dixon plot and secondary replot were performed, respectively.[16] The Dixon plot (Fig. 3a) of slope of lines in Lineweaver–Burk relation versus the inhibitor concentration produced EI dissociation constant (k_i) of 288 μM, whereas the secondary replot (Fig. 3b) of intercept versus inhibitor concentration generated ESI dissociation constant (k'_i) of 1342 μM. The putative binding mode of pinoresinol (Scheme 1) was rationalized that one inhibitor can bind either to active site of free maltase or to maltase-maltose intermediate. The 4.6-time greater values of k'_i suggested a weaker binding of (+)-pinoresinol to maltase-maltose intermediate and indicated that inhibition mechanism is competitive predominant over noncompetitive. Notably, (+)-pinoresinol demonstrates inhibitory effect against intestinal maltase with mixed-type inhibition identical to ferulic acid,[17] a proposed precursor of pinoresinol.

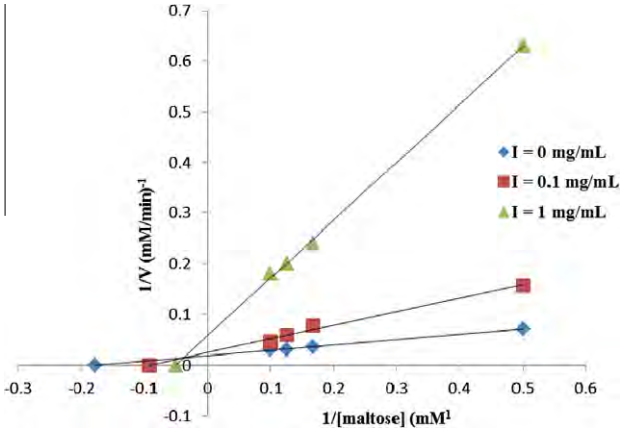

Figure 2. Lineweaver–Burk plot of (+)-pinoresinol (1).

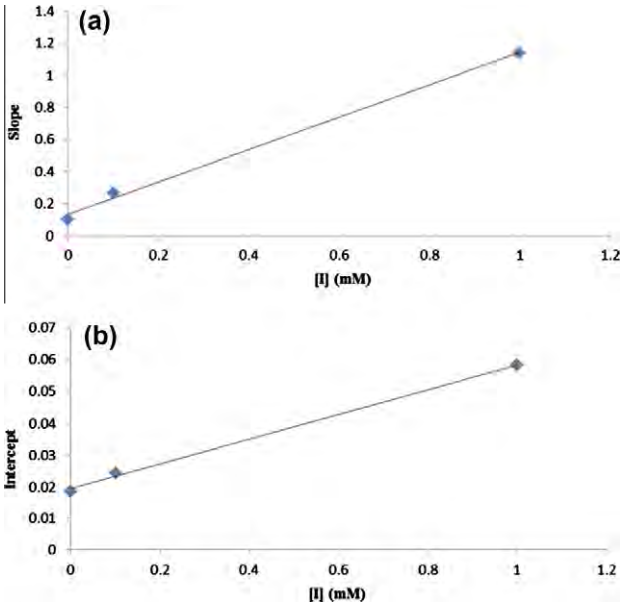

Figure 3. (a) Dixon plot of slope versus concentration of 1, [I], from a Lineweaver–Burk plot for the determination of k_i and (b) secondary plot of intercept versus [I] from a Lineweaver–Burk plot for the determination of k'_i.

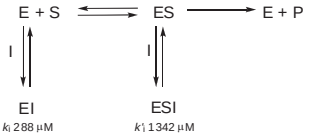

Scheme 1. Putative mechanism of enzymatic hydrolysis of maltose inhibited by (+)-pinoresinol (1, I); where E, S and P are maltase, maltose and glucose, respectively.

In summary, we have succeeded in first identifying (+)-pinoresinol as a putative hypoglycemic agent in defatted sesame seeds, through inhibiting intestinal maltase. We also demonstrated that higher yield of (+)-pinoresinol in defatted sesame seeds can be achieved by extracting with hot water. A mixed-type inhibition mechanism indicates that (+)-pinoresinol can retard enzyme function by not only direct binding to maltase but also interfering maltase-moltose intermediate. Since (+)-pinoresinol also inhibits maltase by noncompetitive manner, it would show synergistic effect with antidibetic drugs such as acarbose in suppressing blood

glucose level, therefore dramatically reducing dose of acarbose used.[18] Pinoresinol is exclusively encountered in sesame and flax seeds[19] and is metabolized in human digestive tract to enterolactone,[20] a principal lignan associated with reduced risk of particular cancers and cardiovascular diseases. Therefore, the intake of defatted sesame seeds possibly not only enhances glycemic control in DM patients but also suppresses the incidence of complications associated with DM.

Acknowledgments

This work was supported by the Thailand Research Fund (DBG5380037) and National Research University Project of CHE and Ratchadaphiseksomphot Endowmwnt Fund (FW645A) and the 90th Anniversary of Chulalongkorn University Fund. T.D. acknowledges Office of the Higher Education Commission for PhD Scholarship. K.K. (under supervision of Professor Hidehiro Sakurai) is grateful to Faculty of Science, Chulalongkorn University and The Graduate University for Advanced Studies for financial support under Student Exchange Program.

Supplementary data

Supplementary data (NMR spectra of isolated compounds) associated with this article can be found, in the online version, at http://dx.doi.org/10.1016/j.bmcl.2012.06.068.

References and notes

1. Zimmet, P.; Alberti, K. G. M. M.; Shaw, J. *Nature* **2001**, *414*, 782.
2. Gallwitz, B. *Diabetes Care* **2009**, *32*, S322.
3. (a) Phuwapraisirisan, P.; Puksasook, T.; Jong-aramruang, J.; Kokpol, U. *Bioorg. Med. Chem. Lett.* **2008**, *18*, 4956; (b) Wacharasindhu, S.; Worawalai, W.; Rungprom, W.; Phuwapraisirisan, P. *Tetrahedron Lett.* **2009**, *50*, 2189; (c) Phuwapraisirisan, P.; Puksasook, T.; Kokpol, U.; Suwanborirux, K. *Tetrahedron Lett.* **2009**, *50*, 5864; (d) Worawalai, W.; Rattanangkool, E.; Vanitcha, A.; Phuwapraisirisan, P.; Wacharasindhu, S. *Bioorg. Med. Chem. Lett.* **2012**, *22*, 1538.
4. Suja, K. P.; Jayalekshmy, A.; Arumughan, C. *J. Agric. Food Chem.* **2004**, *52*, 912.
5. Biswas, A.; Dhar, P.; Ghosh, S. *J. Food Sci.* **2010**, *75*, H274.
6. (a) Takeuchi, H.; Mooi, L. Y.; Inagaki, Y.; He, P. *Biosci. Biotechnol. Biochem.* **2001**, *65*, 2318; (b) Bhuvaneswari, P.; Krishnakumari, S. *Int. J. Pharm. Pharm. Sci.* **2012**, *4*, S527.
7. Figueiredo, A. S.; Modesto-Filho, J. *Braz. J. Pharmacogn.* **2008**, *18*, 77.
8. (a) Shyu, Y.-S.; Hwang, L. S. *Food Res. Int.* **2002**, *35*, 357; (b) Suzuki, N.; Miyase, T.; Ueno, A. *Phytochemistry* **1993**, *34*, 729; (c) Moazzami, A. A.; Andersson, R. E.; Kamal-Eldin, A. *Biosci. Biotechnol. Biochem.* **2006**, *70*, 1478; (d) Andersson, R. E.; Kamal-Eldin, A. *J. Agric. Food Chem.* **2006**, *54*, 633.
9. *(+)-Pinoresinol (1)*: yellow powder; $[\alpha]_D^{25}$ = +38.2 (*c* 0.18, CH_2Cl_2);^{1}H NMR (400 MHz, $CDCl_3$) δ 6.81–6.83 (4H, m), 6.75 (2H, m), 5.54 (2H, s, 2 (OH), 4.67 (2H, d, *J* = 4.0 Hz, H-4 and H-8), 4.24 and 3.80 (each 2H, m, H-2 and H-6), 3.90 (6H, s, 2 (OCH_3), 3.04 (2H, br s, H-3 and H-5); ^{13}C NMR (100 MHz, $CDCl_3$) δ 146.7, 145.3, 132.9, 119.0, 114.3, 108.7, 85.9, 71.7, 56.0, 54.2; ESIMS *m*/*z* 359.1 [M+H]+.
10. Sesamolin (**2**) and sesamin (**3**) was characterized by ^{1}H and ^{13}C NMR as well as comparison with authentic samples. The NMR data of sesaminol monoglucoside (**4**) was coincided well with previous report.[8b]
11. The (α-glucosidase (0.1 U/mL) and substrate (1 mM *p*-nitrophenyl-(α-D-glucopyranoside) were dissolved in 0.1 M phosphate buffer, pH 6.9. A 10 μL of test compound (1 mg/mL in DMSO) was pre-incubated with 40 μL of (α-glucosidase at 37 °C for 10 min. A 50 μL substrate solution was then added to the reaction mixture and incubated at 37 °C for 20 min, and terminated by adding 100 μL of 1 M Na_2CO_3. Enzymatic activity was quantified by measuring the absorbance at 405 nm (Bio-Rad 3550 microplate reader). The percentage inhibition was calculated by $[(A_0–A_1)/A_0] \times 100$, where A_0 is the absorbance without the sample, and A_1 is the absorbance with the sample. The IC_{50} value was determined from a plot of percentage inhibition versus sample concentration. Acarbose® was used as a standard control and the experiment was performed in triplicate.
12. The crude enzyme solution prepared from rat intestinal acetone powder was used as a source of maltase and sucrase. Rat intestinal acetone powder (1 g) was homogenized in 30 mL of 0.9%NaCl solution. After centrifugation (12,000 g × 30 min), the aliquot was subjected to assay. A 10 μL of test compound (1 mg/mL in DMSO) was pre-incubated with crude enzyme solution (as maltase, 20 μ L; as sucrase, 20 μ L, respectively) at 37 °C for 10 min. The substrate solution (maltose: 0.58 mM, 20 μ L; sucrose: 20 mM, 20 μ L, respectively) in 0.1 M phosphate buffer (pH 6.9) was then added to the reaction mixture and incubated at 37 °C for 40 min. The mixture was heated in oven at 80 °C for 15 min to quench the reaction. The concentration of glucose released from the reaction mixture was determined by the glucose oxidase method using a commercial glucose assay kit (SU-GLLQ2, Human). The percentage inhibition was calculated using the same aforementioned expression.
13. Oki, T.; Matsui, T.; Osajima, Y. *J. Agric. Food Chem.* **1999**, *47*, 550.
14. The type of inhibition was investigated by analyzing enzyme kinetic data using the above reaction. Maltase activity was maintained at 0.45 U/mg protein in the presence of (+)-pinoresinol (from 0.1–1.0 mg/mL) at various concentrations of maltase (2, 6, 10, 16, 20 mM). A series of V_{max} and K_m values were obtained from Y intercepts and calculated by slope × V_{max}, respectively.
15. Stein, R. L. *Kinetics of Enzyme Action: Essential Principles for Drug Hunters*; John Wiley & Sons: Singapore, 2011.
16. Nguyen, T. H.; Um, B. H.; Kim, S. M. *J. Food Sci.* **2011**, *76*, H208.
17. Adisakwattana, S.; Chantarasinlapin, P.; Thammarat, H.; Yibchok-Anun, S. *J. Enzyme Inhib. Med. Chem.* **2009**, *24*, 1194.
18. Wang, Y.; Ma, L.; Pang, C.; Huang, M.; Huang, Z.; Gu, L. *Bioorg. Med. Chem. Lett.* **2004**, *14*, 2947.
19. Milder, I. E. J.; Arts, I. C. W.; van de Putte, B.; Venema, D. P.; Hollman, P. C. H. *Brit. J. Nutr.* **2005**, *93*, 393.
20. Liu, Z.; Saarinen, N. M.; Thompson, L. U. *J. Nutr.* **2006**, *136*, 906.

MedChemComm

Dynamic Article Links

Cite this: *Med. Chem. Commun.*, 2012, **3**, 1466

www.rsc.org/medchemcomm

CONCISE ARTICLE

Synthesis of new *N*-substituted aminoquercitols from naturally available (+)-*proto*-quercitol and their α-glucosidase inhibitory activity†

Wisuttaya Worawalai, Sumrit Wacharasindhu and Preecha Phuwapraisirisan*

Received 2nd August 2012, Accepted 17th September 2012
DOI: 10.1039/c2md20227a

Aminocyclitols have been recognized as α-glucosidase inhibitors due to their close structural relationship with sugar. The inhibitory effect can be improved by modifying the cyclic core and *N*-substituted moiety. In the present investigation, a series of new *N*-alkyl and *N*-acyl aminoquercitols have been synthesized using a natural chiral building block, (+)-*proto*-quercitol, and evaluated for α-glucosidase inhibition. *N*-Alkyl aminoquercitols encompassing medium alkyl chains (hexyl to decyl chains) showed highly improved inhibition against rat intestinal maltase, 3–6 fold more potent than antidiabetic drug acarbose. Kinetic study of potent *N*-substituted aminoquercitols indicated that they retarded maltase function in a competitive manner.

Introduction

Aminocyclitols are cycloalkanes bearing at least one free or one substituted amino group in addition to at least three hydroxy groups on the ring atoms.[1] They are a group of natural products possessing significant relevance in medicinal chemistry as they are structural components of a variety of antibiotics and glucosidase inhibitors.[2] Due to their close structural resemblance to sugars, aminocyclitols are also expected to act as carbohydrate mimics, which can be developed as inhibitors of glucosidase-related biological processes such as viral infection, cancer development and diabetes mellitus (DM).[3] Several prominent glucosidase inhibitors derived from aminocyclitols are exemplified by acarbose, voglibose and *N*-octyl-β-valienamine (NOV)[4] (Fig. 1), some of which have been marketed for patients with metabolic disorders such as DM. These potent inhibitors were developed from their parent aminocyclitols by modifying the free amino groups with a variety of hydrophobic and hydrophilic moieties. More interestingly, an increase in hydrophobicity by *N*-alkylation dramatically enhances inhibitory activity owing to additional interaction with a hydrophobic pocket of the enzyme.[5]

Therefore, synthesis of *N*-alkylated aminocyclitols from diverse cyclitol cores with various alkyl chain lengths would be a potential approach to discover a new series of glucosidase inhibitors.[6] However, this approach has been limited, mainly by the lack of new and suitable cyclitol starters.

Quercitol is a cyclitol having five contiguous hydroxy groups on a cyclohexane ring. Although it has four chiral centers and sixteen possible stereoisomers in its family, only (+)-*proto*-, (−)-*proto*- and (−)-*vibo*-quercitols are naturally abundant.[7] Quercitols have been used as chiral building blocks for preparing aminocyclitols and related analogues;[8] however, (+)-*proto*-quercitol is likely to be a potential candidate for large scale synthesis. Due to its proper configuration, exclusive formation of single bis-acetonide is critical to obtain desired products in excellent yield with highly optical purity. This postulation was proved by our previous investigations on the synthesis of α-glucosidase inhibitors such as aminoquercitols,[9] conduritol F and its corresponding inositols,[10] including recent report on synthesis of galactosidase inhibitors NOV and NOEV precursors by Kuno.[4] With the success of our methodology in hand, we herein expand the application to the synthesis of a new series of *N*-acyl and *N*-alkyl substituted aminoquercitols derived from

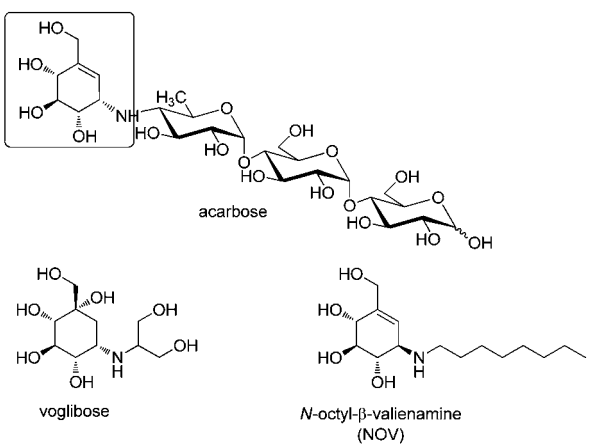

Fig. 1 Chemical structures of aminocyclitols possessing glucosidase inhibition.

Natural Products Research Unit, Department of Chemistry, Faculty of Science, Chulalongkorn University, Bangkok 10330, Thailand. E-mail: preecha.p@chula.ac.th; Fax: +66 2218 7598; Tel: +66 2218 7624

† Electronic supplementary information (ESI) available: Experimental section and NMR spectra of synthesized compounds. See DOI: 10.1039/c2md20227a

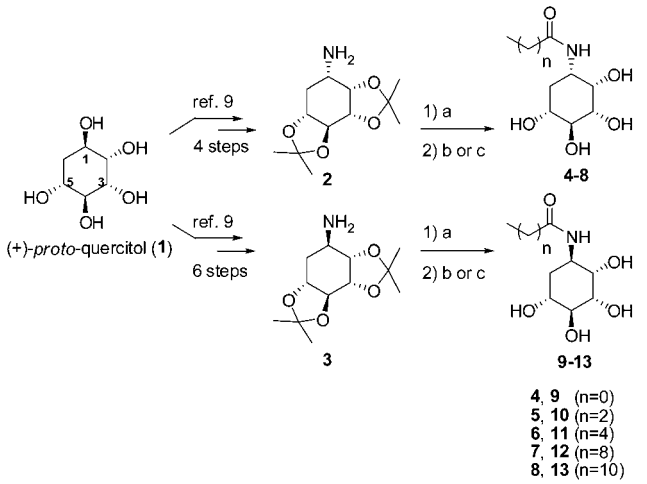

Scheme 1 Synthesis of *N*-acyl aminoquercitols. *Reagents and conditions*: (a) anhydrides, DMAP, TEA, CH_2Cl_2, 33–65%; (b) TFA, THF for **4–7**, 52–74%; (c) HCl–MeOH for **8** and **9–13**, 45% and 52%–quantitative yield.

Table 1 Reaction conditions for reductive amination

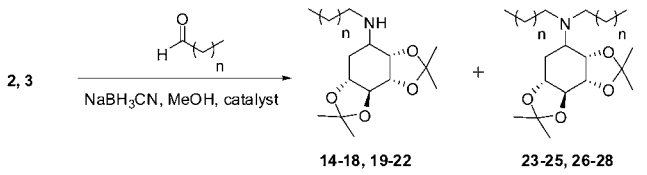

Amine	Aldehyde (*n*)	Catalyst	Yield (%) 2° amine	Yield (%) 3° amine
2	0	AcOH	—	**23** (48%)
2	0	$Ti(O^iPr)_4$	**14** (29%)	**23** (11%)
2	2	AcOH	**15** (34%)	**24** (51%)
2	4	AcOH	**16** (51%)	**25** (38%)
2	8	AcOH	**17** (60%)	—
2	10	AcOH	**18** (50%)	—
3	0	AcOH	—	**26** (45%)
3	2	AcOH	—	**27** (57%)
3	2	$Ti(O^iPr)_4$	**19** (14%)	**27** (26%)
3	4	AcOH	—	**28** (91%)
3	4	$Ti(O^iPr)_4$	**20** (54%)	**28** (16%)
3	8	AcOH	**21** (67%)	—
3	10	AcOH	**22** (32%)	—

naturally available (+)-*proto*-quercitol. The inhibitory activity of *N*-substituted products against α-glucosidases and the mechanism underlying their actions are also described.

Results and discussion

Synthesis of *N*-acyl and *N*-alkyl aminoquercitols

In previous works,[9,10] we discovered an efficient method to isolate (+)-*proto*-quercitol (**1**) from stems of *Arfeuillea arborescens* using hot water for the extraction process, giving us multiple grams of enantiomerically pure **1** in excellent yield. Moreover, the selective protection of natural (+)-*proto*-quercitol (**1**) led us to the preparation of diastereomerically pure aminocyclitols **2** and **3** in good yields.[9]

With these compounds in hand, we began to synthesize the series of *N*-acyl aminoquercitols (**4–13**) as depicted in Scheme 1. With the aim of gaining information on structure–activity relationships, both aminoquercitols **2** and **3** were reacted with the

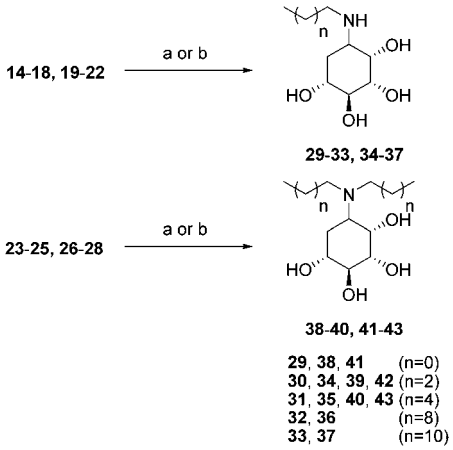

Scheme 2 Synthesis of *N*-alkyl aminoquercitols. *Reagents and conditions*: (a) HCl–MeOH, Dowex 50W-X8 (H^+) for **29–31** (59%–quant. yield), **34** and **35** (85–97%), **38–43** (46%–quant. yield); (b) HCl–MeOH, $NaHCO_3$ for **32** and **33** (75%–quant. yield), **36** and **37** (52–88%).

Table 2 α-Glucosidase inhibitory effect of *N*-substituted aminoquercitols

Compound	IC_{50} (μM) Baker's yeast	Maltase[a]	Sucrase[a]
4	270	180	NI[b]
5	NI	38	NI
6	NI	4.2	NI
7	NI	2.0	NI
8	NI	10	NI
9	150	5.3	5.3
10	1200	19	4.7
11	1700	3.8	6.1
12	NI	3.5	NI
13	NI	7.4	NI
29	NI	NI	NI
30	NI	290	NI
31	NI	2.5	NI
32	NI	2.0	410
33	NI	1.9	NI
34	1200	57	NI
35	400	0.24	NI
36	NI	0.41	NI
37	NI	1.5	NI
38	1600	21	360
39	2300	24	36
40	NI	32	120
41	1600	5.0	NI
42	1800	7.6	NI
43	NI	48	NI
Acarbose®	480	1.5	2.3

[a] α-Glucosidase was obtained from rat small intestine. [b] No inhibition (inhibitory effect 30% at 10 mg mL^{-1} for baker's yeast and at 1 mg mL^{-1} for maltase and sucrase).

Table 3 Inhibitory effect against rat intestinal maltase and kinetic parameters of **7**, **35**, **41**

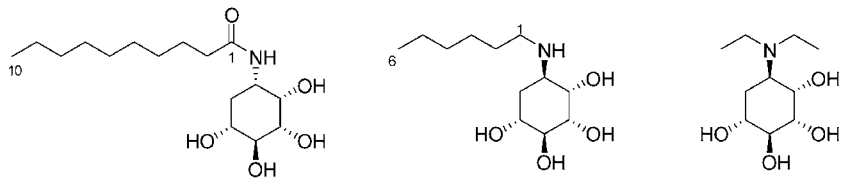

7 **35** **41**

Compound	IC_{50} (μM)	K_i (μM)	Inhibition type
7	2.0	1.5	Competitive
35	0.24	0.73	Competitive
41	5.0	3.5	Competitive
Acarbose	1.5	0.99	Competitive

corresponding anhydrides encompassing various alkyl chain lengths. This design was aimed at determining the optimal length of the aliphatic linker and also exploring the effect of the stereochemistry at C1 for glucosidase inhibition. After acylation, all products were deprotected with either TFA or HCl to afford the *N*-acyl derivatives **4–13** in fair to good yields (Scheme 1).

The search for more potent *N*-substituted aminoquercitols has prompted us to further prepare *N*-alkylated analogues **29–37**. Chemical synthesis of these compounds involves reductive amination between aminoquercitols (**2** and **3**) and various alkyl aldehydes in the presence of reducing agent ($NaBH_3CN$) and acids as catalyst. Notably, the numbers of methylenes in this series were equal to the *N*-acylated analogues (**4–13**). This is for comparative purpose. Surprisingly, treatment of **2** with acetaldehyde in the presence of acetic acid as catalyst did not provide the desired secondary amine **14** but yielded the tertiary amine **23** as the sole product in 48% yield. The dialkylation of amines is commonly encountered due to the occurrence of a second reductive amination mediated by AcOH.[11] To circumvent this problem, reductive amination of **2** with acetaldehyde was carried out in the presence of mild Lewis acid such as $Ti(O^iPr)_4$, therefore producing the desired monoalkylated product **14** together with dialkylated product **23** in a ratio of 3 : 1. Even though the selectivity of this transformation is not impressive, it offers compound diversity, which possibly provides additional information about the structural requirement for glucosidase inhibitory activity. Thus, similar chemistry was applied for the synthesis of monoalkylated analogues and dialkylated analogues from the corresponding amines **2** and **3**. Reductive amination of **2** and **3** with various aldehydes in the presence of $NaBH_3CN$ and catalysts such as either acetic acid or titanium isopropoxide afforded protected monoalkylated (**14–22**) and dialkylated aminoquercitols **23–28** (Table 1). Finally, cleavage of the two acetonide protecting groups in **14–28** under acidic conditions generated the target *N*-alkylated analogues **29–43** in good yields (Scheme 2).

α-Glucosidase inhibitory activity

All target compounds were evaluated for α-glucosidase inhibitory activity using enzymes from two different sources; baker's yeast (type I) and rat intestine (type II), and the results are illustrated in Table 2. Generally, *N*-acyl and *N*-alkyl aminoquercitols displayed weak (IC_{50} 150–2300 μM) to no inhibition against α-glucosidase from baker's yeast. The inhibitory activity of *N*-acyl aminoquercitols (**4–8** and **9–13**) tends to decrease with the extension of chain length, which was supported by the similar results of *N*,*N*-dialkyl aminoquercitols (**38–40** and **41–43**). We supposed that the greater hydrophobicity from the alkyl chain caused a reduction in inhibitory effect. Of all synthesized compounds, **9** showed the highest inhibition with an IC_{50} value of 150 μM, which was three-fold more active than acarbose.

As for type II α-glucosidases, *N*-substituted aminoquercitols inhibited maltase more selectively than sucrase, varying from low (IC_{50} 180–290 μM) to high (IC_{50} 0.24–0.41 μM) potency. Generally, the inhibitory effect increased according to chain length; the maximum inhibitions were observed where *n* was 4 and 8 (Fig. 2). From the *N*-acyl and *N*-alkyl series, **7** ($n = 8$) and **35** ($n = 4$) were the most potent maltase inhibitors with IC_{50} values of 2.0 and 0.24 μM, respectively. However, the inhibitory effect dropped significantly (2–5 times) when *n* reached 10. With a given *n*, the *N*-alkyl series were likely to be more potent than their corresponding *N*-acyl analogues. In addition to the aforementioned factors, a relationship between configuration of C-1

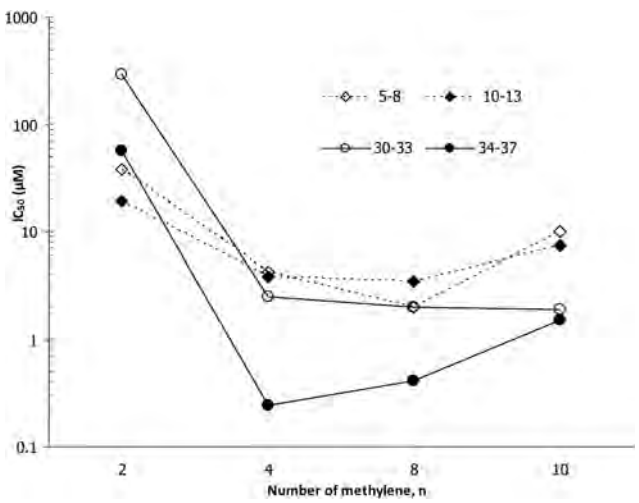

Fig. 2 Inhibition trends of selected *N*-acyl (**5–8** and **10–13**) and *N*-alkyl (**30–33** and **34–37**) aminoquercitols against rat intestinal maltase.

and inhibitory effect was also observed. *N*-Alkyl aminoquercitols **34–36**, all prepared from **3**, apparently exerted stronger inhibition than their corresponding epimers **30–32**, generated from **2**. However, the configuration of C-1 had no impact on the inhibitory activity of the *N*-acyl series. In our experiment, we discovered that **37** was equipotent to acarbose whereas **35** and **36** revealed higher inhibition.

In contrast to the *N*-acyl and *N*-alkyl series, the inhibitory activity of *N*,*N*-dialkyl aminoquercitols **41–43** (IC_{50} 5.0–48 μM) depended largely on the steric hindrance of the alkyl groups whereas the inhibitory effect of the corresponding diastereomers **38–40** (IC_{50} 21–32 μM) was comparable. Compared to the most potent *N*-alkyl aminoquercitol **35**, the corresponding *N*,*N*-dialkyl analogue **43** revealed approximately 200-fold weaker inhibition. A similar trend was also observed in tertiary *N*-alkylated arabinoiminofuranoses, whose inhibitions were approximately 10^2-times less potent than their corresponding secondary amines.[12]

Kinetic study and possible mechanism underlying the maltase inhibition of *N*-substituted aminoquercitols

Apparently, *N*-substituted aminoquercitols selectively inhibited type II, particularly maltase, rather than type I α-glucosidase.

Since rat intestinal maltase used in this experiment and that of humans are categorized into the same group,[13,14] an insight into how *N*-substituted aminoquercitols inhibit maltase function is required for further development in therapeutic application.

We therefore investigated the inhibitory mechanism of **7**, **35** and **41**, all of which are the most potent inhibitors and representatives of *N*-acyl, *N*-alkyl and *N*,*N*-dialkyl aminoquercitols, respectively. Lineweaver–Burk plots of the initial velocity *versus* substrate concentrations in the presence of different concentrations of the inhibitors gave a series of straight lines, all of which intersected at the *Y*-axis (Fig. 3). The analysis revealed the increase in K_m values while V_{max} remained constant. This behavior indicated that **7**, **35** and **41** inhibited maltase in a competitive manner (Table 3) through forming enzyme–inhibitor (EI) complexes, the same as observed in the antidiabetic acarbose.

To envisage the binding affinity between the *N*-substituted aminoquercitols and maltase, secondary replots were performed. The slopes of the lines in the Lineweaver–Burk relation *versus* inhibitor concentration in the secondary replot produced EI dissociation constants (K_i) of 1.5, 0.73 and 3.5 μM for **7**, **35** and **41** (Table 3), respectively. The higher K_i values of **7** and **41** over that of acarbose indicated their weaker EI binding. In contrast,

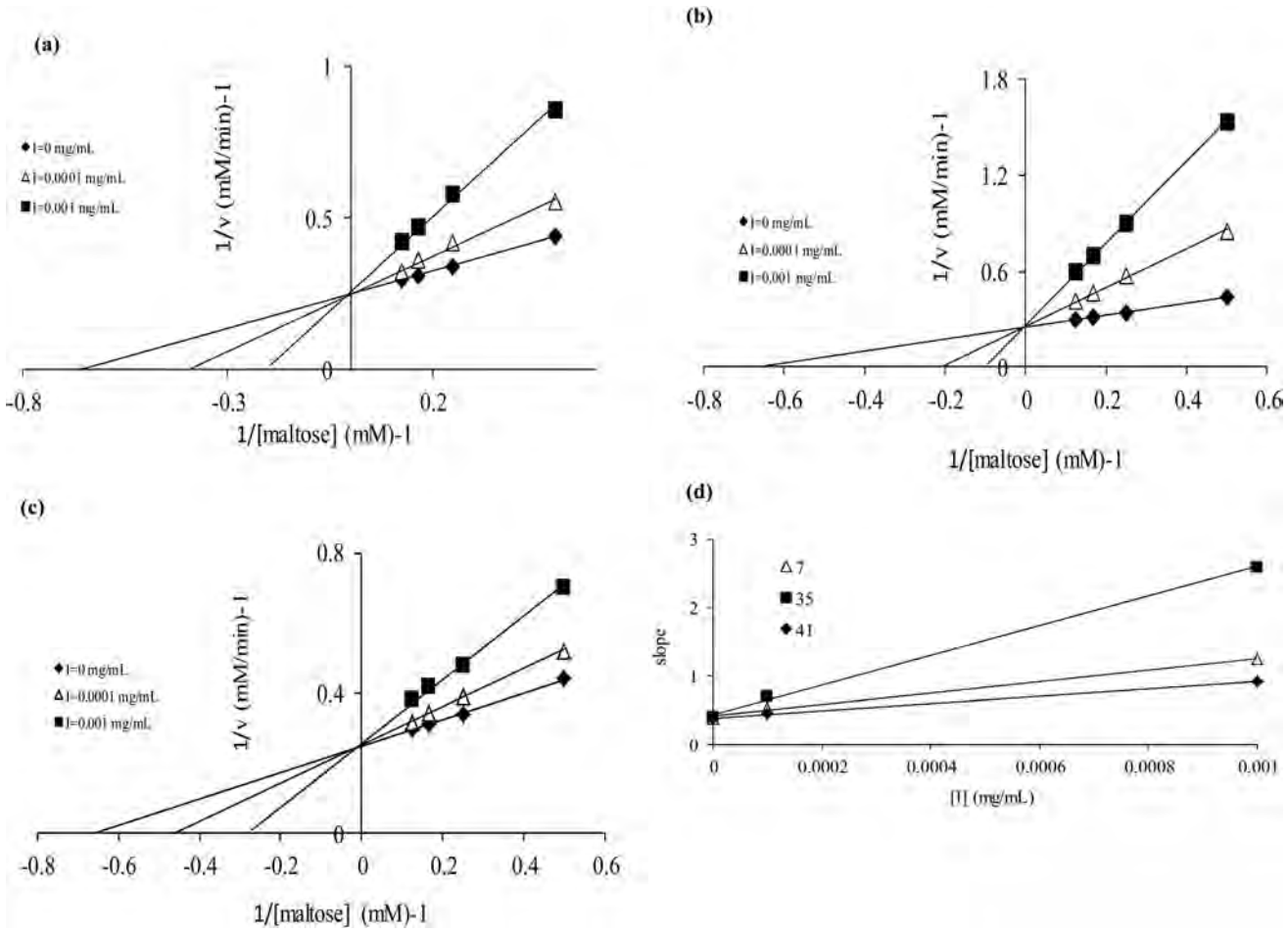

Fig. 3 Lineweaver–Burk plots for inhibitory activity against rat intestinal maltase. (a) *N*-acyl aminoquercitol **7**, (b) *N*-alkyl aminoquercitol **35**, (c) *N*,*N*-dialkyl aminoquercitol **41** and (d) secondary replots of slope *vs.* [I] from a primary Lineweaver–Burk plot for the determination of K_i.

N-alkyl aminoquercitol **35** having a lower K_i obviously bound to maltase more tightly than acarbose. Due to its potent inhibitory effect and strong binding with maltase, **35** could serve as a new candidate for antidiabetic drug development through mainly retarding maltase function.

Conclusion

In summary, we first synthesized a series of *N*-acyl and *N*-alkyl aminoquercitols having different chain lengths from (+)-*proto*-quercitol. Evaluation of their α-glucosidase inhibition revealed that they selectively inhibited rat intestinal maltase (type II glucosidase) rather than yeast glucosidase (type I glucosidase). Of the compounds examined, *N*-alkyl aminoquercitols (**35** and **36**) having medium chains (C_6 and C_{10}) showed highly potent inhibition at sub-micromolar level (IC_{50} 0.24 and 0.41 μM), whereas antidiabetic drug acarbose was 3–6 times less active (IC_{50} 1.5 μM). Although *N*-alkylated aminocyclitols have been expected to exert an improved inhibitory effect, against α-glucosidase, than their unsubstituted precursors, there are few reports[6,12] demonstrating the optimal chain length required for potent activity. Our findings also provide the importance of the hydrophobicity[5] of medium alkyl chains ($\leq C_{10}$) in exerting inhibitory activity, possibly due to being a more preferred structure to fit into the binding site of enzyme.

In addition, the kinetic studies on the mechanism of α-glucosidase inhibition by particularly active compounds (**7**, **35** and **41**) showed competitive inhibition. More importantly, the most potent *N*-alkyl aminoquercitol **35** revealed stronger binding to maltase than acarbose. The synthesis of the new *N*-substituted aminoquercitols reported herein could provide necessary data on the structural requirement for designing other potent α-glucosidase inhibitors.

Acknowledgements

Financial support from the Thailand Research Fund (DBG5380037) is greatly acknowledged. WW is grateful to the Royal Golden Jubilee Ph.D. Program (PHD/0025/2553) for scholarship.

Notes and references

1 A. Delgado, *Eur. J. Org. Chem.*, 2008, 3893–3906.
2 T. Mahmud, *Nat. Prod. Rep.*, 2003, **20**, 137–166.
3 L. Díaz and A. Delgado, *Curr. Med. Chem.*, 2010, **17**, 2393–2418.
4 S. Kuno, A. Takahashi and S. Ogawa, *Bioorg. Med. Chem. Lett.*, 2011, **21**, 7189–7192 and references cited therein.
5 E. Borges de Melo, A. da Silveira Gomes and I. Carvalho, *Tetrahedron*, 2006, **62**, 10277–10302.
6 X. Chen, Y. Fan, Y. Zheng and Y. Shen, *Chem. Rev.*, 2003, **103**, 1955–1977; R. Łysek, C. Schütz, S. Favre, A. C. O'Sullivan, C. Pillonel, T. Krülle, P. M. J. Jung, I. Clotet-Codina, J. A. Esté and P. Vogel, *Bioorg. Med. Chem.*, 2006, **14**, 6255–6282.
7 A. Maras, H. Secen, Y. Sütbeyaz and M. Balci, *J. Org. Chem.*, 1998, **63**, 2039–2041 and references cited therein.
8 S. Ogawa, H. Aoyama and Y. Tezuka, *J. Carbohydr. Chem.*, 2001, **20**, 703–717; S. Ogawa, M. Asada, Y. Ooki, M. Mori, M. Itoh and T. Korenaga, *Bioorg. Med. Chem.*, 2005, **13**, 4306–4314; S. Ogawa and M. Kanto, *J. Nat. Prod.*, 2007, **70**, 493–497; S. Ogawa and M. Kanto, *Curr. Trends Med. Chem.*, 2008, **5**, 1–13.
9 S. Wacharasindhu, W. Worawalai, W. Rungprom and P. Phuwapraisirisan, *Tetrahedron Lett.*, 2009, **50**, 2189–2192.
10 W. Worawalai, E. Rattanangkool, A. Vanitcha, P. Phuwapraisirisan and S. Wacharasindhu, *Bioorg. Med. Chem. Lett.*, 2012, **22**, 1538–1540.
11 A. F. Abdel-Majid, K. G. Carson, B. D. Harris, C. A. Maryanoff and R. Shath, *J. Org. Chem.*, 1996, **61**, 3849–3862.
12 Y. Natori, T. Imahori, K. Murakami, Y. Yoshimura, S. Nakagawa, A. Kato, I. Adachi and H. Takahata, *Bioorg. Med. Chem. Lett.*, 2011, **21**, 738–741.
13 T. Oki, T. Matsui and Y. Osajima, *J. Agric. Food Chem.*, 1999, **47**, 550–553.
14 A. Kimura, J.-H. Lee, I.-S. Lee, H.-S. Lee, K.-H. Park, S. Chiba and D. Kim, *Carbohydr. Res.*, 2004, **339**, 1035–1040.

Accepted Manuscript

Quercitylcinnamates, a new series of antidiabetic bioconjugates possessing α-glucosidase inhibition and antioxidant

Eakkaphon Rattanangkool, Preecha Kittikhunnatham, Thanakorn Damsud, Sumrit Wacharasindhu, Preecha Phuwapraisirisan

PII: S0223-5234(13)00365-6

DOI: 10.1016/j.ejmech.2013.05.047

Reference: EJMECH 6225

To appear in: *European Journal of Medicinal Chemistry*

Received Date: 12 March 2013

Revised Date: 15 May 2013

Accepted Date: 30 May 2013

Please cite this article as: E. Rattanangkool, P. Kittikhunnatham, T. Damsud, S. Wacharasindhu, P. Phuwapraisirisan, Quercitylcinnamates, a new series of antidiabetic bioconjugates possessing α-glucosidase inhibition and antioxidant, *European Journal of Medicinal Chemistry* (2013), doi: 10.1016/j.ejmech.2013.05.047.

Quercityl cinnamates, a new series of antidiabetic bioconjugates possessing α-glucosidase inhibition and antioxidation activity

Highlights

- Novel fifteen quercityl cinnamates (**1a**-**8a**) were synthesized.
- Quercityl caffeate (**6a**) was glucosidase inhibitor more potent than its parent **6**.
- **6a** retained both glucosidase inhibition and antioxidation.
- Mechanism underlying the inhibition of **6a** was mixed-type inhibition.

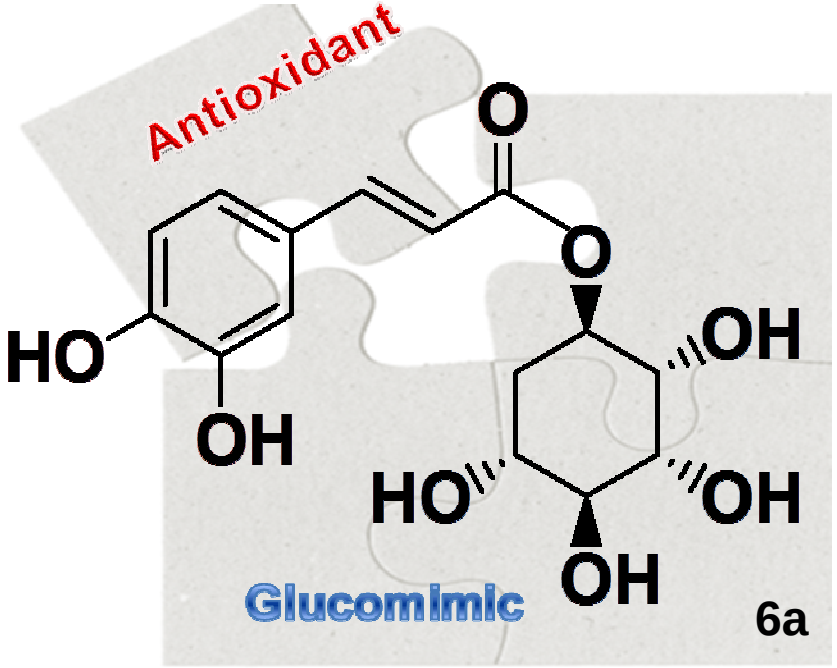
Antioxidant
HO
OH
O
O
OH
HO
OH
OH
Glucomimic
6a

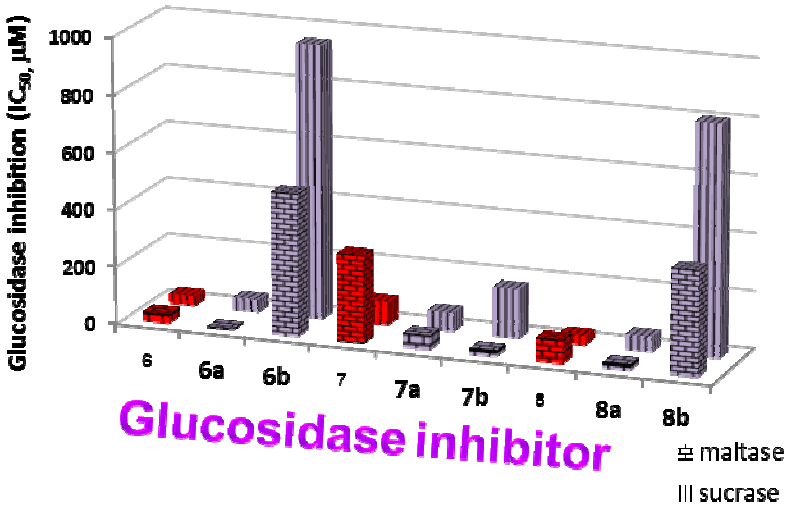
Glucosidase inhibition (IC50, μM)
1000
800
600
400
200
0
6
6a
6b
7
7a
7b
8
8a
8b
Glucosidase inhibitor
maltase
sucrase

Quercitylcinnamates, a new series of antidiabetic bioconjugates possessing α-glucosidase inhibition and antioxidant

Eakkaphon Rattanangkool[a], Preecha Kittikhunnatham[a], Thanakorn Damsud[a,b], Sumrit Wacharasindhu[a], Preecha Phuwapraisirisan[a,*]

[a]*Natural Products Research Unit, Department of Chemistry, Faculty of Science, Chulalongkorn University, Bangkok 10330, Thailand*

[b]*Program of Biotechnology, Faculty of Science, Chulalongkorn University, Bangkok 10330, Thailand*

ABSTRACT

Antidiabetic agents possessing dual functions, α-glucosidase inhibition and antioxidant, have been accepted to be more useful than currently used antidiabetic drugs because they not only suppress hyperglycemia but also prevent risk of complications. Herein, we design antidiabetic bioconjugates comprising of (+)-*proto*-quercitol as a glucomimic and cinnamic analogues as antioxidant moieties. Fifteen quercitylcinnamates were synthesized by direct coupling through ester bond in the presence of DCC and DMAP. Particular quercityl esters **6a**, **7a** and **8a** selectively inhibited rat intestinal maltase and sucrose 4-6 times more potently than their parents **6**, **7** and **8**. Of synthesized bioconjugates, **6a** was the most potent inhibitor against maltase and sucrose with IC_{50} values of 5.31 and 43.65 μM, respectively. Of interest, its inhibitory potency toward maltase was 6 times greater than its parent, caffeic acid (**6**), while its radical scavenging (SC_{50} 0.11 mM) was comparable to that of commercial antioxidant BHA. Subsequent investigation on mechanism underlying inhibitory effect of **6a** indicated that it blocked maltase and sucrose functions by mixed inhibition through competitive and noncompetitive manners.

Keywords: Diabetes mellitus; Glucosidase; Caffeic acid; Bioconjugate; Quercitol

*Corresponding author. Tel.: 662-2187624; fax: 662-2187598.

E-mail address: preecha.p@chula.ac.th (P Phuwapraisirisan).

1. Introduction

Type 2 diabetes is characterized by chronic hyperglycemia and the development of microangiopatic complications such as retinopathy, nephropathy and neuropathy. Aggressive control of blood glucose level is preliminary and effective therapy for diabetic patients and reduces risk of complications [1]. Current evidences suggest that excess plasma glucose drives overproduction of superoxide radicals and other reactive oxygen species, which impair the cells via oxidative stress and account for the pathogenesis of all diabetic complications [2-4]. Therefore, antidiabetic drugs possessing antihyperglycemic effect and radical scarvenging would be potential for diabetic therapy.

In the course of our research on new α-glucosidase inhibitors, we recently reported the synthesis and inhibitory effects of aminoquercitols [5], conduritol F [6] and inositol analogues from naturally available (+)-*proto*-quercitol (Fig. 1). Although (+)-*proto*-quercitol has five contiguous hydroxy groups on cyclohexane ring, exclusive formation of single bis-acetonide is critical to obtain the desired product without stereogenic congeners, in few steps. In fact, (+)-*proto*-quercitol itself does not show inhibitory activity against α-glucosidase possibly due to its water soluble property that enhances ready absorption by small intestine. However, structural modification of (+)-*proto*-quercitol by installing a series of alkyl and acyl motifs [7] or eliminating hydroxyl group [6] led to new generations of quercitol-based analogues with enhanced activity. With the success of this approach in hand, we expand our application by connecting quercitol core with other bioactive residues.

Inspired by chlorogenic acid (Fig. 2A), a well-recognized natural product having both antioxidant [8] and antidiabeticactivities [9], we plan to introduce caffeic acid and other related cinnamic analogues onto quercitol core (Fig. 2B). In the current study, we synthesized fifteen quercitylcinnamates by coupling of (+)-*proto*-quercitol (**10**) and its epimer (**11**) (Scheme 1) with a series of cinnamic analogues (**1**-**8**, Scheme 2). A new series of quercitol-based bioconjugates with improved inhibition were obtained. Structure-activity relationship of the synthesized compounds and mechanism underlying α-glucosidase inhibitory effect of the most potent inhibitor are herein discussed.

2. Results and discussion

2.1. Compound design and synthesis

Crucial to the successful synthesis of all the conjugates described in this work is the selective coupling reaction of cinamic derivatives with the desired hydroxy group on naturally available (+)-*ptoto*-quercitol (**9**) (Scheme 1). Bis-acetonides **10** and **11**were prepared from **9**, which was isolated from the stems of *Arfeuillea arborescens* using the procedure described elsewhere [6,7]. Briefly, (+)-*proto*-quercitol was obtained in 0.3% (w/w) yield as white solid after recrystallization by MeOH. Protection of two diols with

dimethoxypropane gave the target alcohol **10**. In order to investigate the effect of C-1′ configuration on inhibitory effect, the epimer **11** was also synthesized from **10** through oxidation using acetic anhydride/DMSO followed by $LiAlH_4$ reduction, yielding the desired product in 42% yield.

With the chiral coupling partners **10** and **11** in hands**,** the quercitylcinamates **1a**-**8b** were prepared as depicted in Scheme 2. For the esters **1a**-**8a** and their epimers **1b**-**8b**, the synthetic route was straight forward involving the direct coupling reaction between alcohol **10** or **11** with the corresponding cinnamic derivatives **1**-**5** in the presence of *N*,*N*′-dicyclohexylcarbodiimide (DCC) and 4-dimethylaminopyridine (DMAP). Removal of acetonide group underwent smoothly upon treatment of amberlyst-15 in methanol to give esters **1a**-**5a** in 56 - 73 % yields (Scheme 2).

On the other hand, esterification of caffeic acid (**6**), ferulic acid (**7**) and isoferulic acid (**8**) required additional protection step because free phenolic group(s) of those compounds could interfere with the coupling reaction. The silylation of **6**-**8** with *tert*-butyldimethylsilyl chloride (TBDMSCl) not only prevented phenolic group(s) possibly being esterified but also improved solubility of the acids **6**-**8** in CH_2Cl_2, thus facilitating esterification reaction. The syntheses of quercitylcinnamates **6a**-**8b** were accomplished by ester bond formation of protected cinnamic derivatives with the chiral alcohol **10** or **11** followed by double deprotection of silyl and acetonide groups with TBAF and amberlyst-15, respectively. Esters **6a**-**8b** were then isolated in 42-49 % yield as white solid (Scheme 2).

2.2 α-Glucose inhibitory activity and DPPH radical scarvenging

All newly synthesized bioconjugates **1a**-**8b** were subjected to evaluate for their α-glucosidase inhibitory effect and antioxidation (Table 1). The commercial antidiabetic drug acarbose was used as the reference and the parent cinnamic analogues (**1**-**8**) were also validated for comparative purpose. For α-glucosidase inhibitory activity, all bioconjugates showed no inhibition against yeast α-glucosidase (type I α-glucosidase) but some of which inhibited maltase and sucrose, type II α-glucosidases from rat intestine. The bioconjugates **6a**-**8b**, whose structures encompassing caffeoyl, ferulyl and isoferulyl moieties, displayed inhibitory effects in range of 5.31-954.08 μM, whereas **1a**-**5a** were not active. Notably, their cinnamoyl cores in **6a**-**8b** different from those of **1a**-**5b** in having at least one phenolic group, suggesting that this moiety possibly involved in exerting the observed inhibition. It was likely that the more phenolic group in cinnamoyl moiety, the more potent inhibition observed. This result was similar to previous report of intestinal α-glucosidase inhibition of hydroxylated cinnamic derivatives **6**, **7** and **8** [10]. This trend was obviously found in **6a**, whose inhibition against maltase was more potent than those of **7a** (10 times) and **8a** (4 times); while **8a** showed only two times more potent than **7a**.

Further inspection of two quercityl residues (**10** and **11**), installed in the active bioconjugates, on inhibitory effect revealed significant difference in inhibition. Bioconjugates **6a**, **7a** and **8a**, all of which

generated from natural quercitol **10**, showed inhibitory effect 3-94 times more potent than their corresponding C-1′epimers (**6b**, **7b** and **8b**). The difference in inhibitory potency among epimeric analogues was strikingly observed in **6a**, whose inhibition against maltase and sucrose were 93 and 22 times more potent than **6b**. Compared to their corresponding cinnamic precursors (**6**, **7** and **8**), **6a**, **7a** and **8a** showed more improved inhibitory effects (4-6 times), whereas their epimeric analogues (**6b**, **7b** and **8b**) displayed reverse trend (Fig. 3). The observed results suggested that *R* configuration of C-1′ in quercityl moiety was also associated with exerting inhibitory effect, in addition to the presence of more phenolic groups in cinnamoyl residues. The pronounced inhibitions raised by *R* configuration of C-1′ were also supported by a similar trend observed in our previous report of *N*-alkyl aminoquercitols [7]. Of bioconjugates synthesized, **6a** showed most potent inhibition against both maltase and sucrase with IC_{50} values of 5.31 and 43.65 μM, respectively.

As for antioxidation of synthesized bioconjugates, **6a** showed radical scavenging activity toward DPPH with SC_{50} value of 0.11 mM, which was comparable to that of standard antioxidant BHA (SC_{50} 0.10 mM).

2.3 Mechanism underlying inhibitory effect of quercitylcaffeate against rat intestinal α-glucosidase

Since **6a** was the most potent inhibitor in hand, we therefore further study mechanism underlying this inhibitory effect. The Lineweaver-Burk plot of initial velocity versus maltose concentrations in the presence of different concentrations of **6a** gave a series of straight lines, all of which intersected within the second quadrant (Fig 4). The analysis showed that V_{max} decreased with increasing K_m in the presence of increasing concentrations of **6a**. This behavior [11] indicated that **6a** inhibits maltase by two different pathways; competitively forming enzyme-inhibitor (EI) complex and interrupting enzyme-substrate (ES) intermediate by forming enzyme-substrate-inhibitor (ESI) complex in noncompetitive manner. To gain insightful the pathway in which **6a** preferentially proceeded, binding affinities of EI and ESI complexes were determined. Secondary plot of slope against concentration of **6a** (Fig. 5) showed EI dissociation constant (K_i) of 23.8 μM while ESI dissociation constant ($K\hat{}_i$) of 64.5 μM was also deduced from secondary plot of intercept against concentration of **6a** (Fig. 6). A lower dissociation constant of K_i pointed out stronger binding between enzyme and **6a** and suggested preferred competitive over noncompetitive manners. In addition, inhibitory mechanism of **6a** toward sucrase was also determined using similar methodology. Apparently, **6a** also inhibited sucrase through mixed-inhibition (Fig. 7); in which competitive mode (K_i 22.4 μM, Fig. 8) was preferred over noncompetitive manner ($K\acute{}_i$ 47.5 μM, Fig. 9).

3. Conclusions

In summary, we first synthesized fifteen bioconjugates (**1a**-**8b**) comprising two key moieties derived from (+)-*proto*-quercitol as glucomimic and cinnamic analogues as antioxidants. This synthetic design was implemented in the hope that the bioconjugates would provide dual activities, α-glucosidase inhibitory effect and antioxidant activity. Bioconjugates **6a**-**8b**, whose structures encompassing hydroxylated cinnamic analogues, displayed inhibition against rat maltase and sucrase in range of 5.31-954.08 μM. Notably, **6a** and **6b**, the bioconjugates having more phenolic groups in cinnamic core, were likely to provide pronounced inhibition. In addition, the *R* configuration of C-1′ in natural quercitol (**10**) also enhanced inhibitory effects over those of bioconjugates having unnatural quercitol (**11**). Therefore, coupling of quercityl and cinnamic moieties proved to enhance α-glucosidase inhibition. Prominent examples included **6a**, whose inhibitory effect against maltase was 6 times better than those of original caffeic acid (**6**). Of bioconjugates synthesized, **6a** was the most potent α-glucosidase inhibitor, in addition to its radical scarvenging activity equipotent to standard antioxidant, BHA. In addition, mechanism underlying the inhibitory effect of **6a** against maltase and sucrase were proved to be mixed-type inhibition. This suggests proposed guideline for the application of **6a** as single antidiabetic agent or combination with other currently used drugs such as acarbose.

4. Experimental section

4.1 Chemistry

4.1.1 General procedure

All moisture-sensitive reactions were carried out under a nitrogen atmosphere. All solvents were distilled prior to use. HRESI-MS spectra were obtained from a micrOTOF Bruker mass spectrometer. ^{1}H and ^{13}C NMR spectra were recorded ($CDCl_3$ and CD_3OD as solvents) at 400 and 100 MHz, respectively, on a Varian Mercury^{+} 400 NMR spectrometer. Chemical shifts were reported in ppm downfield from TMS or solvent residue. Thin layer chromatography (TLC) was performed on pre-coated Merck silica gel 60 F_{254} plates (0.25 mm thick layer) and visualized under 254 nm UV followed by dipping in $KMnO_4$ solution. Column chromatography was conducted using Merck silica gel 60 (70-230 mesh) or Sephadex LH-20.

*4.1.2 Isolation of (+)-proto-quercitol (**9**) from the stems of Arfeuillea arborescens*

Our improved isolation of (+)-*proto*-quercitol (**9**) was applied [6, 7]. Generally, ground stems (1.0-1.2 kg) of *A. arborescens* were boiled with water (2 ×4 L) for 2 h. The combined decoction was filtered, concentrated to a half and partitioned twice with equal volume of CH_2Cl_2 to remove lipophilic matters. The

aqueous layer was diluted with water in a ratio of 2:1 and applied onto a Diaion HP20 column (1 kg) equilibrated with water. The column was excessively eluted with water (11 L), and the aqueous elutes were lyophilized to yield white powder. More purified (+)-*proto*-quercitol (**9**, 0.3%w/w) was obtained upon crystallization using hot MeOH.

*4.1.3 Synthesis of bis-acetonides **10** and **11***

Bis-acetonides were synthesized using our previous methods [5-7], yielding **10** (79%) and **11** (42%). The ^{1}H and ^{13}C NMR data were matched well the reports.

4.1.4 General protection of phenolic groups

To a solution of **6**, **7** or **8** (1 eq, 2.57 mmol), imidazole (10 eq: 1 OH group) and *tert*-butyldimethylsilyl chloride (TBDMSCl) (10 eq: 1 OH group) in *N*,*N*-dimethylformamide (DMF, 15 mL) in a 50 mL round button flask. The mixture was stirred at room temperature for 1 h under N_2 gas. The reaction mixture was washed with water (3 × 20 mL) and the organic portion was extracted with ethyl acetate (EtOAc) (3×20 mL). The organic layer was washed with saturated aqueous NaCl, followed by dried over Na_2SO_4. After filtration and removal of the solvent under reduced pressure, the crude product was purified by silica gel column to afford **6Si**, **7Si** and **8Si** in 74, 82 and 79 %yield, respectively.

*3,4-Di-O-tert-butyldimetylsilylcaffeic acid (**6Si**)*; white powder; ^{1}H NMR ($CDCl_3$, 400 MHz) δ 7.46 (d, *J* = 15.8 Hz, 1H), 6.83 (d, *J* = 8.8 Hz, 1H), 6.81 (s, 1H), 6.62 (d, *J* = 8.8 Hz, 1H), 6.03 (d, *J* = 15.8 Hz, 1H), 0.77 (d, *J* = 4.5 Hz, 18H), 0.00 (d, *J* = 3.2 Hz, 12H)

*4-O-tert-Butyldimetylsilylferulic acid (**7Si**)*; white powder; ^{1}H NMR ($CDCl_3$, 400 MHz) δ 7.65 (d, *J* = 15.9 Hz, 1H), 6.98 (d, *J* = 8.6 Hz, 1H), 6.95 (s, 1H), 6.79 (d, *J* = 8.6 Hz, 1H), 6.24 (d, *J* = 15.9 Hz, 1H), 3.78 (s, 3H), 0.93 (s, 9H), 0.11 (s, 6H)

*4-O-tert-Butyldimetylsilylisoferulic acid (**8Si**)*; white powder; ^{1}H NMR ($CDCl_3$, 400 MHz) δ .66 (d, *J* = 15.7 Hz, 1H), 6.97 (d, *J* = 8.8 Hz, 1H), 6.95 (s, 1H), 6.79 (d, *J* = 8.8 Hz, 1H), 6.20 (d, *J* = 15.7 Hz, 1H), 3.78 (s, 3H), 0.93 (s, 9H), 0.11 (s, 6H)

4.1.5. General coupling reaction between bis-acetonides and cinnamic or silylated cinnamate derivatives

To a solution of **1, 2, 3, 4** and **5** (2.5 eq) in CH_2Cl_2 (5 mL) were added dicyclohexylcarbodimine (DCC, 2.7 eq) and 4-dimethylaminopyridine (DMAP, catalytic amount). The reaction mixture was stirred at 0 °C for 30 min. **10** or **11** (1 eq) in CH_2Cl_2 was added dropwise at room temperature under N_2 gas. The product was filtrated and solvent was removed under reduced pressure. The crude product was subsequently purified by silica gel column to afford bis-acetonides **1R**-**5R**.

To a solution of **6Si**, **7Si** and **8Si** (11 eq) in CH_2Cl_2 (10 mL) were added DCC (12 eq) and DMAP (catalytic amount). The reaction mixture was stirred at 0 °C for 30 min. **10** or **11** (1 eq) in CH_2Cl_2 was added

dropwise at room temperature under N_2 gas. The bis-acetonides **6R**-**8S** were obtained after purification using silica gel column.

1R; 75 %yield of pale yellow oil; ^{1}H NMR ($CDCl_3$, 400 MHz) δ 7.94 (d, *J* = 16.1 Hz, 1H), 7.43 (d, *J* = 7.6 Hz, 1H), 7.30 (t, *J* = 7.5 Hz, 1H), 6.90 (t, *J* = 7.5 Hz, 1H), 6.85 (d, *J* = 7.6 Hz, 1H), 6.46 (d, *J* = 16.1 Hz, 1H), 5.47 (m, 1H), 4.30 (m, 1H), 4.23 (m, 1H), 3.83 (s, 3H), 3.66 (m, 1H), 3.54 (m, 1H), 2.16 (m, 1H), 2.04 (m, 1H), 1.46 (s, 3H), 1.38 (s, 6H), 1.30 (s, 3H).

1S; 72 %yield of colorless wax; ^{1}H NMR ($CDCl_3$, 400 MHz) δ 7.98 (d, *J* = 16.1 Hz, 1H), 7.45 (d, *J* = 7.5 Hz, 1H), 7.29 (t, *J* = 7.6 Hz, 1H), 7.19 (s, 1H), 6.90 (t, *J* = 7.6 Hz, 1H), 6.85 (d, *J* = 7.5 Hz, 1H), 6.55 (d, *J* = 16.1 Hz, 1H), 5.30 (m, 1H), 4.37 (m, 1H), 4.23 (m, 1H), 3.84 (m, 4H), 3.44 (m, 1H), 2.36 (m, 1H), 1.93 (m, 2H), 1.47 (s, 3H), 1.40 (s, 3H), 1.38 (s, 3H), 1.30 (s, 3H).

2R; 79 %yield of colorless wax; ^{1}H NMR ($CDCl_3$, 400 MHz) δ 7.61 (d, *J* = 16.0 Hz, 1H), 7.24 (t, *J* = 7.9 Hz, 1H), 7.06 (d, *J* = 7.5 Hz, 1H), 6.98 (s, 1H), 6.89 (d, *J* = 7.5 Hz, 1H), 6.36 (d, *J* = 16.0 Hz, 1H), 5.45 (m, 1H), 4.30 (m, 1H), 4.23 (m, 1H), 3.77 (s, 3H), 3.66 (m, 1H), 3.56 (m, 1H), 2.15 m, 1H), 2.06 (m, 1H), 1.46 (s, 3H), 1.39 (s, 6H), 1.20 (s, 3H).

2S; 76 %yield of colorless oil; ^{1}H NMR ($CDCl_3$, 400 MHz) δ 7.65 (d, *J* = 16.0 Hz, 1H), 7.24 (t, *J* = 7.9 Hz, 1H), 7.07 (d, *J* = 7.5 Hz, 1H), 6.99 (s, 1H), 6.89 (d, *J* = 7.5 Hz, 1H), 6.45 (d, *J* = 16.0 Hz, 1H), 5.31 (m, 1H), 4.38 (m, 1H), 4.24 (m, 1H), 3.83 (m, 1H), 3.77 (s, 3H), 3.45 (m, 1H), 2.38 (m, 1H), 1.92 (m, 1H), 1.47 (s, 3H), 1.40 (s, 3H), 1.38 (s, 3H), 1.30 (s, 3H).

3R; 83 %yield of colorless viscous oil; ^{1}H NMR ($CDCl_3$, 400 MHz) δ 7.60 (d, *J* = 16.0 Hz, 1H), 7.42 (d, *J* = 8.7 Hz, 2H), 7.19 (s, 4H), 6.84 (d, *J* = 8.7 Hz, 2H), 6.24 (d, *J* = 16.0 Hz, 1H), 5.45 (m, 1H), 4.30 (m, 1H), 4.23 (m, 1H), 3.78 (s, 3H), 3.65 (m, 1H), 3.54 (m, 1H), 2.15 (m, 1H), 2.05 (m, 1H), 1.47 (s, 3H), 1.39 (s, 6H), 1.31 (s, 3H).

3S; 72 %yield of colorless wax;^{1}H NMR ($CDCl_3$, 400 MHz) δ 7.69 (d, *J* = 15.9 Hz, 1H), 7.49 (d, *J* = 8.4 Hz, 2H), 6.90 (d, *J* = 8.4 Hz, 2H), 6.38 (d, *J* = 15.9 Hz, 1H), 5.35 (m, 1H), 4.43 (m, 1H), 4.30 (m, 1H), 3.87 (m, 1H), 3.83 (s, 3H), 3.50 (m, 1H), 2.43 (m, 1H), 1.98 (m, 1H), 1.53 (s, 3H), 1.46 (s, 3H), 1.44 (s, 3H), 1.36 (s, 3H).

4R; 78 %yield of colorless oil; ^{1}H NMR ($CDCl_3$, 400 MHz) δ 7.64 (d, *J* = 15.9 Hz, 1H), 7.11 (d, *J* = 8.3 Hz, 1H), 7.05 (s, 1H), 6.87 (d, *J* = 8.3 Hz, 1H), 6.30 (d, *J* = 15.9 Hz, 1H), 5.52 (m, 1H), 4.36 (m, 1H), 4.30 (m, 1H), 3.92 (s, 9H), 3.72 (m, 1H), 3.61 (m, 1H), 2.21 (m, 1H), 2.12 (m, 1H), 1.53 (s, 3H), 1.45 (s, 6H), 1.37 (s, 3H).

4S; 81 %yield pale yellow oil; ^{1}H NMR ($CDCl_3$, 400 MHz) δ 7.62 (d, *J* = 15.8 Hz, 1H), 7.05 (d, *J* = 8.2 Hz, 1H), 7.01 (s, 1H), 6.81 (d, *J* = 8.2 Hz, 1H), 6.33 (d, *J* = 15.8 Hz, 1H), 5.31 (s, 1H), 4.38 (m, 1H), 4.24 (m, 1H), 3.83 (m, 7H), 3.45 (m, 2H), 2.37 (m, 1H), 1.90 (m, 1H), 1.48 (s, 3H), 1.40 (s, 3H), 1.38 (s, 3H), 1.30 (s, 3H).

5R; 85 %yield of colorless viscous oil; ^{1}H NMR ($CDCl_3$, 400 MHz) δ 7.56 (d, *J* = 15.9 Hz, 1H), 6.69 (s, 2H), 6.28 (d, *J* = 15.9 Hz, 1H), 5.45 (m, 1H), 4.31 (m, 1H), 4.24 (m, 1H), 3.82 (s, 9H), 3.66 (m, 1H), 3.54 (m, 1H), 2.21 (m, 1H), 2.12 (m, 1H), 1.47 (s, 3H), 1.39 (s, 6H), 1.31 (s, 3H).

6R; 67 %yield of colorless oil; ^{1}H NMR ($CDCl_3$, 400 MHz) δ 7.37 (d, *J* = 15.9 Hz, 1H), 6.80 (d, *J* = 8.7 Hz, 1H), 6.78 (s, 1H), 6.61 (d, *J* = 8.7 Hz, 1H), 6.00 (d, *J* = 15.9 Hz, 1H), 5.30 (m, 1H), 4.17 (m, 1H), 4.09 (m, 1H), 3.51 (m, 1H), 3.40 (m, 1H), 2.00 (m, 1H), 1.91 (m, 1H), 1.32 (s, 3H), 1.24 (s, 6H), 1.16 (s, 3H), 0.78 (s, 18H), 0.00 (s, 12H).

6S; 77 %yield of pale yellow oil; ^{1}H NMR ($CDCl_3$, 400 MHz) δ 7.56 (d, *J* = 15.9 Hz, 1H), 6.96 (d, *J* = 8.7 Hz, 1H), 6.94 (s, 1H), 6.75 (d, *J* = 8.7 Hz, 1H), 6.25 (d, *J* = 15.9 Hz, 1H), 5.29 (brs, 1H), 4.44 (m, 1H), 4.23 (m, 1H), 3.30 (m, 1H), 3.43 (m, 1H), 2.36 (m, 1H), 1.92 (s, 1H), 1.48 (s, 3H), 1.40 (s, 3H), 1.38 (s, 3H), 1.30 (s, 3H), 0.91 (s, 18H), 0.14 (s, 12H).

7R; 68 %yield of colorless oil ^{1}H NMR ($CDCl_3$, 400 MHz) δ 7.47 (d, *J* = 15.8 Hz, 1H), 6.86 (d, *J* = 7.2 Hz, 2H), 6.85 (s, 1H), 6.80 (d, *J* = 7.2 Hz, 1H), 6.12 (d, *J* = 15.8 Hz, 1H), 5.35 (m, 1H), 4.20 (m, 1H), 4.12 (m, 1H), 3.67 (s, 3H), 3.55 (m, 1H), 3.44 (m, 1H), 2.05 (m, 1H), 1.94 (m, 1H), 1.36 (s, 3H), 1.28 (s, 6H), 1.18 (m, 1H), 0.82 (s, 9H), 0.00 (s, 6H).

7S; 69 %yield of colorless oil; ^{1}H NMR ($CDCl_3$, 400 MHz) δ 7.50 (d, *J* = 15.9 Hz, 1H), 6.86 (d, *J* = 7.6 Hz, 1H), 6.83 (s, 1H), 6.67 (d, *J* = 7.6 Hz, 1H), 6.21 (d, *J* = 15.9 Hz, 1H), 5.20 (m, 1H), 4.27 (m, 1H), 4.13 (m, 1H), 3.72 (m, 1H), 3.67 (s, 3H), 3.34 (m, 1H), 2.27 (m, 1H), 1.81 (m, 1H), 1.37 (s, 3H), 1.30 (s, 3H), 1.27 (s, 3H), 1.20 (s, 3H), 0.82 (s, 9H), 0.00 (s, 6H).

8R; 81 %yield of pale yellow oil; ^{1}H NMR ($CDCl_3$, 400 MHz) δ 7.44 (d, *J* = 15.9 Hz, 1H), 6.94 (d, *J* = 8.2 Hz, 1H), 6.89 (s, 1H), 6.68 (d, *J* = 8.2 Hz, 1H), 6.08 (d, *J* = 15.9 Hz, 1H), 5.35 (m, 1H), 4.21 (m, 1H), 4.14 (m, 1H), 3.68 (s, 3H), 3.56 (m, 1H), 3.45 (m, 1H), 2.10 – 1.91 (m, 2H), 1.37 (s, 3H), 1.29 (s, 6H), 1.21 (s, 3H), 0.83 (s, 9H), 0.00 (s, 6H).

8S; 79 %yield of colorless oil; ^{1}H NMR ($CDCl_3$, 400 MHz) δ 7.48 (d, *J* = 15.9 Hz, 1H), 6.95 (dd, *J* = 8.3, 2.0 Hz, 1H), 6.90 (d, *J* = 2.0 Hz, 1H), 6.68 (d, *J* = 8.3 Hz, 1H), 6.18 (d, *J* = 15.9 Hz, 1H), 5.20 (m, 1H), 4.28 (m, 1H), 4.13 (m, 1H), 3.72 (m, 1H), 3.68 (s, 3H), 3.34 (m, 1H), 2.27 (m, 1H), 1.83 (m, 1H), 1.38 (s, 3H), 1.30 (s, 3H), 1.28 (s, 3H), 1.21 (s, 3H), 0.84 (s, 9H), 0.00 (s, 6H).

4.1.6 General deprotection of silyl groups and bis-acetonides

Deprotection of **6R**-**8S**, which contained both silyl groups and bis-acetonides, was performed as follow.To a solution of **6R** (1 eq) in tethahydrofuran (THF) was added TBAF/THF 1.0 M (2 eq: 1 OTBDMS). The mixture was stirred at room temperature for 3 h. The reaction mixture was washed with water (10 mL) and the organic layer was extracted with ethyl acetate (EtOAc) (3 × 15 mL) followed by being dried over Na_2SO_4. After filtration and removal of the solvent under reduced pressure, the crude product was dissolved in methanol (MeOH) and amberlyst-15 (0.5 g: 0.1 mmol) was added into the solution. The reaction mixture was stirred at room temperature for 5 h. After filtration and removal of the solvent under reduced pressure the crude product was purified by Sephadex LH-20 eluted with MeOH to afford **6a**. Compounds **6S**-**8S** were treated using aforementioned procedures to yield corresponding products **6b**-**8b**, respectively.

For deprotection of **1R**-**5R**, which contained only bis-acetonides, general procedures were conducted as follow. To a methanolic solution of **1R** was added amberlyst-15 (0.5 g: 0.1 mmol), and the reaction mixture was stirred at room temperature for 5 h. After filtration and removal of the solvent under reduced pressure, the crude product was purified by Sephadex LH-20 eluted with MeOH to afford **1a**. Compounds **1S**-**5R** were transformed, using the above procedures, to corresponding products **1b**-**5a**, respectively.

*1ℜ-Quercityl-2-methoxycinnamate (**1a**)* 75 %yield of colorless oil; ^{1}H NMR (CD_3OD, 400 MHz) δ 7.97 (d, *J* = 16.2 Hz, 1H, H-3), 7.56 (d, *J* = 6.8 Hz, 1H, Ar-H), 7.38 (t, *J* = 7.4 Hz, 1H, Ar-H), 7.03 (d, *J* = 6.8 Hz, 1H, Ar-H), 6.96 (t, *J* = 7.4 Hz, 1H, Ar-H), 6.53 (d, *J* = 16.2 Hz, 1H, H-2), 5.10 (m, 1H, H-1′), 3.94 (brs, 1H), 3.89 (s, 3H, OMe), 3.84 – 3.60 (m, 3H), 1.99 (m, 2H, H-6′); ^{13}C NMR (CD_3OD, 100 MHz) δ 168.0, 160.0, 142.1, 133.2, 130.0, 124.2, 121.9, 118.8, 112.5, 76.0, 73.5, 72.9, 71.5, 70.8, 56.2, 32.9; HRESIMS *m/z* 347.1100 $[M + Na]^+$ (calcd for $[C_{16}H_{16}NaO_7]^+$ 347.1107).

*1ℑ-Quercityl-2-methoxycinnamate (**1b**)* 79 %yield of colorless oil; ^{1}H NMR (CD_3OD, 400 MHz) δ 7.92 (d, *J* = 16.2 Hz, 1H, H-3), 7.49 (dd, *J* = 8.0, 4.0 Hz, 1H, Ar-H), 7.28 (t, *J* = 7.5 Hz, 1H, Ar-H), 6.95 (d, *J* = 8.0 Hz, 1H, Ar-H), 6.88 (t, *J* = 7.5 Hz, 1H, Ar-H), 6.52 (d, *J* = 16.2 Hz, 1H, H-2), 4.85 (m, 1H, H-1′), 4.02 (s, 1H), 3.81 (s, 3H, OMe), 3.52 – 3.24 (m, 3H), 1.93 (m, 2H, H-6′); ^{13}C NMR (CD_3OD, 100 MHz) δ 168.6, 160.0, 142.0, 133.1, 130.0, 124.3, 121.9, 119.2, 112.5, 76.1, 73.6, 72.2, 71.5, 70.8, 56.1, 32.9; HRESIMS *m/z* 347.1108 $[M + Na]^+$ (calcd for $[C_{16}H_{20}NaO_7]^+$ 347.1107).

*1ℜ-Quercityl-3-methoxycinnamate (**2a**)* 85 %yield of colorless oil; ^{1}H NMR (CD_3OD, 400 MHz) δ 7.65 (d, *J* = 16.0 Hz, 1H, H-3), 7.32 (t, *J* = 7.8 Hz, 1H, Ar-H), 7.18 (d, *J* = 7.8 Hz, 1H, Ar-H), 7.15 (s, 1H, H-5), 6.98 (d, *J* = 7.8 Hz, 1H, Ar-H), 6.52 (d, *J* = 16.0 Hz, 1H, H-2), 5.11 (brs, 1H, H-1′), 3.93 (brs, 1H), 3.82 (s, 3H, OMe), 3.76 – 3.55 (m, 3H), 1.99 (m, 2H, H-6′); ^{13}C NMR (CD_3OD, 100 MHz) δ 167.4, 161.6, 146.7, 137.0, 131.1, 121.9, 118.9, 117.6, 114.1, 75.9, 73.4, 73.0, 71.5, 70.8, 55.9, 32.9; HRESIMS *m/z* 347.1110 $[M + Na]^+$ (calcd for $[C_{16}H_{16}NaO_7]^+$ 347.1107).

*1ℑ-Quercityl-3-methoxycinnamate (**2b**)* 73 %yield of colorless oil; ^{1}H NMR (CD_3OD, 400 MHz) δ 7.72 (d, *J* = 16.0 Hz, 1H, H-3), 7.31 (t, *J* = 7.8 Hz, 1H, Ar-H), 7.18 (d, *J* = 8.2 Hz, 1H, Ar-H), 7.15 (s, 1H, H-5), 6.97 (dd, *J* = 8.2, 1.6 Hz, 1H, H-9), 6.54 (d, *J* = 16.0 Hz, 1H, H-2), 4.85 (m, 1H, H-1′), 4.11 (s, 1H), 3.82 (s, 3H, OMe), 3.64 – 3.33 (m, 3H), 2.01 (m, 2H, H-6′); ^{13}C NMR (CD_3OD, 100 MHz) δ 167.8, 161.6, 146.6, 137.2, 131.1, 121.8, 119.2, 117.4, 114.1, 76.1, 73.6, 72.2, 71.6, 70.8, 55.8, 32.9; HRESIMS *m/z* 347.1107 $[M + Na]^+$ (calcd for $[C_{16}H_{20}NaO_7]^+$ 347.1107).

*1ℜ-Quercityl-4-methoxycinnamate (**3a**)* 78 %yield of white solid; ^{1}H NMR (CD_3OD, 400 MHz) δ 7.64 (d, *J* = 15.9 Hz, 1H, H-3), 7.56 (d, *J* = 8.6 Hz, 2H, H-5 and H-9), 6.95 (d, *J* = 8.6 Hz, 2H, H-6 and H-8), 6.37 (d, *J* = 15.9 Hz, 1H, H-2), 5.11 (m, 1H, H-1′), 3.96 – 3.59 (m, 4H), 3.83 (s, 3H, OMe), 1.99 (m, 2H, H-6′); ^{13}C NMR (CD_3OD, 100 MHz) δ 167.8, 163.3, 146.6, 131.1, 131.1, 128.2, 115.9, 115.5, 115.5, 76.0, 73.5, 72.8, 71.5, 70.8, 55.9, 33.0; HRESIMS *m/z* 347.1104 $[M + Na]^+$ (calcd for $[C_{16}H_{20}NaO_7]^+$ 347.1107).

*1′S-Quercityl-4-methoxycinnamate (**3b**)* 78 %yield of colorless oil; ^{1}H NMR (CD_3OD, 400 MHz) δ 7.61 (d, *J* = 15.9 Hz, 1H, H-3), 7.47 (d, *J* = 8.5 Hz, 2H, H-5 and H-9), 6.86 (d, *J* = 8.5 Hz, 2H, H-6 and H-8), 6.31 (d, *J* = 15.9 Hz, 1H, H-2), 4.85 (m, 1H, H-1′), 4.01 (s, 1H), 3.74 (s, 3H, OMe), 3.56 – 3.31 (m, 3H), 1.98-1.83 (m, 2H, H-6′); ^{13}C NMR (CD_3OD, 100 MHz) δ 168.3, 163.3, 146.5, 131.0, 131.0, 128.4, 116.2, 115.5, 115.5, 76.1, 73.6, 72.3, 71.4, 70.8, 55.9, 32.9; HRESIMS *m/z* 347.1103 $[M + Na]^+$ (calcd for $[C_{16}H_{20}NaO_7]^+$ 347.1107).

*1′R-Quercityl-3,4-dimethoxycinnamate (**4a**)* 85 %yield of colorless oil; ^{1}H NMR (CD_3OD, 400 MHz) δ 7.62 (d, *J* = 15.9 Hz, 1H, H-3), 7.22 (s, 1H, H-5), 7.17 (d, *J* = 8.2 Hz, 1H, Ar-H), 6.97 (d, *J* = 8.2 Hz, 1H, Ar-H), 6.40 (d, *J* = 15.9 Hz, 1H, H-2), 5.11 (m, 1H, H-1′), 3.97 – 3.56 (m, 4H), 3.86 (s, 6H, 2×OMe), 2.00 (m, 2H, H-6′); ^{13}C NMR (CD_3OD, 100 MHz) δ 167.8, 153.0, 150.8, 146.9, 128.7, 124.2, 116.3, 112.7, 111.9, 76.0, 73.5, 72.9, 71.5, 70.8, 56.8, 56.5, 33.0; HRESIMS *m/z* 377.1203 $[M + Na]^+$ (calcd for $[C_{17}H_{22}NaO_8]^+$ 377.1212).

*1′S-Quercityl-3,4-dimethoxycinnamate (**4b**)* 79 %yield of colorless oil; ^{1}H NMR (CD_3OD, 400 MHz) δ 7.60 (d, *J* = 15.9 Hz, 1H, H-3), 7.12 (s, 1H, H-5), 7.09 (d, *J* = 8.2 Hz, 1H, Ar-H), 6.88 (d, *J* = 8.2 Hz, 1H, Ar-H), 6.33 (d, *J* = 15.9 Hz, 1H, H-2), 4.82 (m, 1H, H-1′), 4.01 (brs, 1H), 3.77 (s, 6H, 2×OMe), 3.52-3.25 (m, 3H), 2.05-1.85 (m, 2H, H-6′); ^{13}C NMR (CD_3OD, 100 MHz) δ 168.2, 152.9, 150.8, 146.7, 128.9, 124.0, 116.5, 112.7, 111.6, 76.1, 73.6, 72.3, 71.4, 70.8, 56.5, 56.5, 33.0; HRESIMS *m/z* 377.1209 $[M + Na]^+$ (calcd for $[C_{17}H_{22}NaO_8]^+$ 377.1212).

*1′R-Quercityl-3,4,5-trimethoxycinnamate (**5a**)* 83 %yield of colorless oil; ^{1}H NMR (CD_3OD, 400 MHz) δ 7.62 (d, *J* = 15.9 Hz, 1H, H-3), 6.93(s, 1H, Ar-H), 6.91(s, 1H, Ar-H), 6.48 (d, *J* = 15.9 Hz, 1H, H-2), 5.12 (m, 1H, H-1′), 4.05–3.55 (m, 4H), 3.86 (s, 9H, 3×OMe), 2.00 (m, 2H, H-6′); ^{13}C NMR (CD_3OD, 100 MHz) δ 167.5, 154.9, 146.8, 146.4, 131.5, 118.1, 118.0, 106.9, 106.8, 76.0, 73.5, 73.0, 71.5, 70.8, 61.2, 56.8, 56.8, 33.0; HRESIMS *m/z* 407.1310 $[M + Na]^+$ (calcd for $[C_{18}H_{24}NaO_9]^+$, 407.1318).

*1′R-Quercitylcaffeate (**6a**)* 84 %yield of yellow oil; ^{1}H NMR (CD_3OD, 400 MHz) δ 7.45 (d, *J* = 15.9 Hz, 1H, H-3), 6.95 (d, *J* = 1.6 Hz, 1H, H-5), 6.86 (dd, *J* = 8.2, 1.6 Hz, 1H, H-9), 6.69 (d, *J* = 8.2 Hz, 1H, H-8), 6.16 (d, *J* = 15.9 Hz, 1H, H-2), 5.00 (m, 1H, H-1′), 3.83 (brs, 1H), 3.68 – 3.45 (m, 3H), 1.89 (m, 2H, H-6′); ^{13}C NMR (CD_3OD, 100 MHz) δ 168.0, 149.7, 147.4, 146.9, 127.7, 123.1, 116.6, 115.3, 114.9, 76.0, 73.5, 72.8, 71.6, 70.8, 32.9; HRESIMS *m/z* 325.0930 $[M - H]^-$ (calcd for $[C_{15}H_{17}O_8]^-$ 325.0923).

*1′S-Quercitylcaffeate (**6b**)* 84 %yield of yellow oil; ^{1}H NMR (CD_3OD, 400 MHz) δ 7.51 (d, *J* = 15.9 Hz, 1H, H-3), 6.95 (d, *J* = 1.8 Hz, 1H, H-5), 6.88 (dd, *J* = 8.1, 1.8 Hz, 1H, H-9), 6.68 (d, *J* = 8.1 Hz, 1H, H-8), 6.20 (d, *J* = 15.9 Hz, 1H, H-2), 4.81 (m. 1H, H-1′), 4.00 (brs, 1H), 3.54–3.25 (m, 3H), 1.99-1.78 (m, 2H, H-6′); ^{13}C NMR (CD_3OD, 100 MHz) δ168.5, 148.7, 147.3, 146.9, 127.8, 123.0, 116.5, 115.2, 115.2, 76.1, 73.6, 72.3, 71.3, 70.8, 32.9; HRESIMS *m/z* 349.0899 $[M + Na]^+$ (calcd for $[C_{15}H_{18}NaO_8]^+$ 349.0899).

*1′R-Quercitylferurate (**7a**)* 79 %yield of yellow less oil; ^{1}H NMR (CD_3OD, 400 MHz) δ 7.51 (d, *J* = 15.9 Hz, 1H, H-3), 7.11 (d, *J* = 1.6 Hz, 1H, H-5), 6.99 (dd, *J* = 8.2, 1.6 Hz, 1H, H-9), 6.72 (d, *J* = 8.2 Hz, 1H, H-8), 6.27 (d, *J* = 15.9 Hz, 1H, H-2), 5.01 (m, 1H, H-1′), 3.85–3.45 (m, 4H), 3.86 (s, 3H, OMe), 1.85 (m, 2H, H-6′); ^{13}C NMR (CD_3OD, 100 MHz) δ 168.0, 150.8, 149.4, 147.3, 127.6, 124.3, 116.5, 115.3, 111.8, 76.0, 73.4, 72.8, 71.5, 70.8, 56.5, 33.0; HRESIMS *m/z* 363.1057 $[M + Na]^+$ (calcd for $[C_{16}H_{20}NaO_8]^+$ 363.1056).

*1′S-Quercitylferurate (**7b**)* 79 %yield of colorless oil; ^{1}H NMR (CD_3OD, 400 MHz) δ 7.58 (d, *J* = 15.9 Hz, 1H, H-3), 7.09 (s, 1H, H-5), 6.99 (d, *J* = 8.2 Hz, 1H, Ar-H), 6.72 (d, *J* = 8.2 Hz, 1H, Ar-H), 6.29 (d, *J* = 15.9 Hz, 1H, H-2), 4.73 (m, 1H, H-1′), 4.01 (brs, 1H), 3.79 (s, 3H, OMe), 3.52 – 3.23 (m, 3H), 1.99-1.84 (m, 2H, H-6′); ^{13}C NMR (CD_3OD, 100 MHz) δ 168.5, 150.7, 149.4, 147.2, 127.8, 124.1, 116.6, 115.6, 111.9, 76.1, 73.6, 72.4, 71.3, 70.9, 56.5, 32.9; HRESIMS *m/z* 363.1057 $[M + Na]^+$ (calcd for $[C_{16}H_{20}NaO_8]^+$ 363.1056).

*1′R-Quercitylisoferulate (**8a**)* 76 %yield of yellow oil; ^{1}H NMR (CD_3OD, 400 MHz) δ 7.56 (d, *J* = 15.9 Hz, 1H, H-3), 7.08 (s, 1H, H-5), 7.07 (d, *J* = 8.2 Hz, 1H, Ar-H), 6.95 (d, *J* = 8.2 Hz, 1H, Ar-H), 6.30 (d, *J* = 15.9 Hz, 1H, H-2), 5.10 (m, 1H, H-1′), 3.92 (s, 1H), 3.89 (s, 3H, OMe), 3.77 – 3.58 (m, 3H), 1.99 (m, 2H, H-6′); ^{13}C NMR (CD_3OD, 100 MHz) δ 167.8, 151.7, 148.0, 147.0, 128.8, 123.0, 115.9, 114.8, 112.6, 76.0, 73.4, 72.8, 71.5, 70.8, 56.4, 32.9; HRESIMS *m/z* 363.1054 $[M + Na]^+$ (calcd for $[C_{16}H_{20}NaO_8]^+$ 363.1056).

*1′S-Quercitylisoferulate (**8b**)* 64 %yield of yellow oil; ^{1}H NMR (CD_3OD, 400 MHz) δ 7.54 (d, *J* = 15.9 Hz, 1H, H-3), 6.99 (s, 1H, H-5), 6.97 (d, *J* = 8.2 Hz, 1H, Ar-H), 6.85 (d, *J* =8.2 Hz, 1H, Ar-H), 6.25 (d, *J* = 15.9 Hz, 1H, H-2), 4.73 (m, 1H, H-1′), 4.00 (brs, 1H), 3.79 (s, 3H, OMe), 3.48 (t, *J* = 9.3 Hz, 1H), 3.41 – 3.32 (m, 1H), 3.26 (m, 1H), 1.92 (m, 2H, H-6′); ^{13}C NMR (CD_3OD, 100 MHz) δ 168.3, 151.6, 148.1, 146.9, 129.0, 122.8, 116.2, 114.8, 112.6, 76.1, 73.6, 72.3, 71.4, 70.9, 56.5, 32.9; HRESIMS *m/z* 363.1056 $[M + Na]^+$ (calcd for $[C_{16}H_{20}NaO_8]^+$ 363.1056).

4.2 α-Glucosidase inhibitory activity

Inhibitory activity of test compound against α-glucosidase from baker's yeast was assessed based on *p*-nitrophenoxide colorimetric method [12]. Briefly, A 10 μL of test compound (1 mg/mL in DMSO) was pre-incubated with 40 μL of α-glucosidase (0.1 U/mL in 0.1 M phosphate buffer, pH 6.9) at 37 °C for 10 min. The mixture was added with 50 μL substrate solution (1 mM *p*-nitrophenyl-α-D-glucopyranoside, PNPG) and incubated for additional 20 min. The resulting mixture was quenched by adding 100 μL of 1 M Na_2CO_3. *p*-Nitrophenoxide ion liberated from the enzymatic reaction was monitored at 405 nm by Bio-Rad 3550 microplate reader. The percentage inhibition was calculated by $[(A_0–A_1)/A_0] \times 100$, where A_1 and A_0 are the absorbance with and without the sample, respectively. The IC_{50} value was deduced from a plot of percentage inhibition versus sample concentration and acarbose was used as a positive control.

The inhibitory activity of the test compounds against α-glucosidases from rat intestine (as maltase and sucrase) was validated on the basis of glucose oxidase colorimetric method [13]. Maltase and sucrase was obtained from rat intestinal acetone powder (Sigma, St**.** Louis). Generally, the powder (1 g) was homogenized with 0.9% NaCl solution (30 mL). The aliquot containing both maltase and sucrase was obtained upon centrifugation (12,000 g) for 30 min. The test compound (1 mg/mL, 10 μL) was pre-incubated with crude enzyme solution (as maltase, 20 μL; as sucrase, 20 μL, respectively) at 37 °C for 10 min. The substrate solution (maltose: 0.58 mM, 20 μL; sucrose: 20 mM, 20 μL, respectively) in 0.1 M phosphate buffer (pH 6.9) was therefore added to the reaction mixture and incubated at 37 °C for additional 40 min. The mixture was heated in oven at 80 °C for 15 min to quench the reaction. The concentration of glucose released from the reaction mixture was determined by the glucose oxidase method using a commercial glucose assay kit (SU-GLLQ2, Human). The percentage inhibition was calculated using the above expression.

4.3 Kinetic study of α-glucosidase inhibition

The type of inhibition was investigated by analyzing enzyme kinetic data using aformentioned reactions. Maltase and sucrase activities were maintained at 0.45 and 0.09 U/mg protein, respectively, in the presence of inhibitor (from 0-20.4 μM) at various concentrations of maltose ranging from 1.0-20.0 mM. A series of V_{max} and K_m values were obtained from Y intercepts and calculated by slope × V_{max}, respectively.

4.4 DPPH radical scavenging

Radical scavenging activity was validated using DPPH colorimetric method [14]. Briefly, a sample solution (10 μL at concentrations of 0.1, 1.0 and 10.0 mg/mL) was added to 0.1 mM methanolic solution of DPPH (150 μL). The mixture was kept dark at room temperature in incubator shaker for 15 min. The absorbance of the resulting solution was measured at 517 nm with a 96-well microplate reader. The percentage scavenging was calculated by $[(A_0–A_1)/A_0] \times 100$, where A_0 is the absorbance without the sample whereas A_1 is the absorbance with the sample. The SC_{50} value was deduced from a plot of percentage scavenging versus sample concentration. BHA was used as a standard antioxidant.

Acknowledgments

This work (DBG5380037) was supported by Thailand Research Fund and Chulalongkorn University. ER and TD are PhD candidates supported by Chulalongkorn University Dutsadi Phiphat Scholarship and The

Commission of Higher Education, respectively. PK is undergraduate student supported through the Development and Promotion of Science and Technology Talents Project (DPST).

References

[1] P. Zimmet, K.G.M.M. Alberti, J. Shaw, Global and societal implications of the diabetes epidemic, Nature 414 (2001) 782-787.

[2] V. Bocci, I. Zanardi, M.S.P. Huijberts, V. Travagli, Diabetes and chronic oxidative stress. A perspective based on the possible usefulness of ozone therapy, Diabetes Metab. Syndr. Clin. Res. Rev. 2 (2011) 45-49.

[3] M. Brownlee, Biochemistry and molecular cell biology of diabetic complications, Nature 414 (2001) 813-820.

[4] A.C. Maritim, R.A. Sanders, J.B. Watkins III, Diabetes, oxidative stress, and antioxidants: A review, J. Biochem. Mol. Toxicol. 17 (2003) 24-38.

[5] S. Wacharasindhu, W. Worawalai, W. Rungprom, P. Phuwapraisirisan, (+)-*proto*-Quercitol, a natural versatile chiral building block for the synthesis of the alpha-glucosidase inhibitors, 5-amino-1,2,3,4-cyclohexanetetrols, Tetrahedron Lett. 50 (2009) 2189-2192.

[6] W. Worawalai, E. Rattanangkool, A. Vanitcha, P. Phuwapraisirisan, S. Wacharasindhu, Concise synthesis of (+)-conduritol F and inositol analogues from naturally available (+)-*proto*-quercitol and their glucosidase inhibitory activity, Bioorg. Med. Chem. Lett.22 (2012) 1538-1540.

[7] W. Worawalai, S. Wacharasindhu, P. Phuwapraisirisan, Synthesis of new *N*-substituted aminoquercitols from naturally available (+)-*proto*-quercitol and their alpha-glucosidase inhibitory activity, Med. Chem. Comm. 3 (2012) 1466-1470.

[8] Y. Sato, S.Itagaki, T. Kurokawa, J. Ogura, M. Kobayashi, T. Hirano, M. Sugawara, K. Iseki, In vitro and in vivo antioxidant properties of chlorogenic acid and caffeic acid, Int. J. Pharmaceut. 403 (2011) 136-138.

[9] A. Hunyadi, A. Martins, T.J. Hsieh, A. Seres, I. Zupkó, Chlorogenic acid and rutin play a major role in the in vivo anti-diabetic activity of *Morus alba* leaf extract on type II diabetic rats, PLoSOne 11 (2012) e50619.

[10] S. Adisakwattana, P. Chantarasinlapin, H. Thammarat, S. Yibchok-Anun, A series of cinnamic acid derivatives and their inhibitory activity on intestinal alpha-glucosidase, J. Enzym. Inhib. Med. Chem. 24 (2009) 1194-1200.

[11] R.L. Stein, Kinetics of Enzyme Action: Essential Principles for Drug Hunters, John Wiley & Sons, Singapore, 2011.

[12] A. Schäfer, P. Högger, Pharmaceutical and nutraceutical effects of *Pinuspinaster* bark extract, Diabetes Res. Clin. Pract. 77 (2007) 41-46.

[13] D. Barham, P. Trinder, An improved colour reagent for the determination of blood glucose by the oxidase system, Analyst 97 (1972) 142-145.

[14] A.L. Dawidowicz, D. Wianowska, M. Olszowy, On practical problems in estimation of antioxidant activity of compounds by DPPH method (Problems in estimation of antioxidant activity), Food Chem. 131 (2012) 1037-1043.

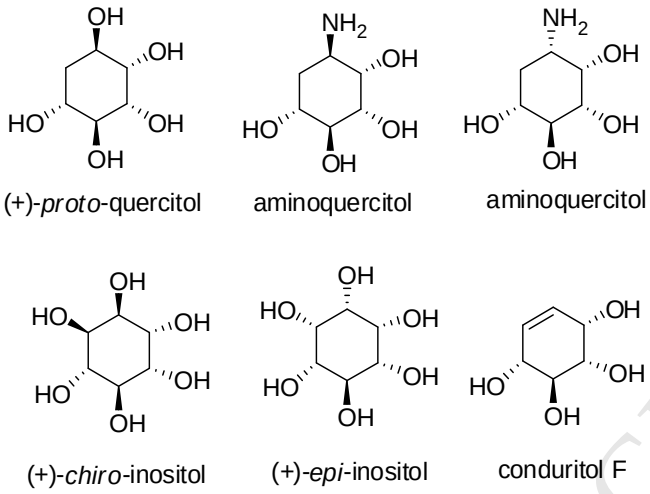

Fig. 1. Structures of (+)-*proto*-quercitol and its synthetic analogues.

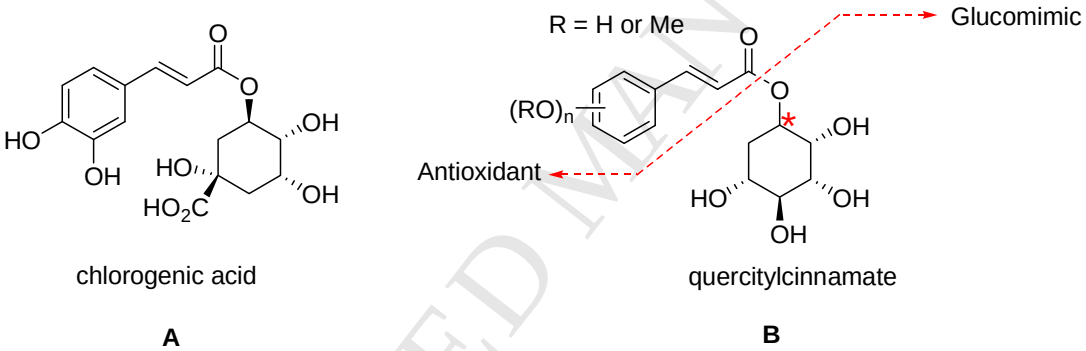

Fig. 2. Structures of chlorogenic acid (**A**) and designed quercitylcinnamates (**B**) encompassing antioxidant and glucomimic residues.

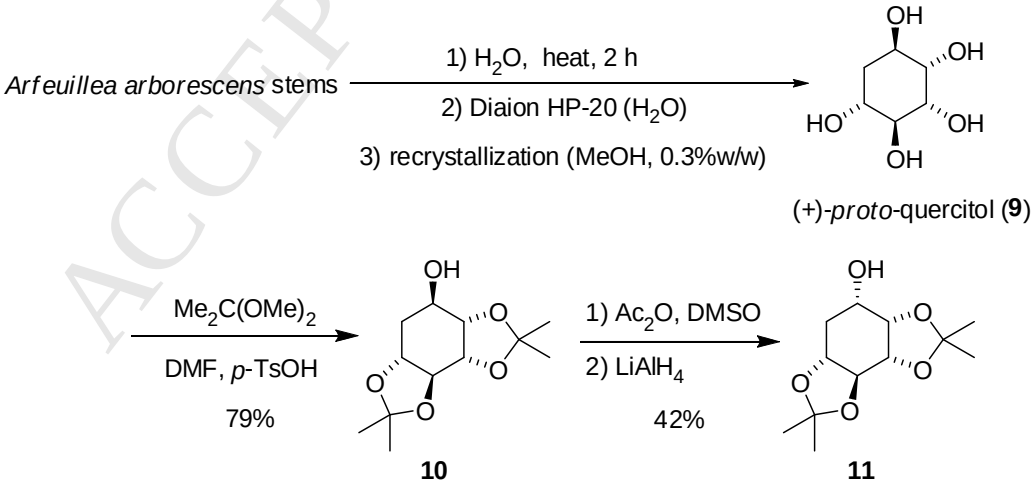

Scheme 1. Isolation of (+)-*proto*-quercitol and synthesis of bis-acetonides **10** and **11**

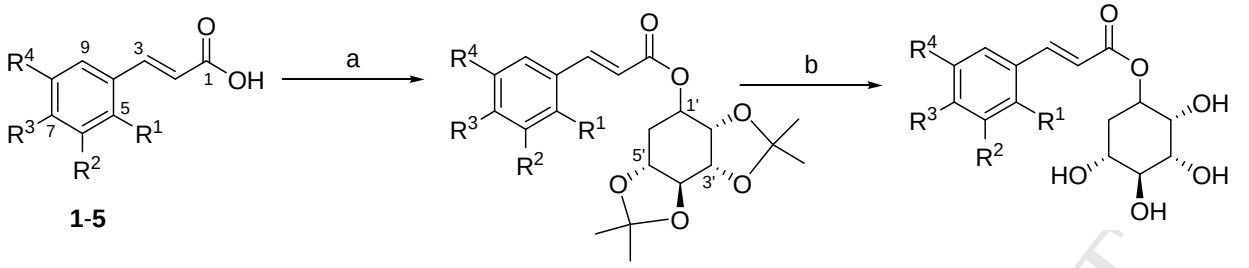

R^1 = OMe, R^2 = R^3 = R^4 = H; **1**
R^1 = R^3 = R^4 = H, R^2 = OMe; **2**
R^1 = R^2 = R^4 = H, R^3 = OMe; **3**
R^1 = R^4 = H, R^2 = R^3 = OMe; **4**
R^1 = H, R^2 = R^3 = R^4 = OMe; **5**

R^1 = OMe, R^2 = R^3 = R^4 = H, 1'*R*; **1R**
R^1 = OMe, R^2 = R^3 = R^4 = H, 1'*S*; **1S**
R^1 = R^3 = R^4 = H, R^2 = OMe, 1'*R*; **2R**
R^1 = R^3 = R^4 = H, R^2 = OMe, 1'*S*; **2S**
R^1 = R^2 = R^4 = H, R^3 = OMe, 1'*R*; **3R**
R^1 = R^2 = R^4 = H, R^3 = OMe, 1'*S*; **3S**
R^1 = R^4 = H, R^2 = R^3 = OMe, 1'*R*; **4R**
R^1 = R^4 = H, R^2 = R^3 = OMe, 1'*S*; **4S**
R^1 = H, R^2 = R^3 = R^4 = OMe, 1'*R*; **5R**

R^1 = OMe, R^2 = R^3 = R^4 = H, 1'*R*; **1a**
R^1 = OMe, R^2 = R^3 = R^4 = H, 1'*S*; **1b**
R^1 = R^3 = R^4 = H, R^2 = OMe, 1'*R*; **2a**
R^1 = R^3 = R^4 = H, R^2 = OMe, 1'*S*; **2b**
R^1 = R^2 = R^4 = H, R^3 = OMe, 1'*R*; **3a**
R^1 = R^2 = R^4 = H, R^3 = OMe, 1'*S*; **3b**
R^1 = R^4 = H, R^2 = R^3 = OMe, 1'*R*; **4a**
R^1 = R^4 = H, R^2 = R^3 = OMe, 1'*S*; **4b**
R^1 = H, R^2 = R^3 = R^4 = OMe, 1'*R*; **5a**

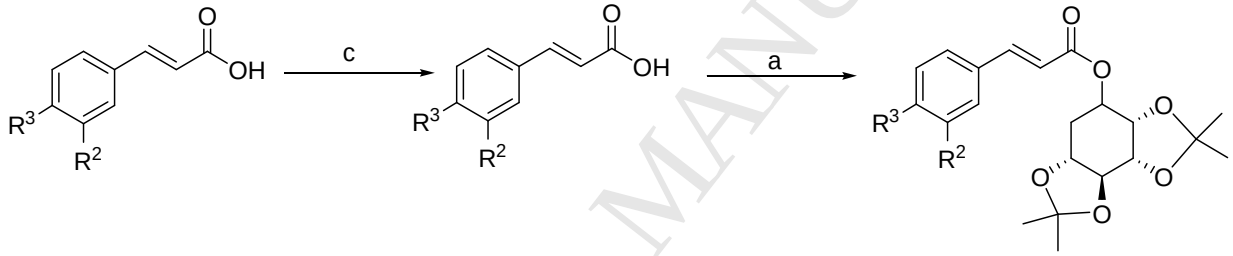

R^2 = R^3 = OH; **6**
R^2 = OMe, R^3 = OH; **7**
R^2 = OH, R^3 = OMe; **8**

R^2 = R^3 = $O(CH_3)_2SiC(CH_3)_3$; **6Si**
R^2 = OMe, R^3 = $O(CH_3)_2SiC(CH_3)_3$; **7Si**
R^2 = $O(CH_3)_2SiC(CH_3)_3$, R^3 = OMe; **8Si**

R^2 = R^3 = $O(CH_3)_2SiC(CH_3)_3$, 1'*R*; **6R**
R^2 = R^3 = $O(CH_3)_2SiC(CH_3)_3$, 1'*S*; **6S**
R^2 = OMe, R^3 = $O(CH_3)_2SiC(CH_3)_3$, 1'*R*; **7R**
R^2 = OMe, R^3 = $O(CH_3)_2SiC(CH_3)_3$, 1'*S*; **7S**
R^2 = $O(CH_3)_2SiC(CH_3)_3$, R^3 = OMe, 1'*R*; **8R**
R^2 = $O(CH_3)_2SiC(CH_3)_3$, R^3 = OMe, 1'*S*; **8S**

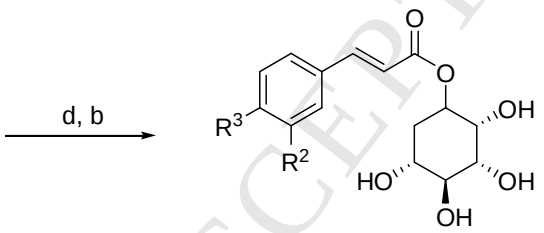

R^2 = R^3 = OH, 1'*R*; **6a**
R^2 = R^3 = OH, 1'*S*; **6b**
R^2 = OMe, R^3 = OH, 1'*R*; **7a**
R^2 = OMe, R^3 = OH, 1'*S*; **7b**
R^2 = OH, R^3 = OMe, 1'*R*; **8a**
R^2 = OH, R^3 = OMe, 1'*S*; **8b**

Scheme 2. Synthesis of quercetylcinnamates. Reagents and conditions: (a) **10** or **11**, DCC, DMAP, CH_2Cl_2, 0 °C to rt; (b) amberlyst-15, MeOH; (c) TBDMSCl, imidazole, DMF, rt; (d) TBAF, THF, rt

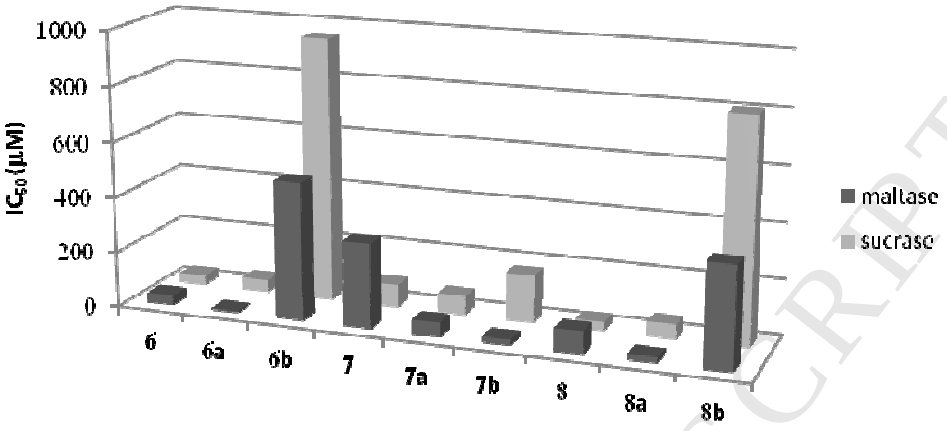

Fig. 3. Inhibition trends of bioconjugates **6a-8b** compared to their cinnamic parents **6-8**.

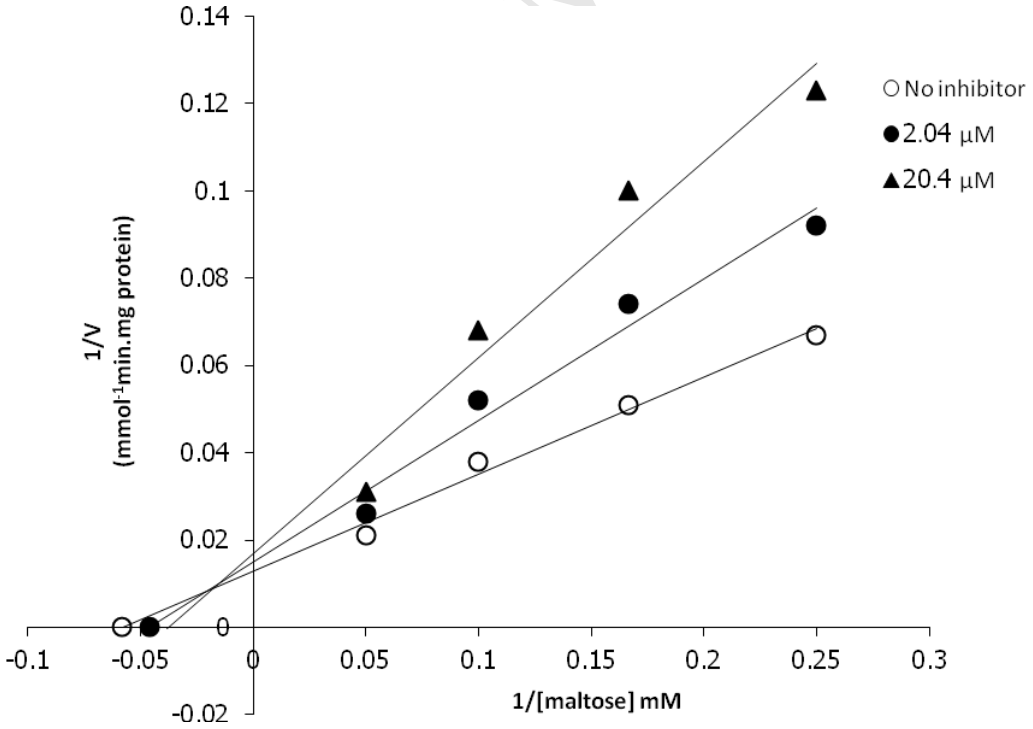

Fig. 4. Lineweaver-Burk plots for inhibitory activity of **6a** against maltase.

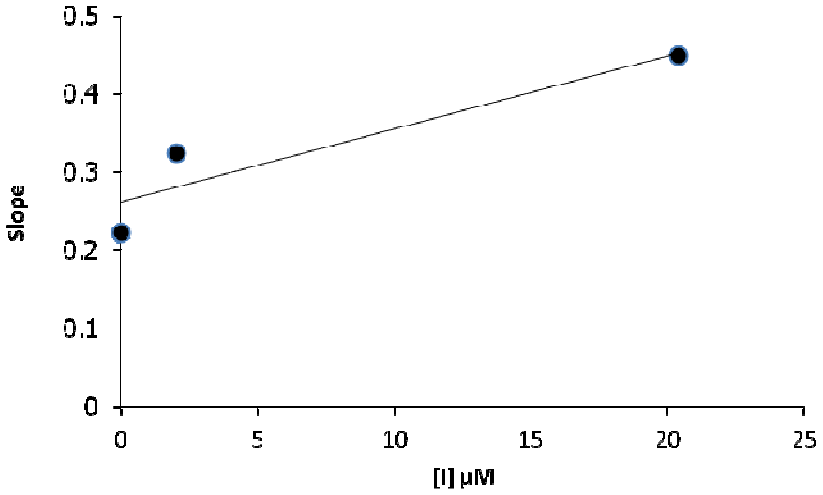

Fig. 5. Secondary plot of slope *vs* [I] for determination of K_i of **6a** against maltase.

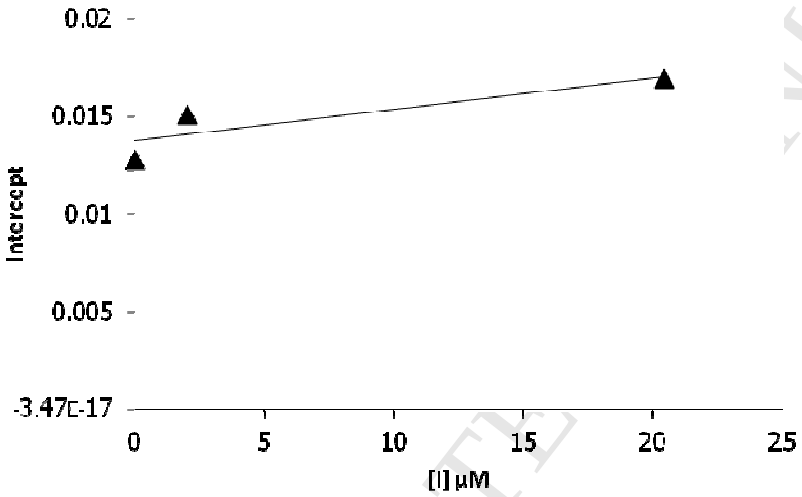

Fig. 6. Secondary plot of intercept *vs* [I] for determination of K'_i of **6a** against maltase.

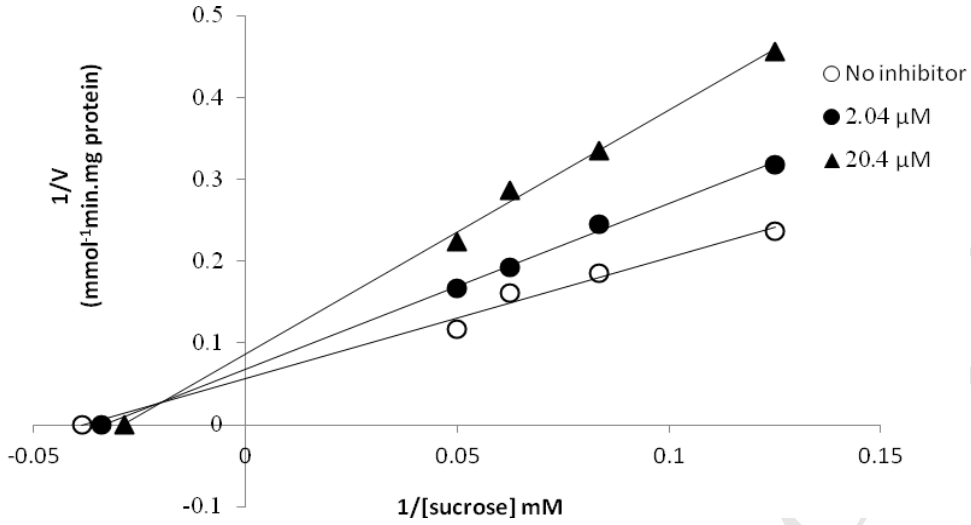

Fig. 7. Lineweaver-Burk plots for inhibitory activity of **6a** against sucrase.

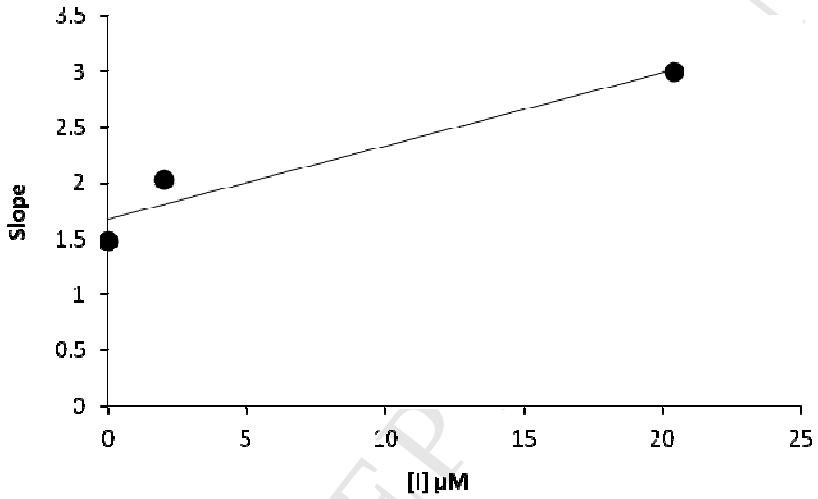

Fig. 8. Secondary plot of slope *vs* [I] for determination of K_i of **6a** against maltase.

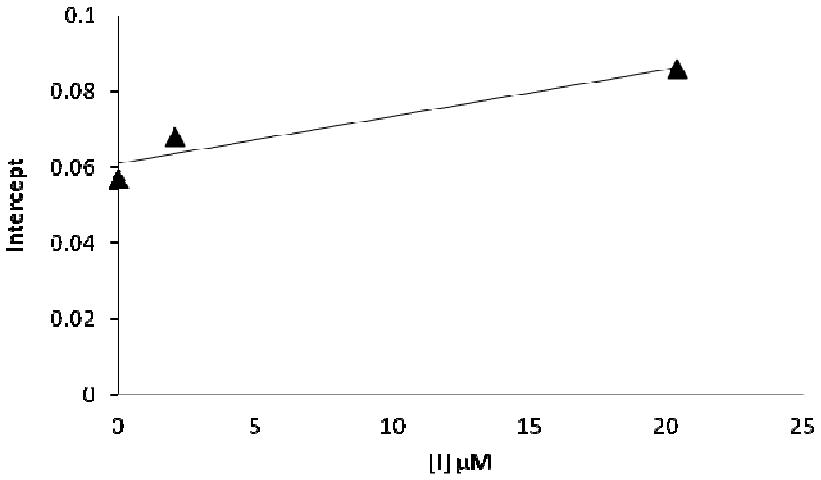

Fig. 9. Secondary plot of intercept *vs* [I] for determination of K_i' of **6a** against sucrase.

Table 1. α-Glucosidase inhibitory effect and radical scavenging activity of quercityl-cinnamates

Compounds	α-Glucosidase inhibitory effect (IC_{50}, μM)			Radical scavenging (SC_{50}, mM)
	Baker's yeast glucosidase	Maltase	Sucrase	
1a	NI[a]	NI	NI	NS[b]
1b	NI	NI	NI	NS
2a	NI	NI	NI	NS
2b	NI	NI	NI	NS
3a	NI	NI	NI	NS
3b	NI	NI	NI	NS
4a	NI	NI	NI	NS
4b	NI	NI	NI	NS
5a	NI	NI	NI	NS
6	NI	34.69±0.74	87.45±0.62	0.15
6a	NI	5.31±0.10	43.65±0.30	0.11
6b	NI	497.48±0.50	954.08±0.50	NS
7a	NI	51.93±0.20	67.21±0.20	NS
7b	NI	21.07±0.15	171.43±0.35	NS
8a	NI	20.81±0.14	53.00±0.32	NS
8b	NI	367.15±0.42	805.48±0.65	NS
Acarbose®	403.9±0.40	1.50±0.14	2.30±0.02	ND[d]
BHA	ND	ND	ND	0.10

[a]No inhihition (inhibitory effect less than 30% at concentration of 10 mg/mL)
[b]No scavenging(inhibitory effect less than 50% at concentration of 10 mg/mL)
[c]Not determined

Table 2. Kinetic data of α-glucosidase inhibition of **6a**.

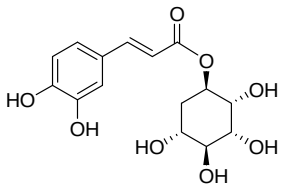

α-Glucosidase	Inhibition type	K_i(μM)	K_i' (μM)	K_m (mM)
Maltase	Mixed-inhibition	23.8	64.5	17.3
sucrase	Mixed-inhibition	22.4	47.5	25.9

Supporting Information

Quercitylcinnamates, a new series of antidiabetic bioconjugates possessing α-glucosidase inhibition and antioxidant

Eakkaphon Rattanangkool[a], Preecha Kittikhunnatham[a], Thanakorn Damsud[a,b], Sumrit Wacharasindhu[a], Preecha Phuwapraisirisan[a,*]

[a]*Natural Products Research Unit, Department of Chemistry, Faculty of Science, Chulalongkorn University, Bangkok 10330, Thailand*

[b]*Program of Biotechnology, Faculty of Science, Chulalongkorn University, Bangkok 10330, Thailand*

Figures 1-30: ^{1}H and ^{13}C NMR spectra of **1a-8b**

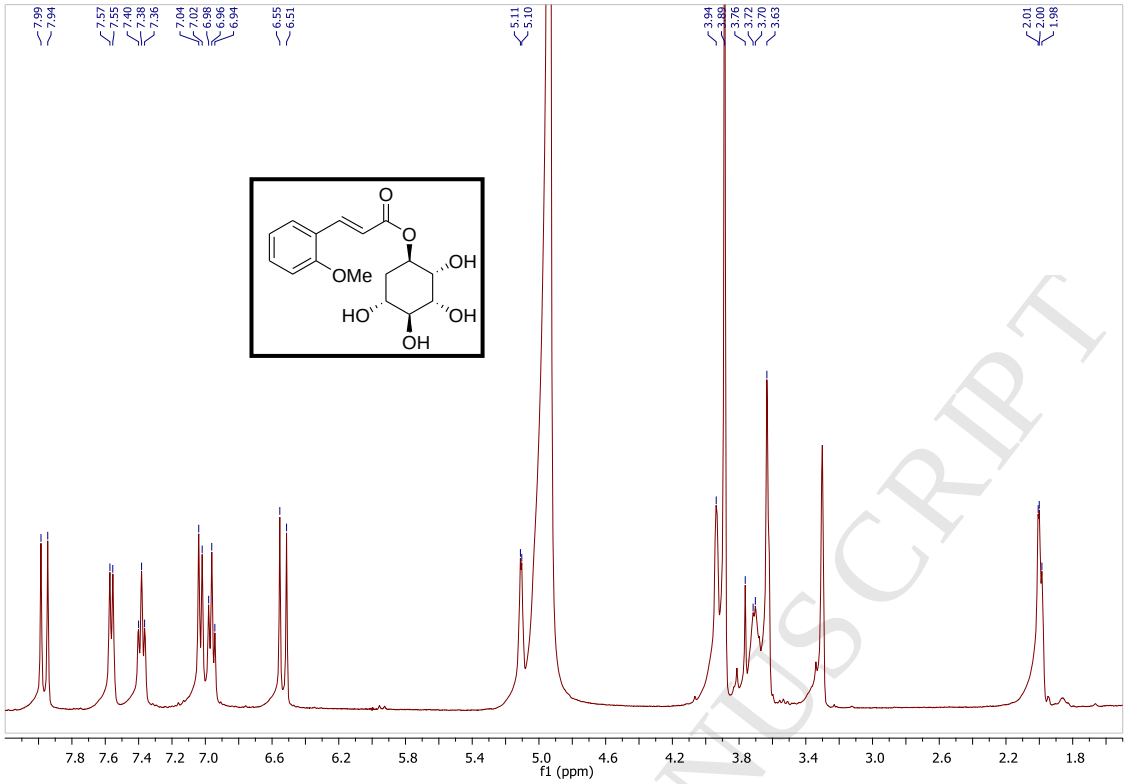

Figure 1. ^{1}H NMR spectrum of **1a** (CD_3OD)

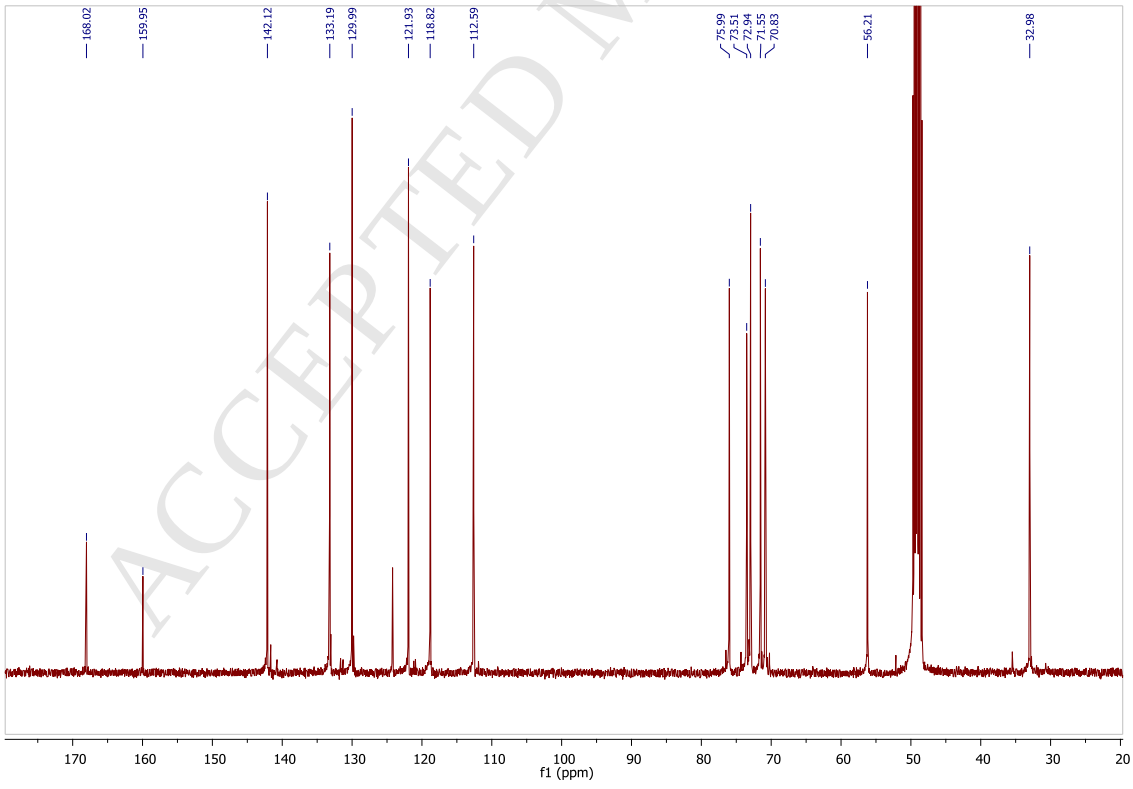

Figure 2. ^{13}C NMR spectrum of **1a** (CD_3OD)

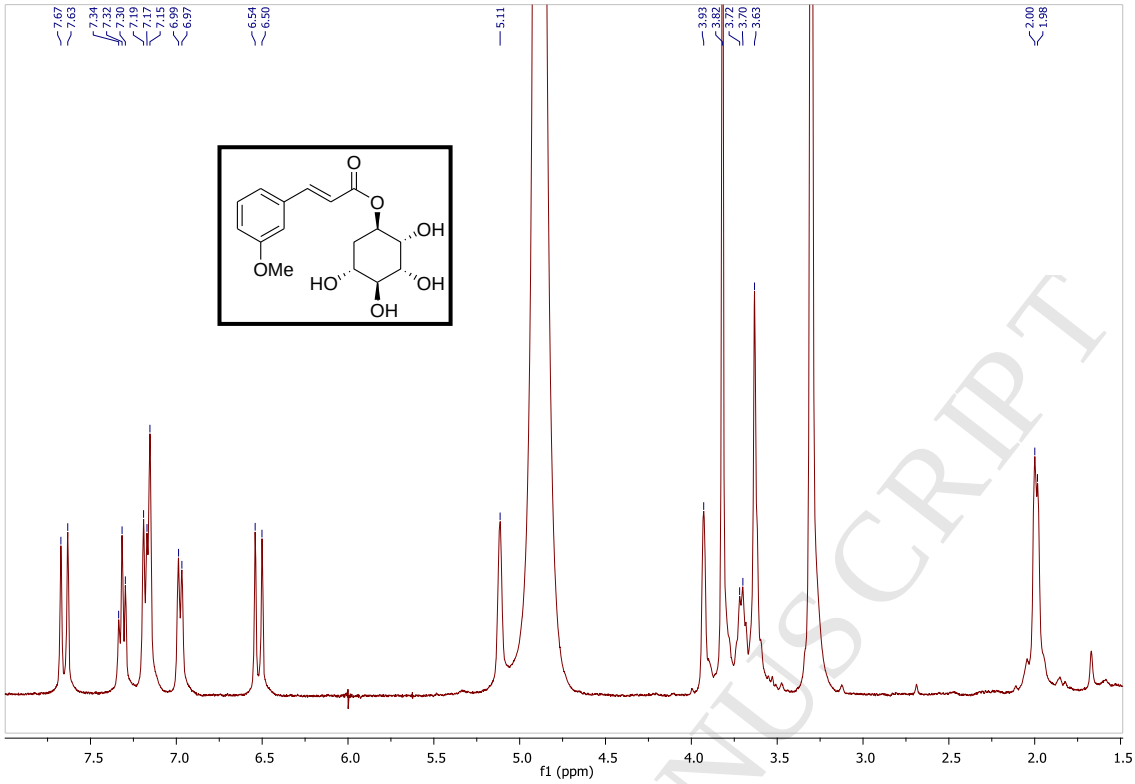

Figure 3. ^{1}H NMR spectrum of **2a** (CD_3OD)

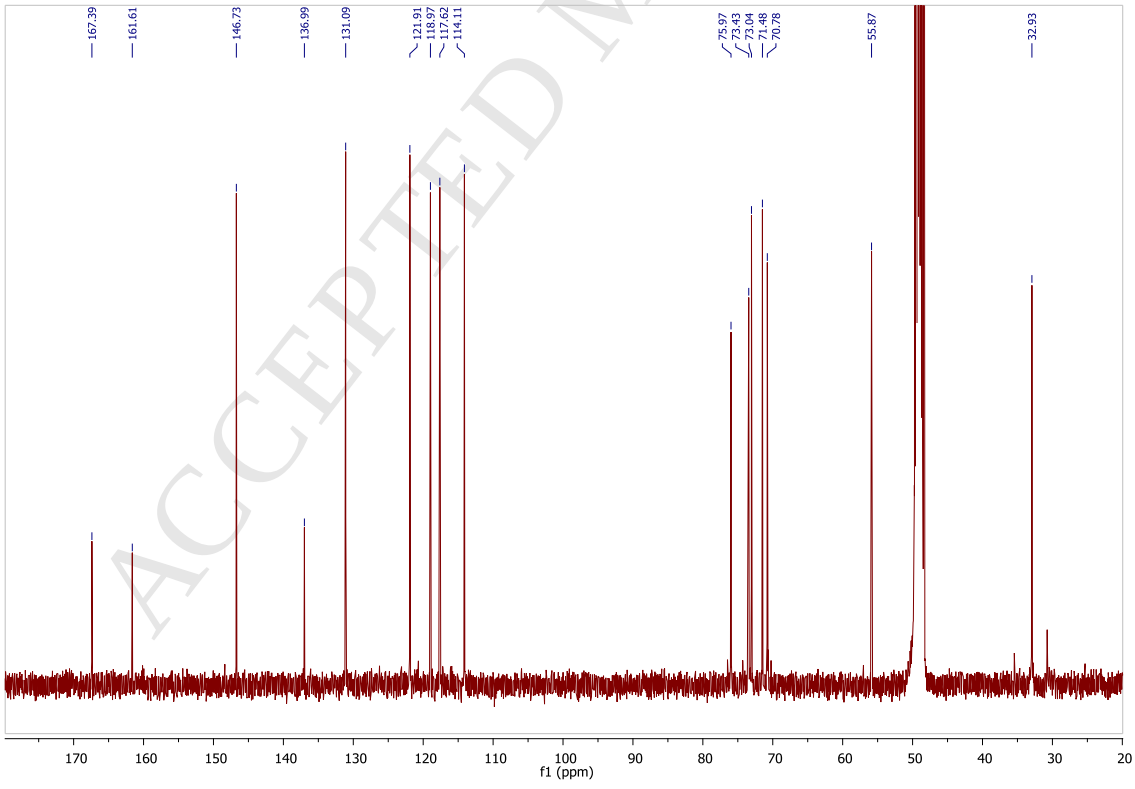

Figure 4. ^{13}C NMR spectrum of **2a** (CD_3OD)

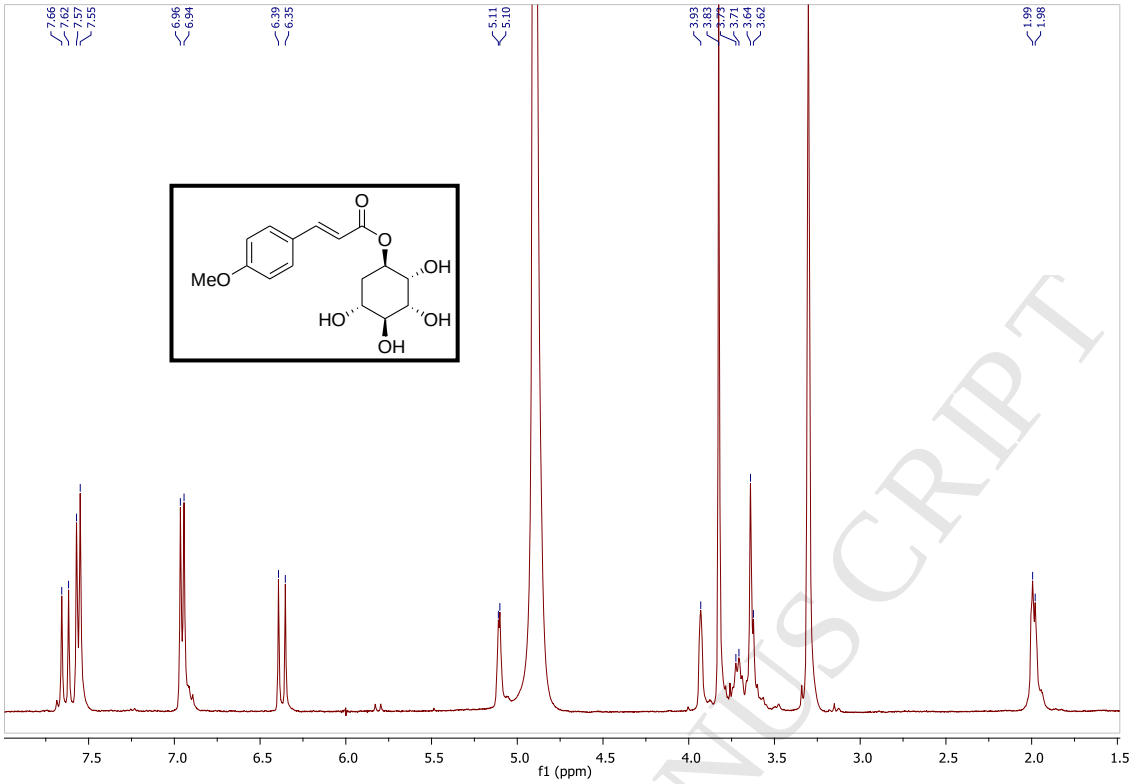

Figure 5. ^{1}H NMR spectrum of **3a** (CD_3OD)

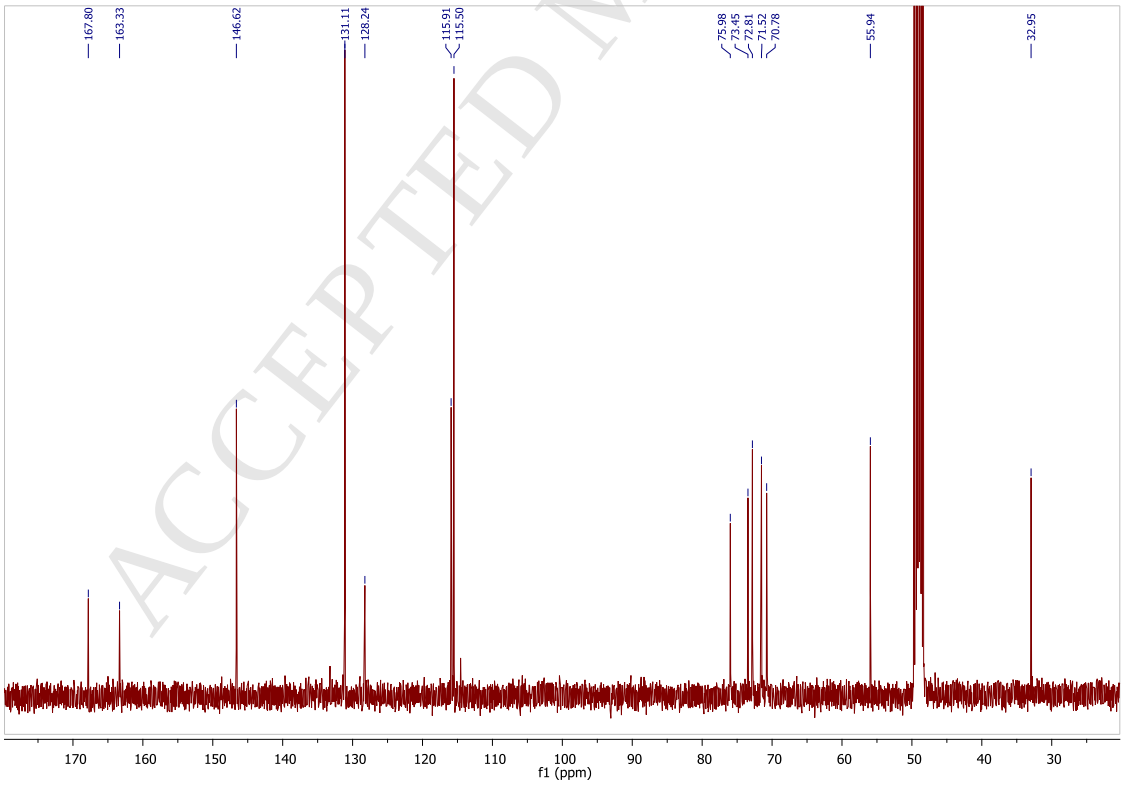

Figure 6. ^{13}C NMR spectrum of **3a** (CD_3OD)

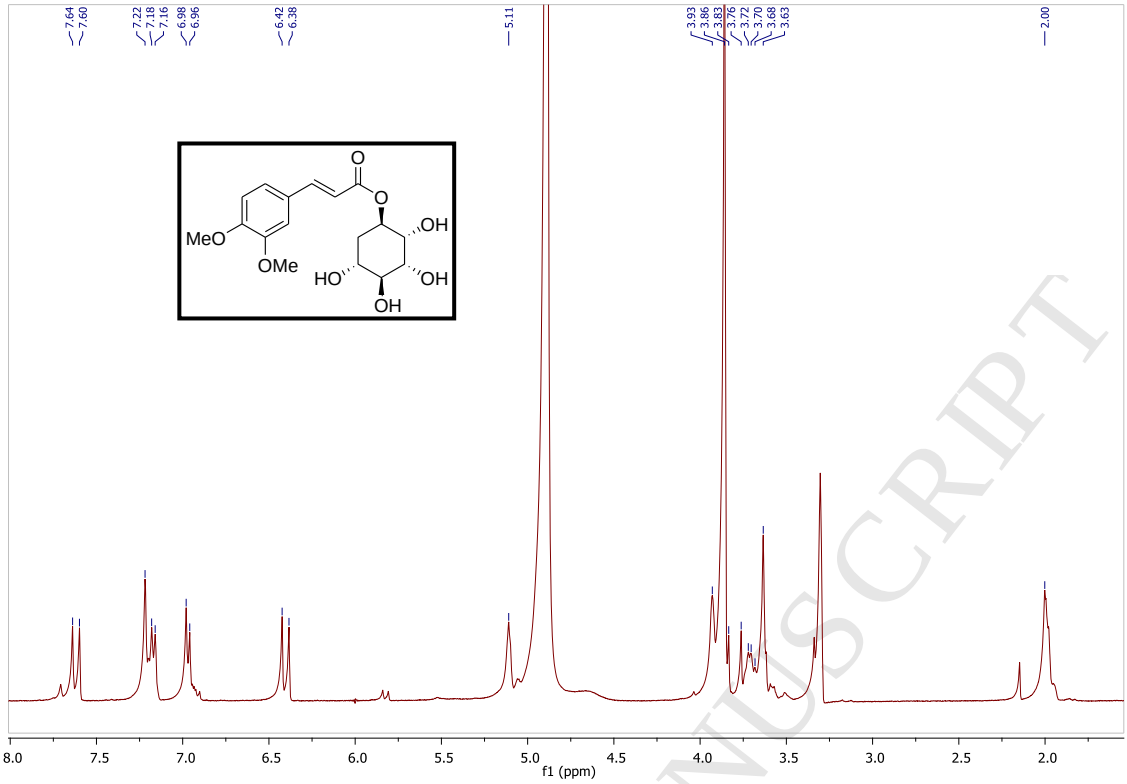

Figure 7. ^{1}H NMR spectrum of **4a** (CD_3OD)

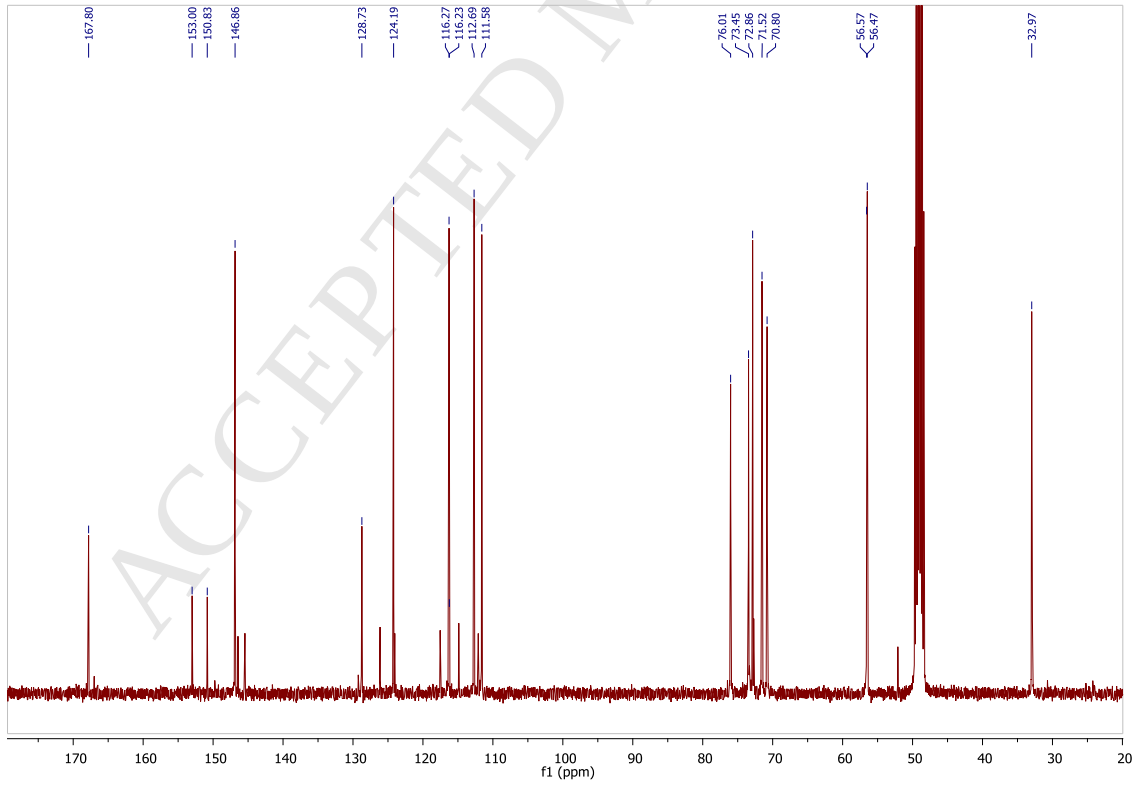

Figure 8. ^{13}C NMR spectrum of **4a** (CD_3OD)

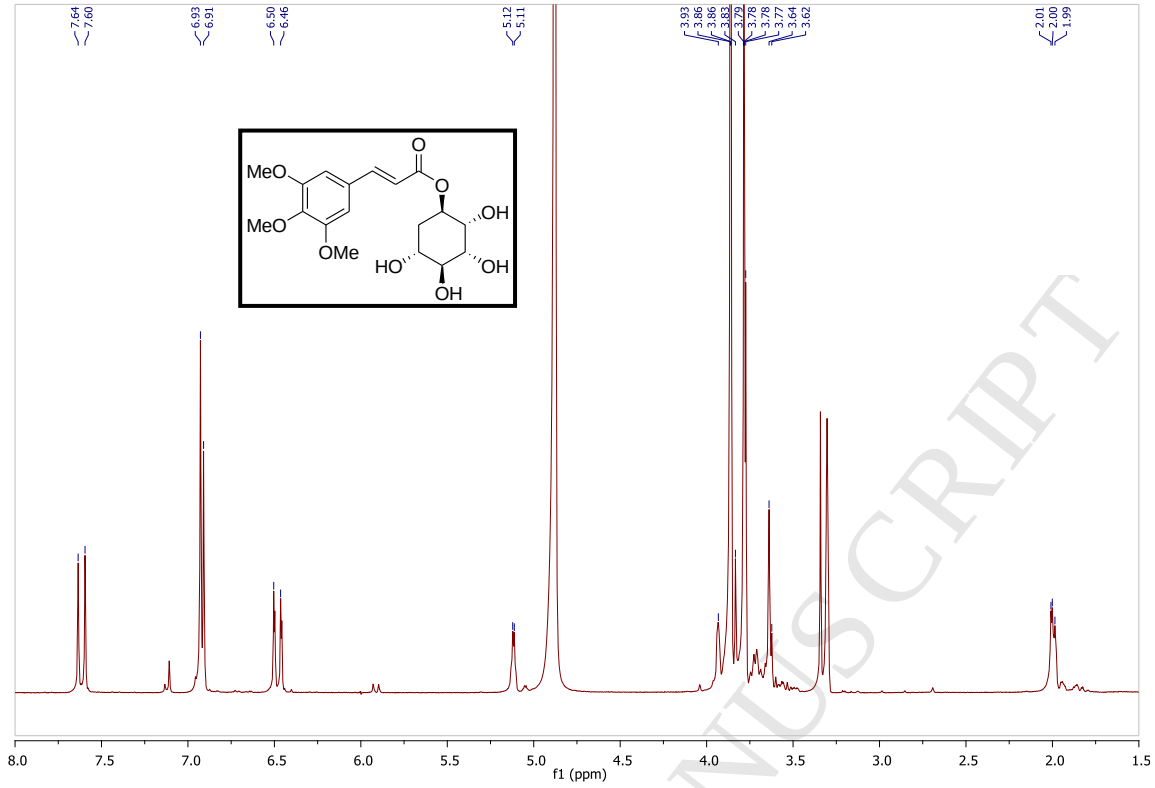

Figure 9. ^{1}H NMR spectrum of **5a** (CD_3OD)

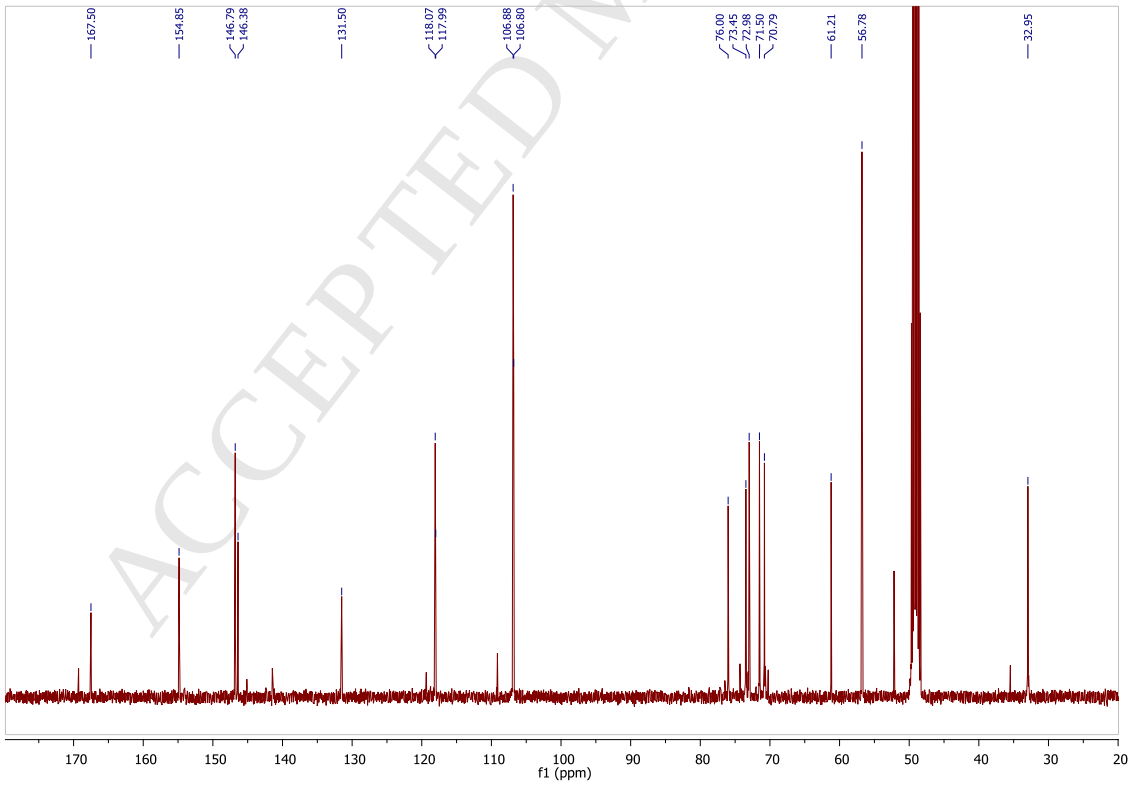

Figure 10. ^{13}C NMR spectrum of **5a** (CD_3OD)

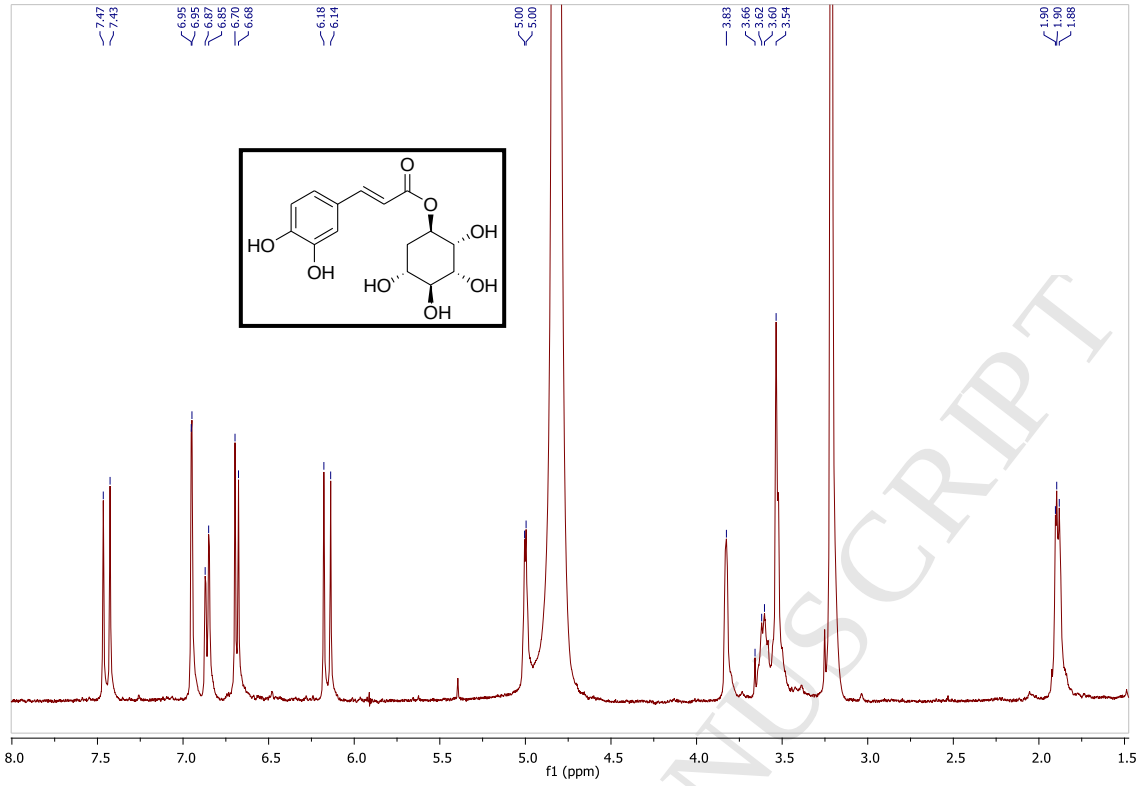

Figure 11. ^{1}H NMR spectrum of **6a** (CD_3OD)

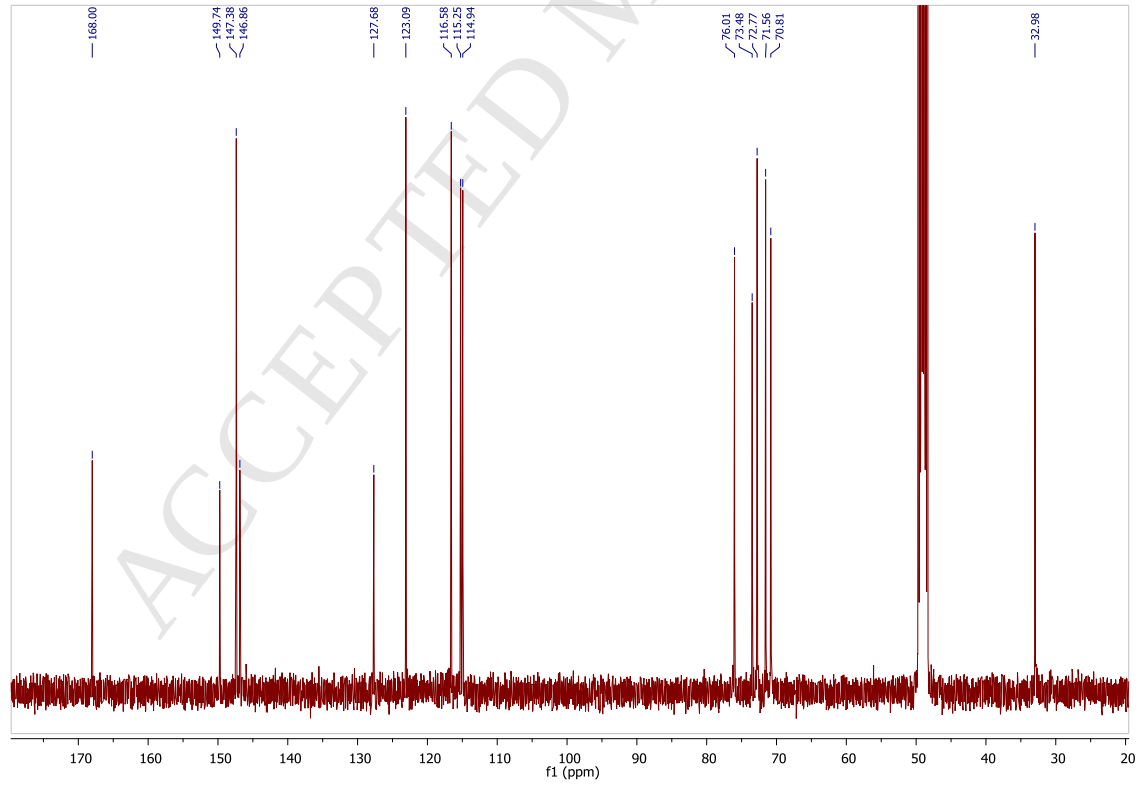

Figure 12. ^{13}C NMR spectrum of **6a** (CD_3OD)

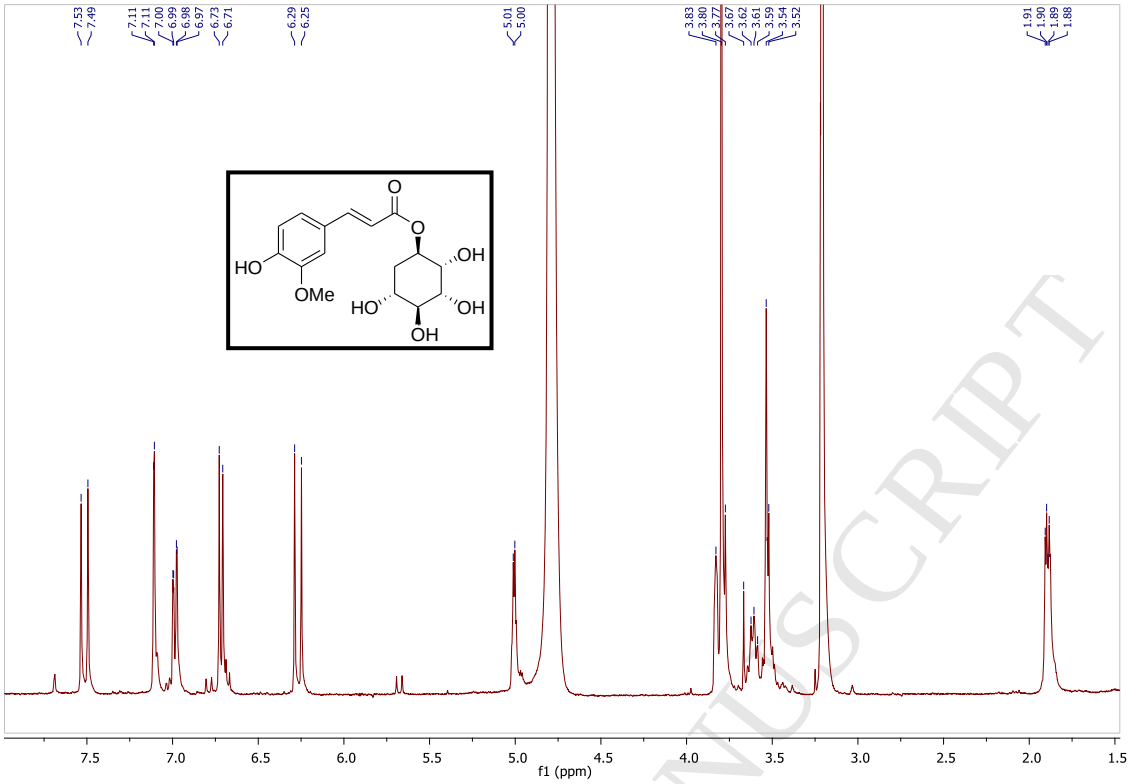

Figure 13. ^{1}H NMR spectrum of **7a** (CD_3OD)

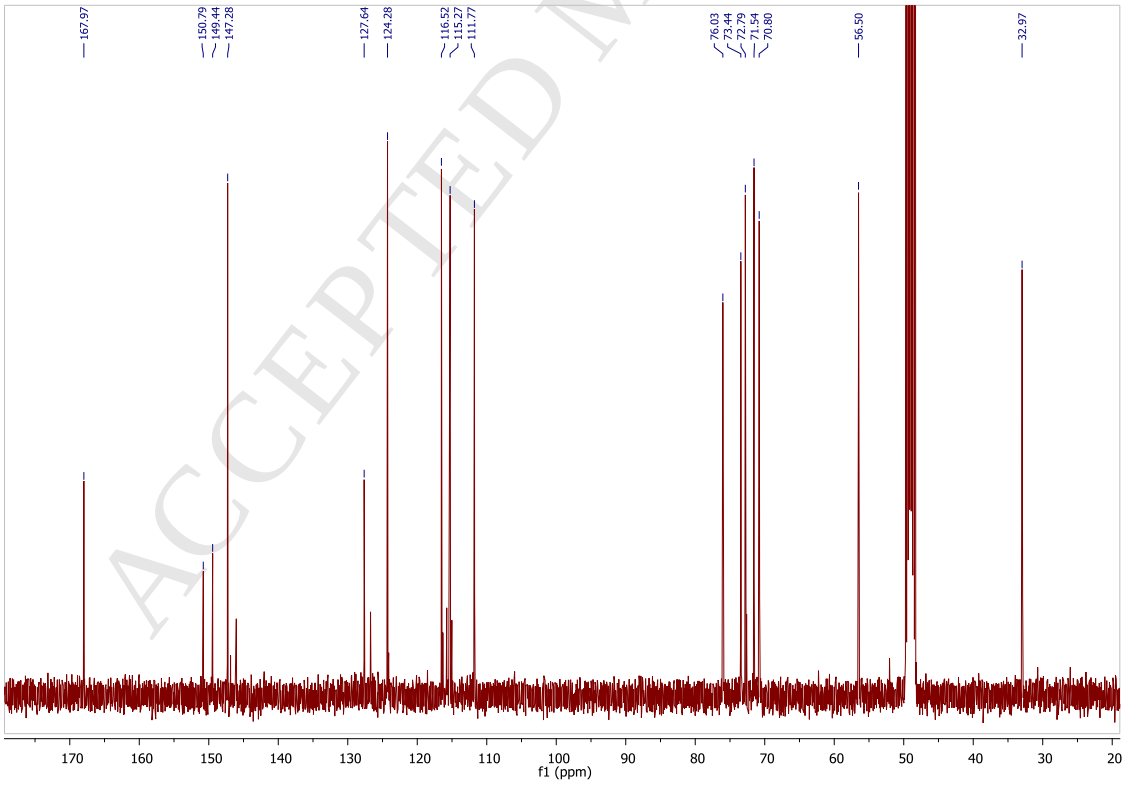

Figure 14. ^{13}C NMR spectrum of **7a** (CD_3OD)

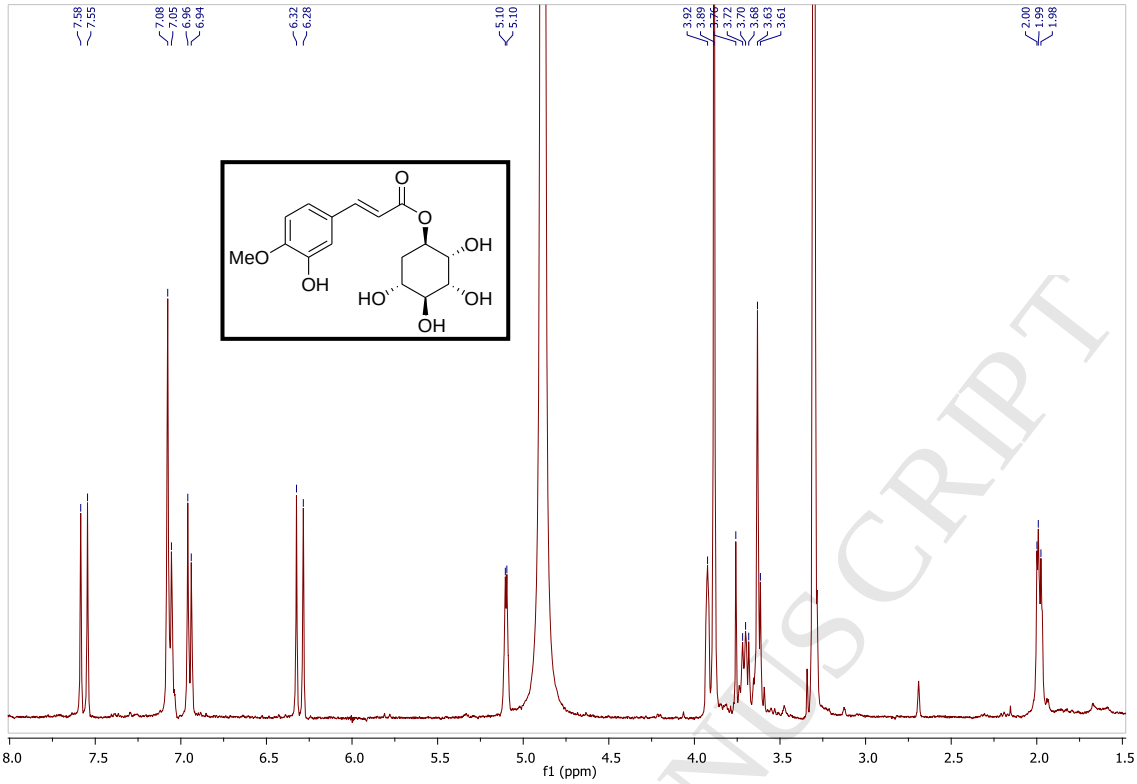

Figure 15. ^{1}H NMR spectrum of **8a** (CD_3OD)

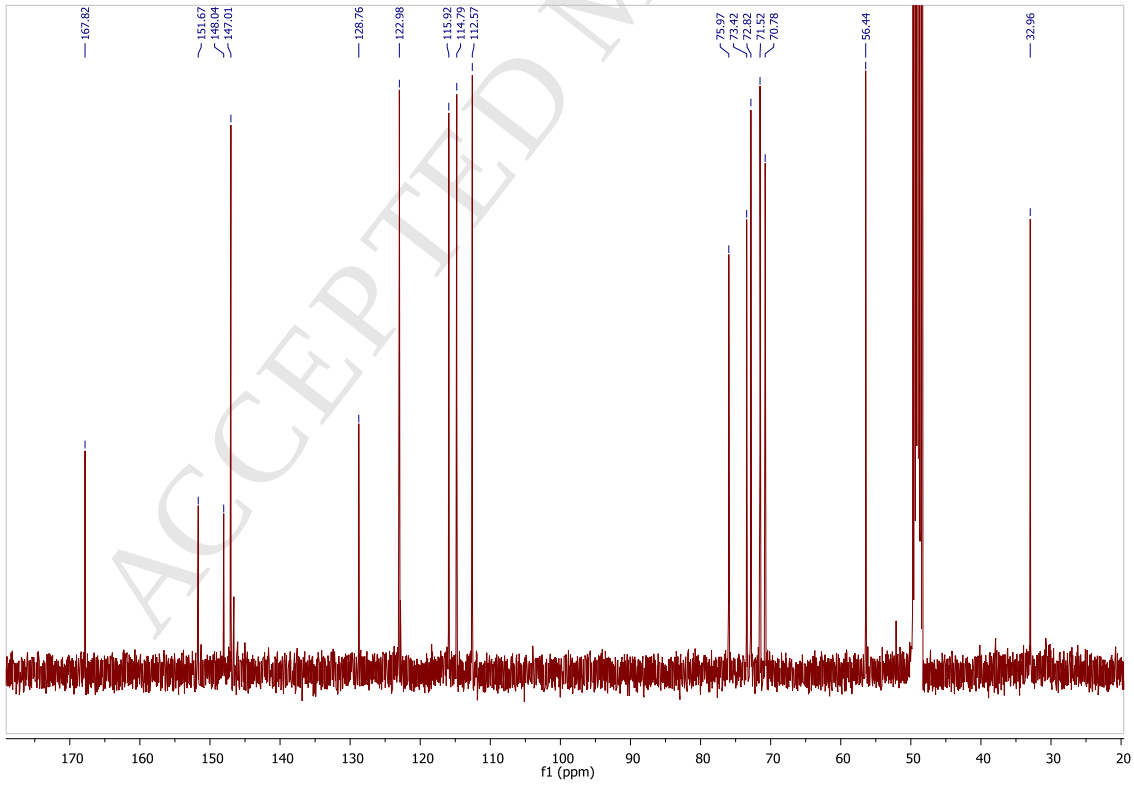

Figure 16. ^{13}C NMR spectrum of **8a** (CD_3OD)

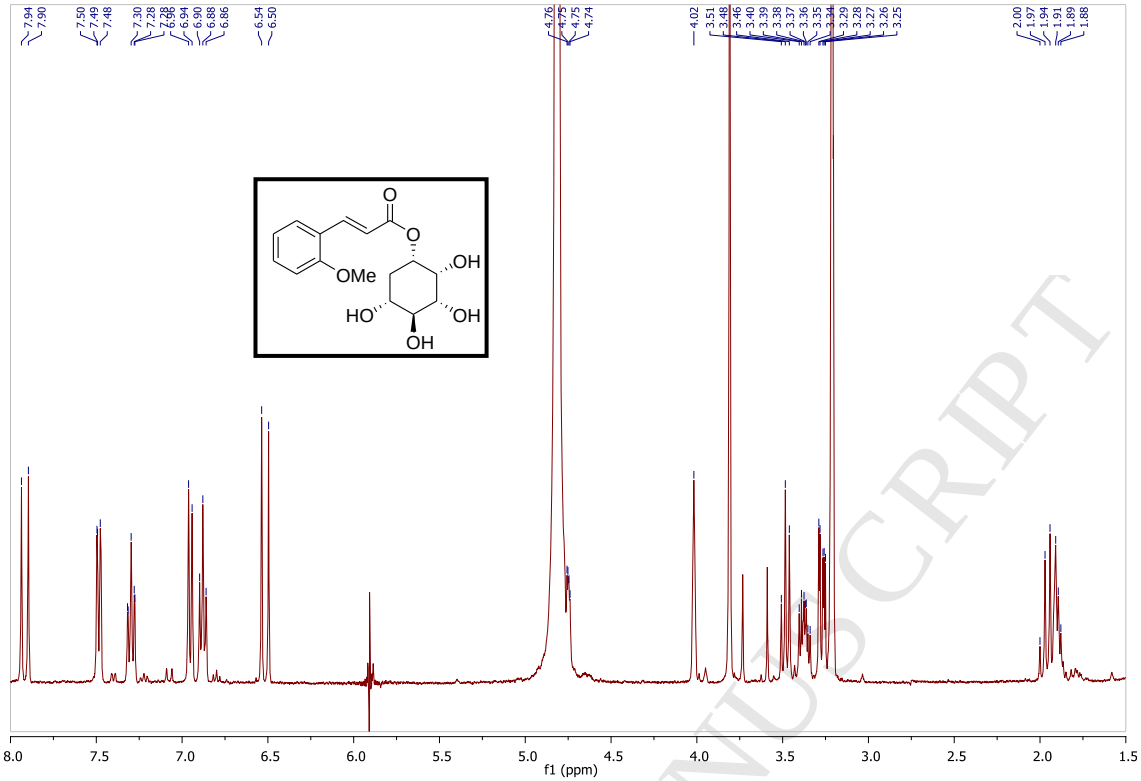

Figure 17. ^{1}H NMR spectrum of **1b** (CD_3OD)

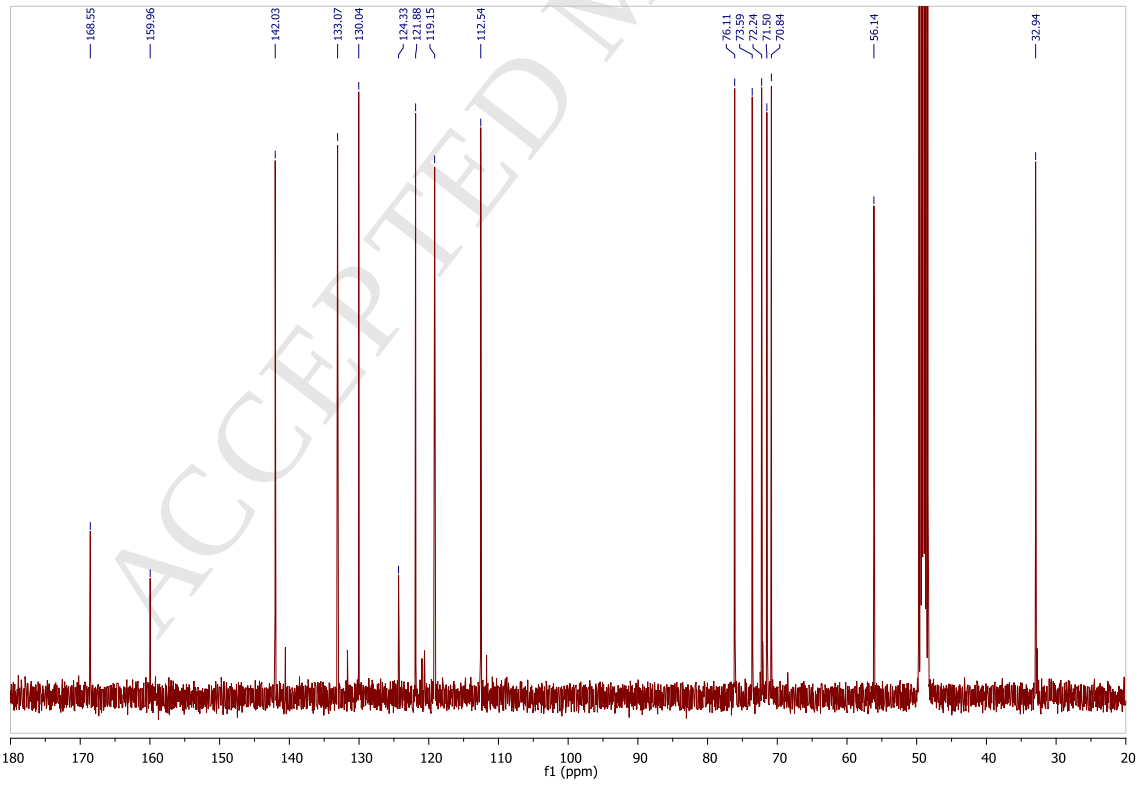

Figure 18. ^{13}C NMR spectrum of **1b** (CD_3OD)

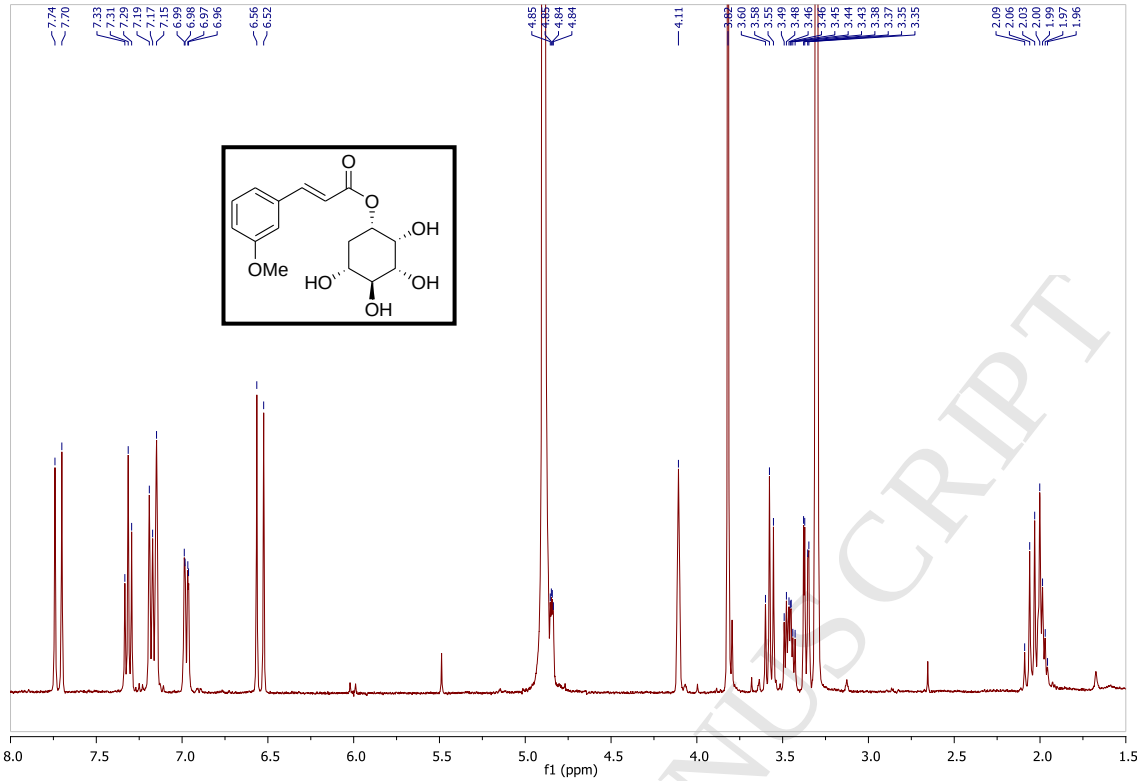

Figure 19. ^{1}H NMR spectrum of **2b** (CD_3OD)

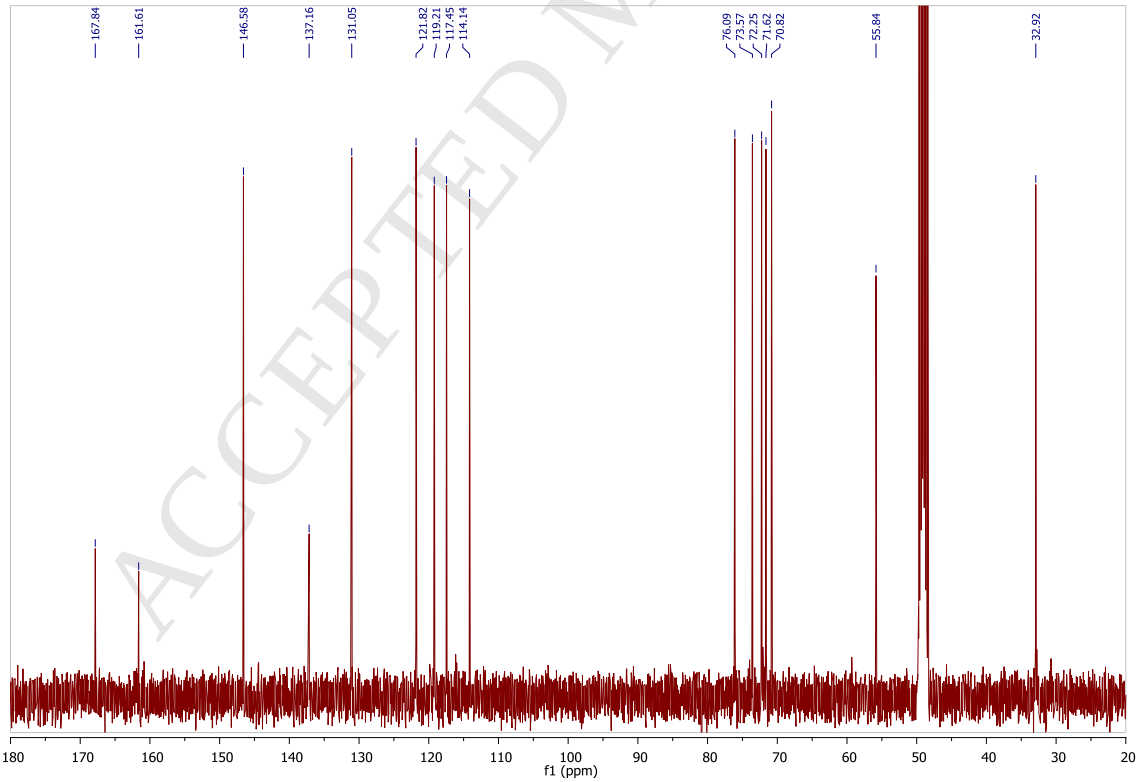

Figure 20. ^{13}C NMR spectrum of **2b** (CD_3OD)

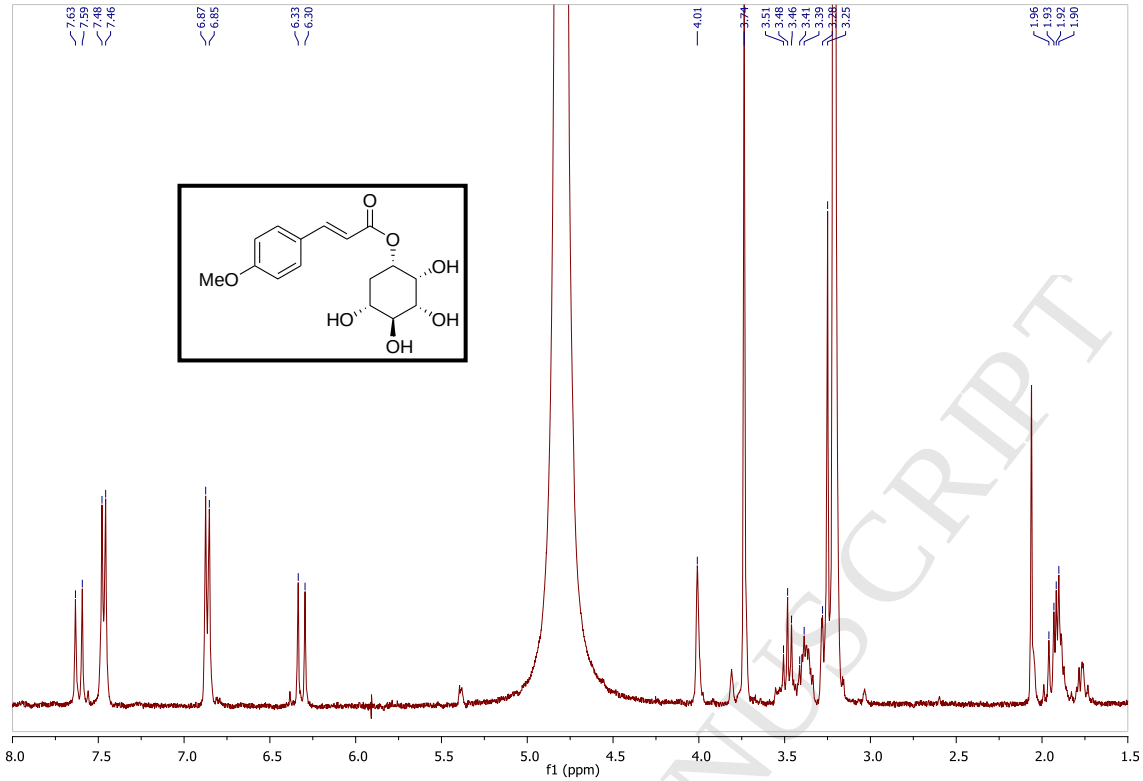

Figure 21. ^{1}H NMR spectrum of **3b** (CD_3OD)

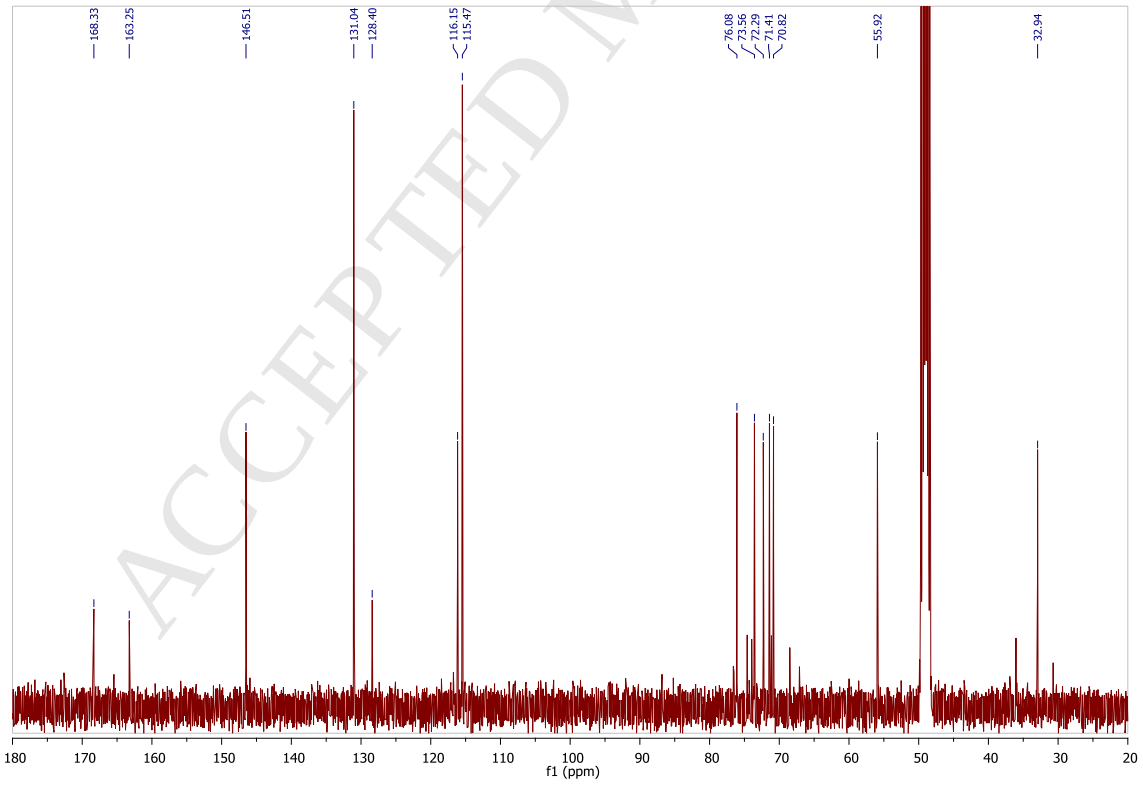

Figure 22. ^{13}C NMR spectrum of **3b** (CD_3OD)

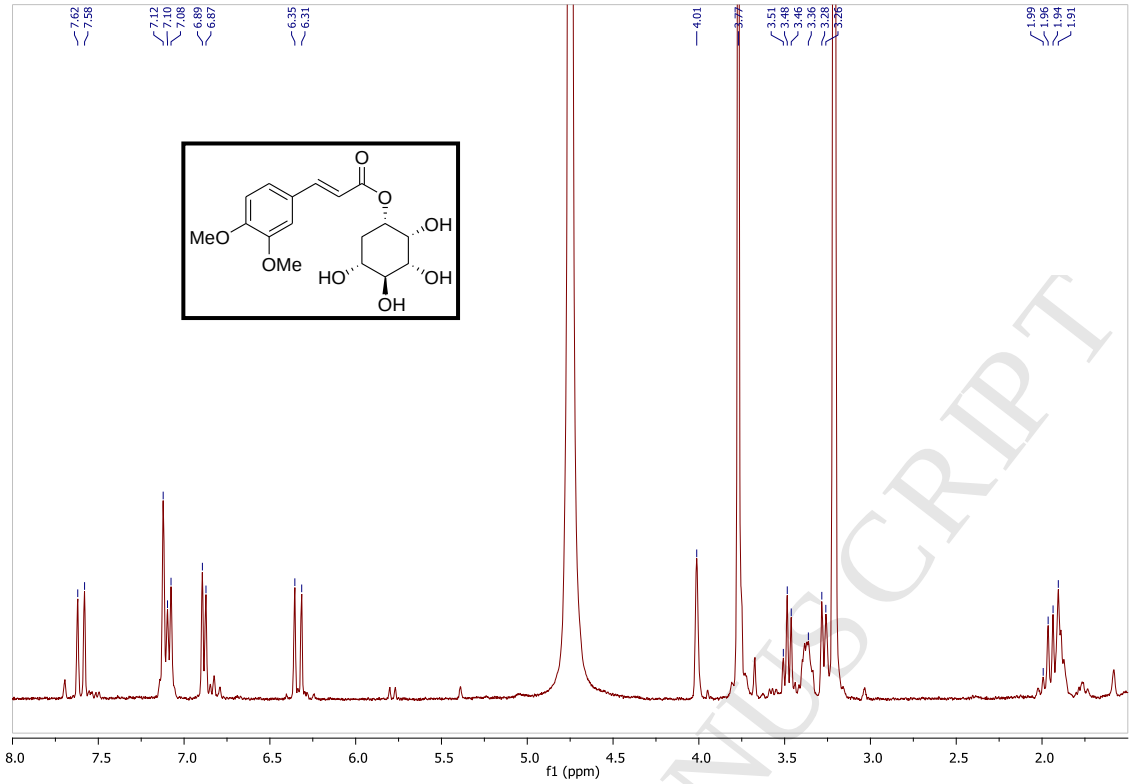

Figure 23. ^{1}H NMR spectrum of **4b** (CD_3OD)

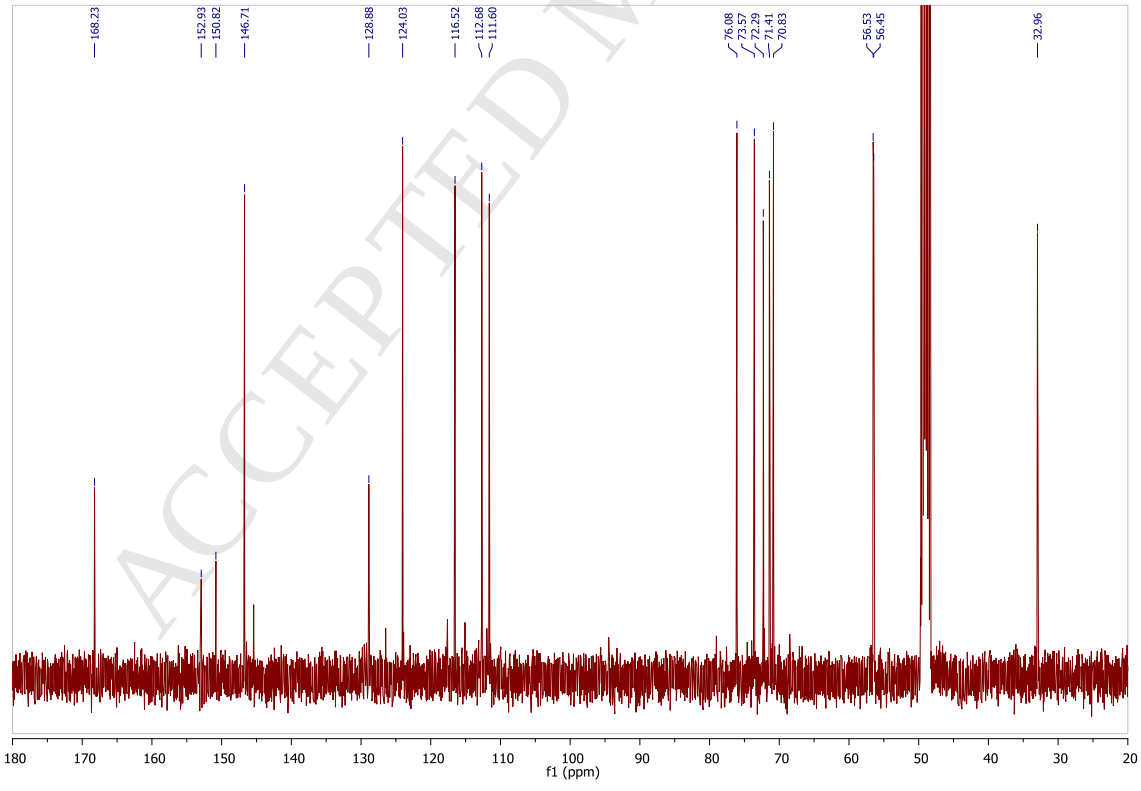

Figure 24. ^{13}C NMR spectrum of **4b** (CD_3OD)

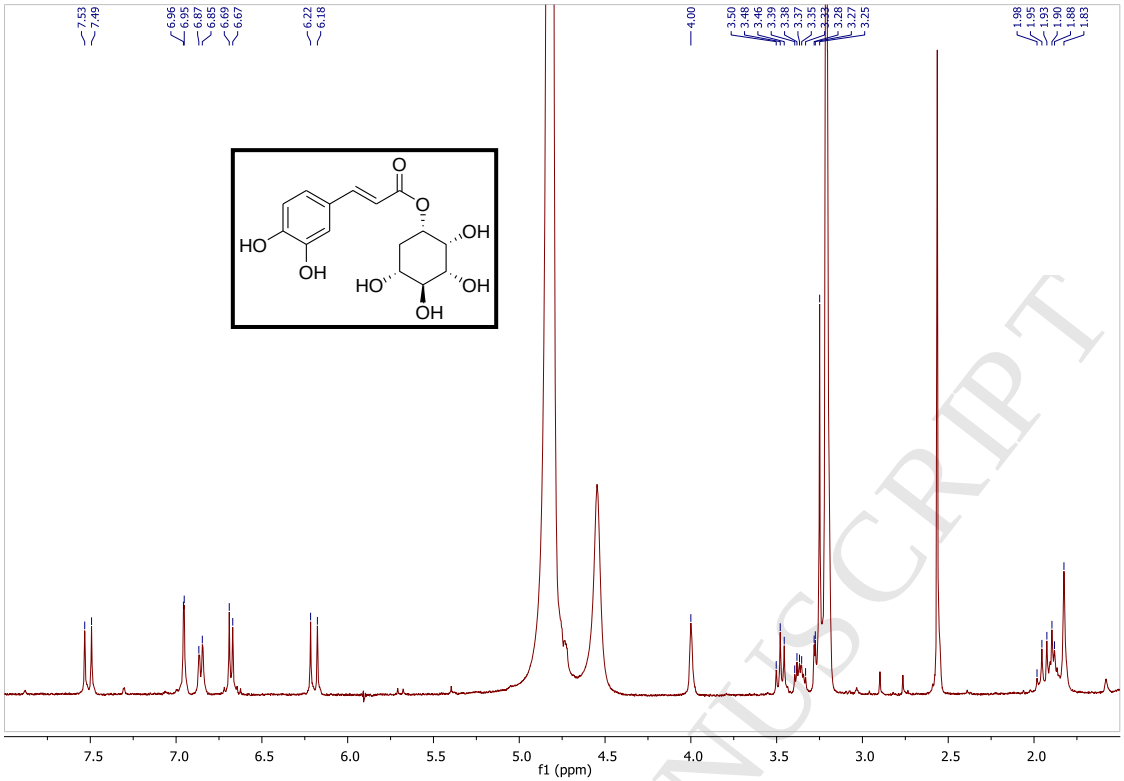

Figure 25. ^{1}H NMR spectrum of **6b** (CD_3OD)

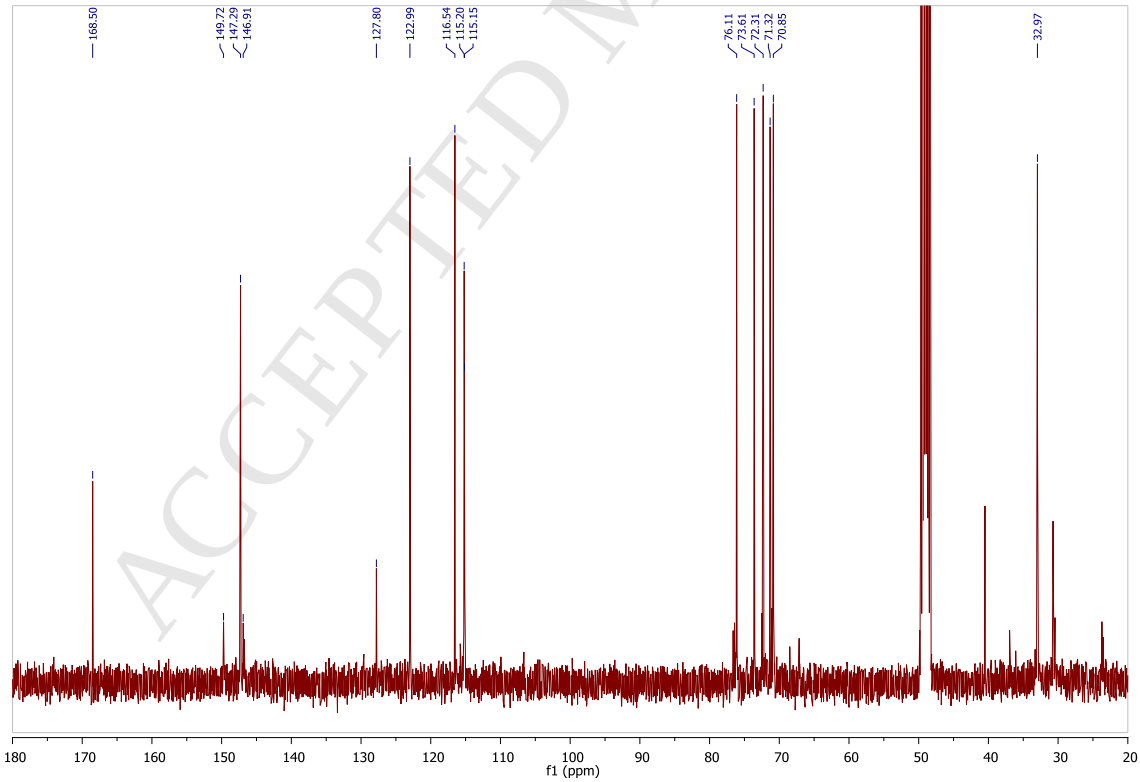

Figure 26. ^{13}C NMR spectrum of **6b** (CD_3OD)

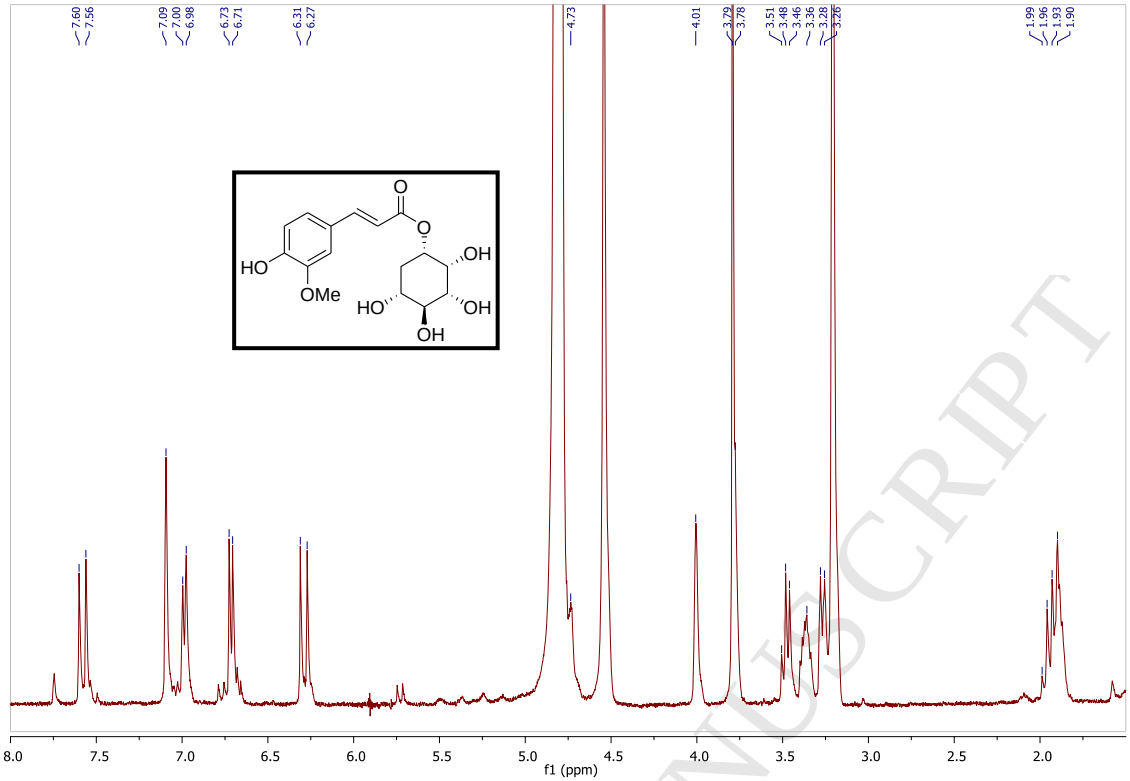

Figure 27. ^{1}H NMR spectrum of **7b** (CD_3OD)

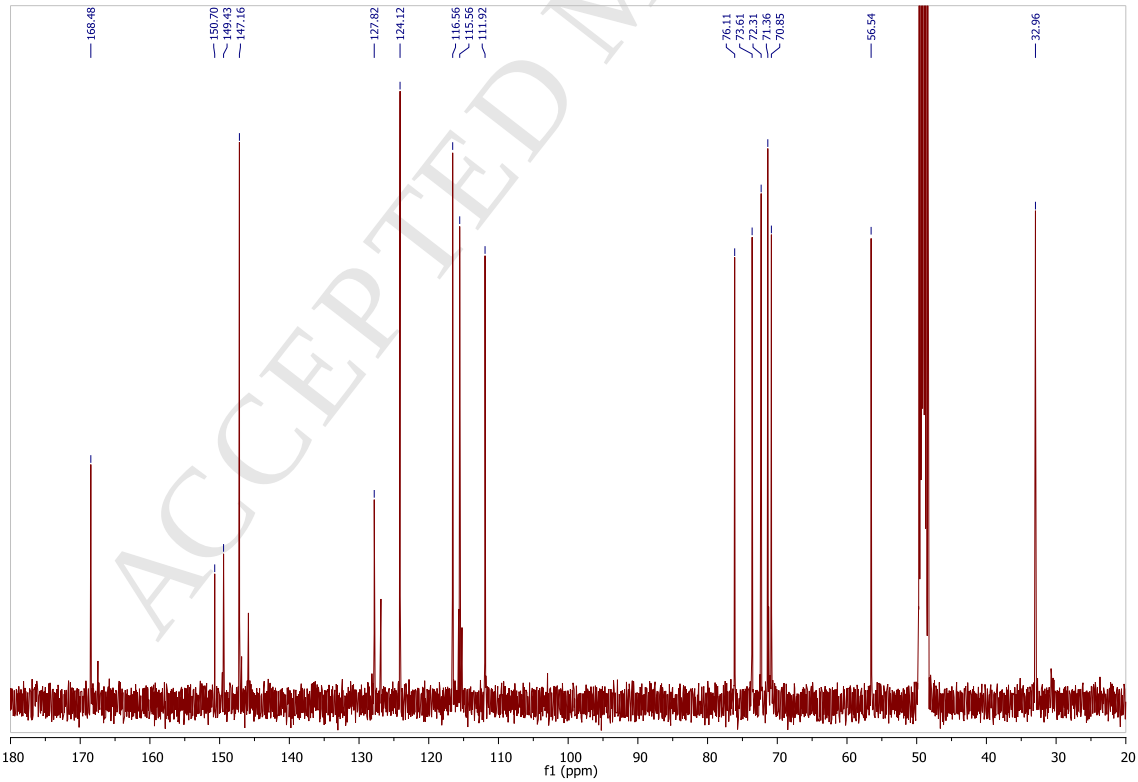

Figure 28. ^{13}C NMR spectrum of **7b** (CD_3OD)

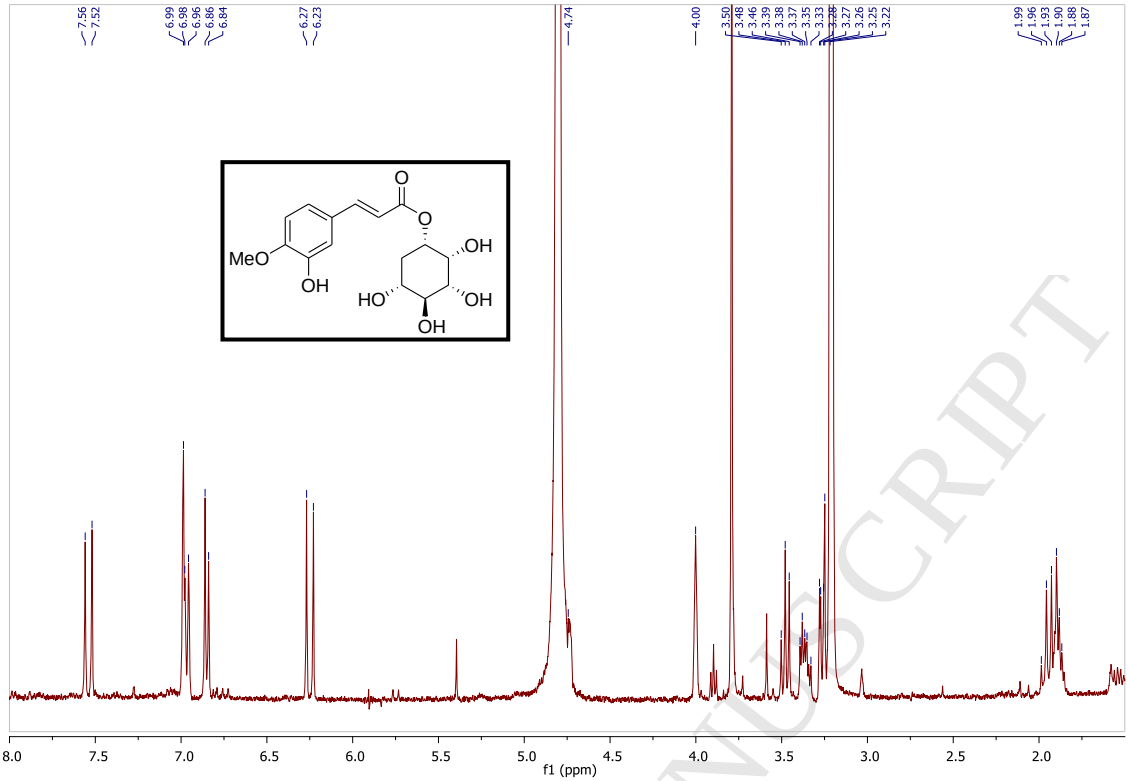

Figure 29. ^{1}H NMR spectrum of **8b** (CD_3OD)

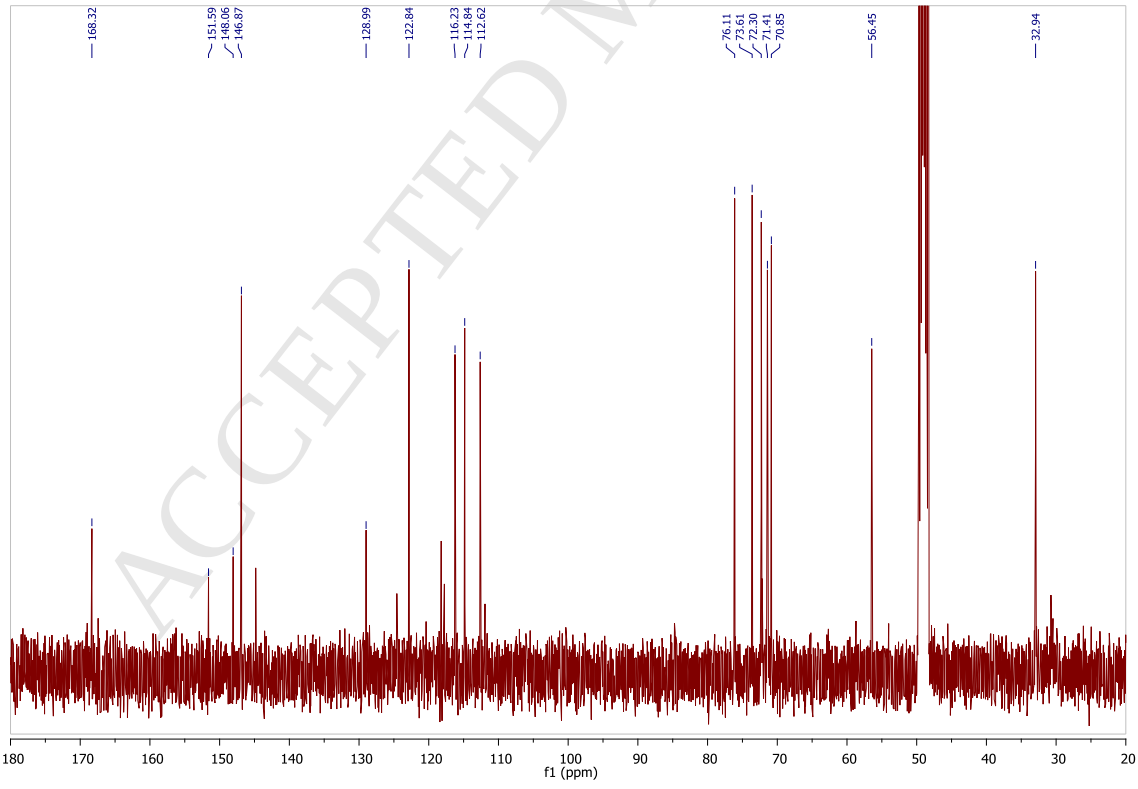

Figure 30. ^{13}C NMR spectrum of **8b** (CD_3OD)

Bioorganic & Medicinal Chemistry Letters 22 (2012) 1538–1540

Contents lists available at SciVerse ScienceDirect

Bioorganic & Medicinal Chemistry Letters

journal homepage: www.elsevier.com/locate/bmcl

Concise synthesis of (+)-conduritol F and inositol analogues from naturally available (+)-*proto*-quercitol and their glucosidase inhibitory activity

Wisuttaya Worawalai, Eakkaphon Rattanangkool, Avassaya Vanitcha, Preecha Phuwapraisirisan, Sumrit Wacharasindhu *

Natural Products Research Unit, Department of Chemistry, Faculty of Science, Chulalongkorn University, Bangkok 10330, Thailand

ARTICLE INFO

Article history:
Received 23 October 2011
Revised 24 December 2011
Accepted 4 January 2012
Available online 10 January 2012

Keywords:
Conduritol-F
α-Glucosidase
Quercitoll
Inositol
Diabetes mellitus

ABSTRACT

An effective synthesis of (+)-conduritol F, (+)-*chiro*- and (+)-*epi*-inositols from naturally available (+)-*proto*-quercitol is described. This synthetic method provides a concise synthesis of cyclitols in enantiomerically pure form. Of the synthesized cyclitols, (+)-conduritol F potently inhibits type I α-glucosidase with an IC_{50} value of 86.1 μM, which is five times greater than the standard antidiabetic drug, acarbose.

Conduritols are cyclitol derivatives possessing four contiguous hydroxyl groups on cyclohexene ring. There are ten possible stereoisomers; four enantiomeric pairs (conduritols B, C, E and F) and two *meso*-forms (conduritols A and D) (Fig. 1). Interest in conduritols and their analogues have been amplified due to synthetic challenge and presence of a variety of biological activities such as antifeedant, antibiotics, antileukemics and growth-regulation.[1] Currently, as a vital motif in potent anticancer narciclasine[2] and antidiabetic conduritol A,[3] facile and efficient synthetic approaches have been developed to produce optically pure conduritols in large quantity.

Over the course of our current research on new chemical entities as glycosidase inhibitors,[4] we recently reported the synthesis and inhibitory activity of amino quercitols from naturally available (+)-*proto*-quercitol.[4b] Although the starting quercitol has five contiguous hydroxyl groups on cyclohexane ring, exclusive formation of single bis-acetonide is crucial to obtain optically pure amino quercitols in few steps. With the success of our approach in hand, we expand the application to the synthesis other cyclitols.

Conduritol F is our first target because of prominent bioactivities and low natural abundance. Regardless of the presence of an unsaturation in conduritol F and one additional hydroxyl group in (+)-*proto*-quercitol, their gross structure and relative configuration are identical. Thus, dehydration of starting material would readily generate the desired product. Although several conduritols, including conduritol F, have been principally prepared through microbial and photo-oxidations of halogenated benzene,[2,5] vicinal-diols obtained after oxidation inevitably existed as a mixture of two or more stereoisomers. Therefore, preparation of conduritol F from optically pure starting materials is likely to be a method of choice to circumvent such problems. However, these approaches were limited by low yield of conduritol F obtained.[6] In this Letter, we report a short and effective synthesis of (+)-conduritol F and its inhibitory activity against types I and IIα-glucosidase. In addition,

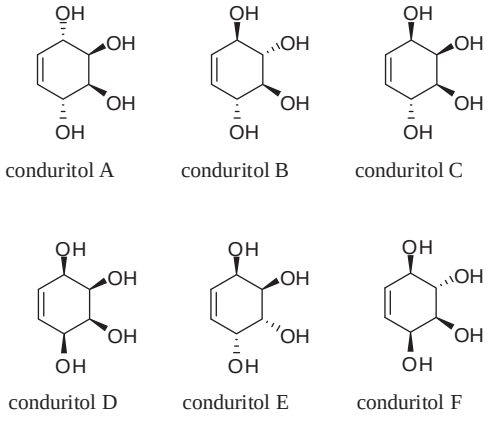

Figure 1. Structures of conduritols.

* Corresponding author.
E-mail address: sumrit.w@chula.ac.th (S. Wacharasindhu).

0960-894X/$ - see front matter © 2012 Elsevier Ltd. All rights reserved.
doi:10.1016/j.bmcl.2012.01.007

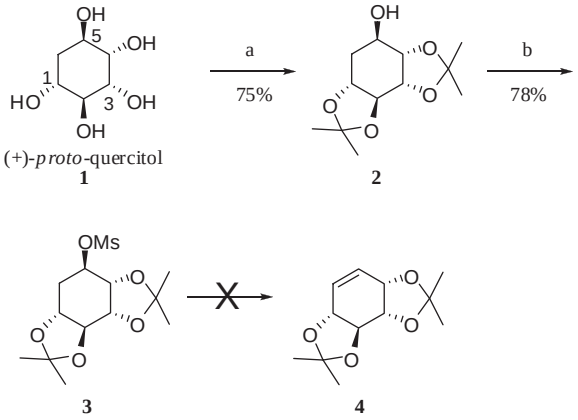

Scheme 1. Reagents and conditions: (a) 2,2-dimethoxypropane, *p*-TsOH, DMF, 75%; (b) $MeSO_2Cl$, Et_3N, DMAP, 78%.

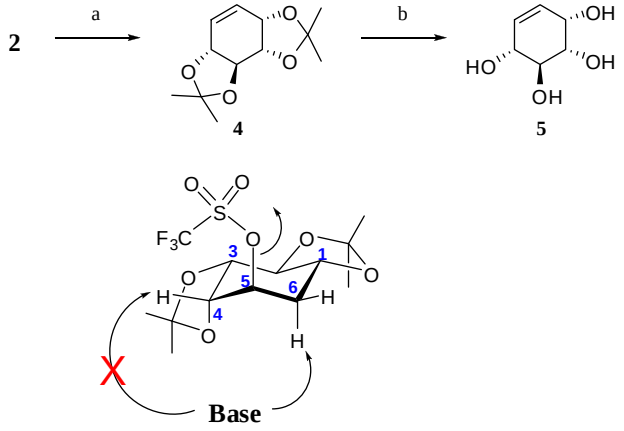

Scheme 2. Reagents and conditions: (a) Tf_2O, pyridine, −10 °C, 12 h, 68%; (b) 1.25MHCl/MeOH, rt, 4 h, quant.

the synthesis process also allowed us to prepare two corresponding inositols, (+)-*epi*- and (+)-*chiro*-isomers.

Our first attempt to synthesize conduritol F from the naturally available (+)-*proto*-quercitol was depicted in Scheme 1. The starting material utilized in this work was facilely isolated from the stems of *Arfeuillea arborescens* using method developed in our laboratory.[7] Notably, this method provides an efficient process, yielding a multiple gram of enantiomerically pure **1** (0.3% yield). It is also environmentally friendly as water is used during extraction and isolation. With compound **1** in hand, the bis-diol moiety was then preferentially protected as the corresponding acetonide to provide the desired compound **2** in an excellent yield. Since one hydroxyl group remains unprotected, it was thus activated with mesyl chloride to afford mesylate ester **3** in 78% yield. Unfortunately, elimination of **3** using various bases such as DBU, pyridine, and *t*-BuOK, in the hope that it would be converted to the protected conduritol **4**, was unsuccessful. More than 80% of **3** was recovered along with **4** in less than 5%. We hypothesized that mesyl group may not be a good leaving group under these conditions.

Having fail elimination reaction of **3** under basic conditions, we turned our focus on olefin formation directly via bis-acetonide **2** using strong dehydrating agents such as thionyl chloride, phosphorusoxychloride, Martin's reagent and trifluoromethanesulfonic anhydride. Treatment of **2** with $SOCl_2$ or $POCl_3$ in pyridine generated the complex mixtures along with trace amount of the desired alkene **4**. Moreover, Martin's sulfurane dehydrating agent was also employed in dry toluene under reflux but inseparable mixture along with 50% starting material were recovered. Fortunately, dehydration of **2** took place smoothly upon addition of Tf_2O in pyridine at −10 °C, affording the protected conduritol F (**4**) as the sole product (Scheme 2). This alternative route not only provided us a short-step conversion of (+)-*proto*-quercitol to conduritol F but also generated the desired product without any congeners.

The specificity of this elimination step is possibly attributed to steric effect. The bulky acetonide may block the proton abstraction at C-4 whereas *trans*-diaxial orientation of H-6_{ax} and the leaving group trifluoromethanesulfonyl facilitates E2 pathway, hence generating protected alkene **4**. Eventually, conduritol F (**5**) was obtained by deprotection of **4** with methanolic HCl. The NMR data and specific rotation (+79.5, c 1.12, MeOH) of our prepared conduritol F[8] were completely identical to those previously reported,[6a,9] confirming the absolute configuration as (+)-conduritol F.

The success in preparation of optically pure (+)-conduritol F allows us to access other cyclitols. The protected conduritol **4** could serve as a chiral building block for single-step conversion to

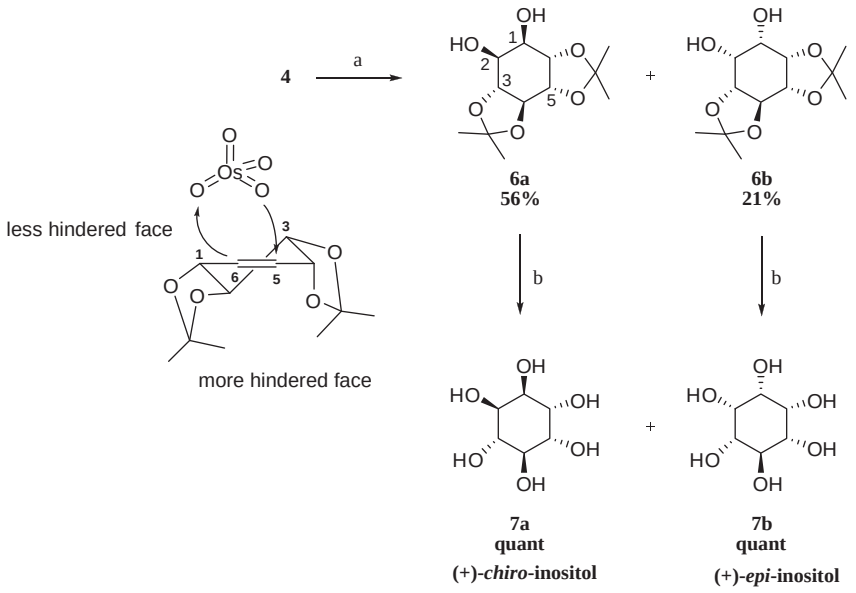

Scheme 3. Reagents and conditions: (a) OsO_4, NMO, *t*-BuOH/H_2O (1:1), 0 °C; (b) Amberlyst-15, MeOH/H_2O (7:3).

Table 1
α-Glucosidase inhibitory effect of cyclitols **1**, **5**, **7a** and **7b**

	IC_{50} (μM)		
Cyclitol	Baker's yeast	Maltase[a]	Sucrase[a]
1	NI[b]	NI	NI
5	86.1 ± 0.5	NI	NI
7a	1256.1 ± 1.7	NI	NI
7b	475.7 ± 0.9	NI	NI
Acarbose	403.9 ± 0.4	1.50 ± 0.14	2.38 ± 0.02

[a] α-Glucosidase was obtained from rat small intestine.
[b] NI, no inhibition, inhibitory effect less than 30% at 10 mg/mL.

inositol derivatives. Dihydroxylation of **4** using OsO_4 led to the formation of readily separable 3:1 diastereomeric inositols[10] **6a** and **6b** in 77% yield (Scheme 3). The selective formation of **6a** over **6b** could be rationalized by preferential osmylation on the less hindered face of alkene. Consequently, **6a** and **6b** were deprotected by Amberlyst-15 to quantitatively afford (+)-*chiro*-inositol (**7a**)[11] and (+)-*epi*-inositol (**7b**),[12] respectively.

(+)-Conduritol F (**5**) and inositols (**7a** and **7b**) were evaluated for α-glucosidase inhibitory activity using enzymes from two different sources; baker's yeast (type I) and rat small intestine (type II). They selectively inhibited α-glucosidase from baker's yeast,[13] in which **5** displayed highest inhibition with an IC_{50} value of 86.1 μM (Table 1). A potent inhibitory effect (6–16 times) of **5** over its corresponding diols, (+)-*chiro*-inositol (**7a**) and (+)-*epi*-inositol (**7b**), indicates that a half-chair conformation of cyclohexene moiety is more critical in binding active site of the enzyme than additional dihydroxy groups. This observation was also supported by a very low inhibition of (+)-*proto*-quercitol (**1**), a hydroxylated cyclitol of **5**. However, all cyclitols evaluated did not inhibit maltase and sucrase, type II α-glucosidases from rat small intestine.

In summary, we have simply and efficiently achieved short synthesis steps for (+)-conduritol F and inositols: (+)-*chiro*- and (+)-*epi*-inositols, from naturally available (+)-*proto*-quercitol. A key step involves dehydration of protected (+)-*proto*-quercitol (**2**) after addition of Tf_2O in pyridine, therefore taking a total of three steps to produce optically pure conduritol F in excellent yield. Furthermore, our method also provides rapid access to corresponding dihydroxy analogues, (+)-*chiro*- and (+)-*epi*-inositols. A potent inhibition of conduritol F, selectively against typeI α-glucosidase, over related compounds as well as antidiabetic drug acarbose suggests that its half-chair conformation is critical for its biological activity.

Acknowledgments

This work was supported by the Thailand Research Fund (DBG5380037) and Faculty of Science through the Research Strategic Plan (A1B1-6). W.W., E.R. and A.V. are grateful to the Royal Golden Jubilee Ph.D. Program (PHD/0025/2553), Chulalongkorn University Dutsadi Phiphat and Development and Promotion of Science and Technology Talents Project (DPST), respectively, for scholarships.

Supplementary data

Supplementary data (full experimental details and characterization data for **2**, **4**, **5**, **6a**, **6b**, **7a** and **7b**) associated with this article can be found, in the online version, at doi:10.1016/j.bmcl.2012.01.007.

References and notes

1. For recent review of conduritols see: Gültekin, M. S.; Çelik, M.; Balci, M. *Curr. Org. Chem.* **2004**, *8*, 1159.
2. Kornienko, A.; Evidente, A. *Chem. Rev.* **1982**, *2008*, 108.
3. Borges de Melo, E.; da Silveira Gomes, A.; Carvalho, I. *Tetrahedron* **2006**, *62*, 10277.
4. (a) Phuwapraisirisan, P.; Puksasook, T.; Jong-aramruang, J.; Kokpol, U. *Bioorg. Med. Chem. Lett.* **2008**, *18*, 4956; (b) Wacharasindhu, S.; Worawalai, W.; Rungprom, W.; Phuwapraisirisan, P. *Tetrahedron Lett.* **2009**, *50*, 2189; (c) Phuwapraisirisan, P.; Puksasook, T.; Kokpol, U.; Suwanborirux, K. *Tetrahedron Lett.* **2009**, *50*, 5864.
5. (a) Duchek, J.; Adams, D. R.; Hudlicky, T. *Chem. Rev.* **2011**, *111*, 4223; (b) Klbaş, B.; Balci, M. *Tetrahedron* **2011**, *67*, 2355; (c) Finn, K. J.; Collins, J.; Hudlicky, T. *Tetrahedron* **2006**, *62*, 7471; (d) Ogawa, S.; Uetsuki, S.; Tezuka, Y.; Morikawa, T.; Takahashi, A.; Sato, K. *Bioorg. Med. Chem. Lett.* **1999**, *11*, 1493.
6. (a) Cerè, V.; Mantovani, G.; Peri, F.; Pollicino, S.; Ricci, A. *Tetrahedron* **2000**, *56*, 1225; (b) Chiara, J. L.; Valle, N. *Tetrahedron: Asymmetry* **1995**, *6*, 1895; (c) Akiyama, T.; Shima, H.; Ohnari, M.; Okazaki, T.; Ozaki, S. *Bull. Chem. Soc. Jpn.* **1993**, *66*, 3760; (d) Akiyama, T.; Shima, H.; Ozaki, S. *Tetrahedron Lett.* **1991**, *32*, 5593.
7. Briefly, ground stems (1 kg) of *A. arborescens* were boiled with water (4 L) for 3 h. The decoction was filtered and partitioned twice with equal volume of CH_2Cl_2. The aqueous layer was loaded onto a column chromatography filled with wet Diaion HP20 (1 kg) and excessively eluted with H_2O (10 L). The combined aqueous elutes were lyophilized to afford white powder (3 g), which was subsequently purified by crystallization using hot MeOH.
8. (+)-Conduritol F (**5**): colorless oil, $[\alpha]_D^{25}$ = +79.5 (*c* 1.12, CH_3OH); ^1H NMR (CD_3OD, 400 MHz) δ 5.71 (ddd, *J* = 9.9, 4.8, 1.9 Hz, 1H), 5.64 (dd, *J* = 10.1, 2.0 Hz, 1H), 4.09 (t, *J* = 4.4 Hz, 1H), 3.85 (d, *J* = 7.6 Hz, 1H), 3.54 (dd, *J* = 10.4, 7.7 Hz, 1H), 3.35 (dd, *J* = 10.3, 4.0 Hz, 1H); ^{13}C NMR (CD_3OD, 100 MHz) δ 133.8, 128.0, 74.0, 73.9, 72.7, 68.0.
9. (a) Kwon, Y.-U.; Lee, C.; Chung, S.-K. *J. Org. Chem.* **2002**, *67*, 3327; (b) Heo, J.-N.; Holson, E. B.; Roush, W. R. *Org. Lett.* **2003**, *5*, 1697.
10. An attempt to address configurations of newly generated dihydroxy groups of **6a** and **6b** by NOESY could not be performed since severely overlapped signals of hydroxylated methine protons. However, significant difference in methyl signals of acetonides was observed; **6b** showed separated four methyl resonances whereas 6a demonstrated only three signals.
11. (+)-*chiro*-Inositol (**7a**): pale yellow oil: $[\alpha]_D^{25}$ = +81.9 (*c* 0.45, H_2O); ^1H NMR (D_2O, 400 MHz) δ 3.81 (br s, 2H), 3.54 (br d, *J* = 7.2 Hz, 2H), 3.37 (br d, *J* = 7.2 Hz, 2H); ^{13}C NMR (D_2O, 100 MHz) δ 72.8, 71.7, 70.5.
12. (+)-*epi*-Inositol (**7b**): white solid: $[\alpha]_D^{25}$ = +36.0 (*c* 0.27, H_2O); ^1H NMR (D_2O, 400 MHz) δ 3.86 (br s, 1H), 3.81 (br s, 1H), 3.53 (br s, 2H), 3.37 (dd, *J* = 7.2, 2.4 Hz, 1H), 3.28 (dd, *J* = 9.6, 2.4 Hz, 1H); ^{13}C NMR (D_2O, 100 MHz) δ 74.5, 72.8, 71.8, 71.7, 70.5.
13. Freeman previously reported inhibitory effect of conduritol F against β-galactosidase with an IC_{50} value of 600 μM; Freeman, S.; Hudlicky, T. *Bioorg. Chem. Med. Lett.* **2004**, *14*, 1209.

NPC Natural Product Communications

2013
Vol. 8
No. 0
1 - 4

First Identification of α-Glucosidase Inhibitors from Okra (*Abelmoschus esculentus*) Seeds

Wannisa Thanakosai [a,b] and Preecha Phuwapraisirisan[b,*]

[a]*Program of Biotechnology*, *Faculty of Science*, *Chulalongkorn University*, *Bangkok 10330*, *Thailand*
[b]*Natural Products Research Unit, Department of Chemistry*, *Faculty of Science*, *Chulalongkorn University*, *Bangkok 10330*, *Thailand*

preecha.p@chula.ac.th

Received: April 6th, 2013; Accepted: April 30th, 2013

Infusion of roasted okra seeds has long been consumed in Turkey for diabetes mellitus therapy. Previous reports of a hypoglycemic effect observed in rats administrated with okra seed extract indicated a possible connection with inhibition of intestinal α-glucosidase. An attempt to identify active components was first herein conducted using α-glucosidase-inhibition-guided isolation, yielding two major flavonol glucosides named isoquercetin (**2**) and quercetin-3-*O*-β-glucopyranosyl-(1‴→6″)-glucoside (**3**). They selectively inhibited rat intestinal maltase and sucrase, in which isoquercetin (**2**) was 6-10 times more potent than its related diglucoside **3**. This result suggested that an increase in hydrophilicity by the additional glucose residue in **3** led to a significant decline in the inhibitory effect and raised the possible involvement of the free 3-OH in exerting the inhibition. Our postulation was evaluated by examining α-glucosidase inhibition of quercetin (**1**), and the aglycone of **2** and **3**, whose 3-OH is free from any glucose moiety. Interestingly, **1** displayed a broad inhibitory effect toward rat intestinal and baker's yeast α-glucosidases, with improved potency. A kinetic study of **1** indicated that it inhibited maltase by two distinct mechanisms, in competitive (K_i 462 μM) and noncompetitive (K'_i 2153 μM) manners, whereas the mechanism underlying the inhibition of sucrase was verified as being of a competitive behavior (K_i 218 μM).

Keywords: Okra, *Abelmoschus* esculentus, Hypoglycemic, Diabetes mellitus, α-Glucosidase, Quercetin.

Maintaining good glycemic control is critical in diabetes therapy because it is associated with marked reduction in risk of developing complications such as cardiovascular diseases, neuropathy and retinopathy. Therefore, antihyperglycemic agents, particularly α-glucosidase inhibitors, are expected to provide such beneficial effects. Acarbose and voglibose are instances of potent α-glucosidase inhibitors currently used for diabetes therapy. They not only suppress postprandial glucose but also reduce the triglyceride level, body weight and systolic blood pressure. However, long-term intake of acarbose and voglibose resulted in undesired effects such as flatulence and diarrhea [1]. Therefore, new α-glucosidase inhibitors having minimized side effects are continuously required.

Edible plants are a prolific source of α-glucosidase inhibitors [2], in addition to their beneficial nutrition and safety on prolonged consumption. Prominent examples include corchoruside A, a flavonoid glycoside having a caffeoyl moiety isolated from *Corchorus olitorius* [3], which inhibited α-glucosidase three times more potently than acarbose. In the present study, we are intrigued by *Abelmoschus esculentus*, typically known as okra, because of its antidiabetic potential [4]. Okra fruit is high in mucilage [5,6], which was believed to delay glucose absorption into the bloodstream by its excellent water-holding and gel-forming capabilities. However, Palanuvej and coworkers [7] demonstrated that mucilage yield, glucose entrapping capability, and α-glucosidase inhibition of fruit aqueous extract were relatively low. Thus, the antidiabetic activity reported by Tomada [4] is not likely to be due to the mucilage.

Alternatively, roasted seeds, which are popularly consumed in Turkey as an herbal infusion, have long been recognized to attenuate blood glucose level. This ethnopharmacological claim was supported by *in vivo* antihyperglycemic activity. Oral administration of an aqueous extract in hyperglycemic rats prevented high blood glucose levels while a more pronounced and significant effect was observed in streptozotocin-induced diabetic rats [8]. However, there is no informative clue implied from early reports describing a possible mechanism underlying the hypoglycemic effect of okra seeds. Herein, we propose that α-glucosidase inhibition is one pathway in which okra seeds possibly exert their effect. An attempt to identify the active components in okra seeds resulted in the isolation of flavonol glucosides **2** and **3**. The mechanism underlying the inhibition is also reported.

An attempt to identify the active compounds responsible for suppressing blood glucose level was performed using an α-glucosidase inhibitory assay as guidance, coupled with chromatographic separation. The methanolic extract of the seeds when fractionated by vacuum column chromatography, afforded four major fractions. The combined second fraction (Fr2) displayed the highest inhibitory activity against rat intestinal maltase (76.3%) and sucrose (69.8%) (Figure 1). Further purification of the active fraction afforded the two principal components, which based on NMR and MS data, were identified as isoquercetin (**2**) and quercetin-3-*O*-β-glucopyranosyl-(1‴→6″)-glucoside (**3**) [9,10].

Flavonol glucosides **2** and **3** were subjected to evaluation for their inhibitory effects against α-glucosidases from two different sources, baker's yeast and rat intestine. Apparently, they selectively inhibited rat intestinal maltase and sucrose, whereas inhibitory activity against baker's yeast α-glucosidase was not observed (Table 1). Isoquercetin (**2**) revealed inhibition toward maltase and sucrase with IC_{50} values of 64.1 and 42.5 μM, respectively, which were 10 and 5 times, respectively, more potent than its corresponding diglucoside **3**. This observation suggested that the

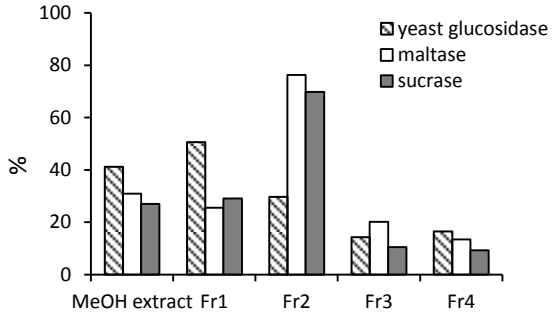

Figure 1: α-Glucosidase inhibitory effect of methanol extract and fractions after first-step purification, examined at concentration of 1.0 mg/mL.

increase in hydrophilicity by the extra glucose moiety in **3** dramatically reduced the inhibitory effect. We subsequently investigated the inhibitory activity of quercetin, the aglycone of **2** and **3**, in order to gain insight into the effect of 3-OH in exerting inhibition. Quercetin (**1**) used in our experiment was prepared from commercially available rutin by HCl-catalyzed hydrolysis.

Table 1: α-Glucosidase inhibitory effect of flavonoids **1-3**.

Compds	IC_{50} (μM)		
	Baker's yeast	Maltase	Sucrase
1	62.8 ± 2.1	12.3 ± 0.6	31.7 ± 1.5
2	NI[a]	64.1 ± 3.3	42.5 ± 1.2
3	NI	646 ± 5.8	265.7 ± 3.1
Acarbose	403.9 ± 0.4	1.50 ± 0.14	2.38 ± 0.02

[a]No inhibition, inhibitory effect less than 30% at 10 mg/mL.

Interestingly, **1** displayed a broad inhibitory effect against baker's yeast α-glucosidase (IC_{50} 62.8 μM), rat intestinal maltase (IC_{50} 12.3 μM) and sucrase (IC_{50} 31.7 μM), with improved potency (Table 1). Therefore, the presence of the free 3-OH in quercetin is required for α-glucosidase inhibition. To gain insight into the mechanism underlying this inhibitory effect, a kinetic study of **1** toward maltase and sucrase, instead of baker's yeast α-glucosidase, was carried out.

We designed such an experiment based on the fact that maltase and sucrase are more closely relevant to the α-glucosidases present in the human small intestine [11]. The Lineweaver–Burk plot of 1/v and 1/[maltose] (Figure 2) demonstrated a series of straight lines; all of which had different Y intercepts but intersected in the second quadrant. Kinetic analysis showed that V_{max} decreased with elevated K_m in the presence of increasing concentrations of **1**, therefore suggesting that maltase was inhibited by quercetin (**1**) in two distinct manners, competitive and noncompetitive (Table 2). This phenomenon could be rationalized by simultaneous formation of an enzyme-inhibitor (EI) complex in a competitive manner and an enzyme-substrate-inhibitor (ESI) complex in a noncompetitive manner.

To envisage the pathway in which quercetin (**1**) preferentially proceeded, the dissociation constants of EI (K_i) and ESI (K'_i) complexes were determined. The secondary plot of slope of lines in the Lineweaver–Burk relation versus the inhibitor concentration produced a K_i value of 462 μM, whereas the secondary plot of intercept versus inhibitor concentration generated a K'_i value of 2153 μM (Table 2). An approximately 5-fold lower dissociation constant of the EI complex suggested a closer binding between quercetin (**1**) and maltase and pointed out that competitive inhibition was predominant over noncompetitive behavior (Scheme 1). In addition, we also investigated the mechanism underlying the inhibitory effect of quercetin (**1**) against sucrase using the

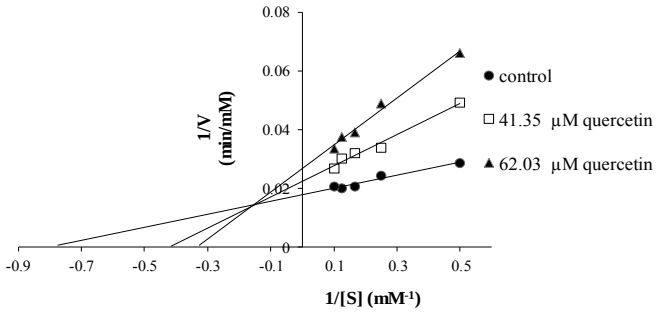

Figure 2: Lineweaver-Burk plot for inhibitory activity of quercetin (**1**) against rat intestinal maltase.

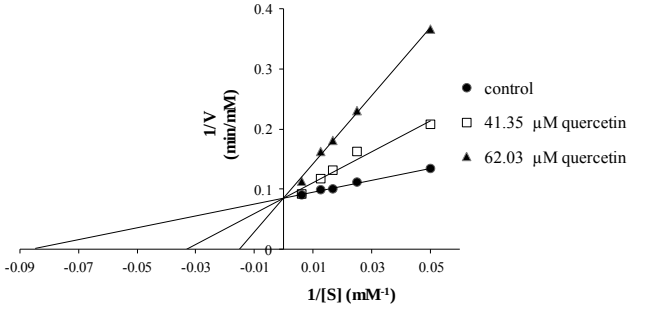

Figure 3: Lineweaver-Burk plot for inhibitory activity of quercetin (**1**) against rat intestinal sucrase.

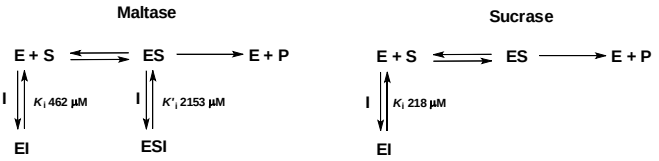

Scheme 1: Proposed inhibition mechanisms of quercetin (**1**, I) against maltase and sucrase; where E, S and P are maltase (or sucrase), maltose (or sucrose) and glucose, respectively.

Table 2: Kinetic data of intestinal α-glucosidase inhibition by quercetin (**1**).

Flavonoid	Maltase		Sucrase	
	K_i (μM)	Inhibition type	K_i (μM)	Inhibition type
1	462 2153[a]	Mixed	218	Competitive

[a] K'_i value for noncompetitive manner.

aforementioned approach. The Lineweaver–Burk plot of **1** against sucrase (Figure 3) revealed a series of straight lines, all of which intersected at the Y axis. Kinetic analysis revealed that K_m increased while V_{max} remained constant in the presence of increasing concentrations of **1**, therefore indicating competitive inhibition (Scheme 1) with a K_i value of 218 μM (Table 2).

Quercetin (**1**) was previously reported as a potent inhibitor against baker's yeast α-glucosidase. However, the mechanism underlying the inhibitory effect reported by two groups is different; it was first reported as a noncompetitive inhibitor by Lee [12] and subsequently as a mixed-type of noncompetitive and anticompetitive inhibitor by Li [13]. Although a significant amount of **1** could not be detected in our experiment, its corresponding glucosides **2** and **3** could be transformed into aglycone **1** by lactase phlorizin hydrolase [14,15], an extracellular enzyme located at the brush border membrane of intestinal cells. In addition, Turkish ethnopharmacological use of roasted okra seeds as an infusion is likely to enhance liberation of quercetin from its glycosides by thermal-assisted hydrolysis.

In summary, we are the first to identify flavonol glucosides **2** and **3**, present in okra seeds, as the major inhibitors against α-glucosidase. The glucosides **2** and **3** possibly exert a beneficial effect on diabetes mellitus therapy by being transformed into the active quercetin (**1**), which can attenuate blood glucose levels through inhibiting maltase and sucrase functions. The highly improved inhibitory effect of **1** over **2** and **3** indicated that free 3-OH is required for retarding the α-glucosidase function. The mechanism underlying the inhibition of quercetin discovered in our investigation suggested a possible guidance for the use of okra seeds as a single alternative drug or in combination with currently used antidiabetic drugs.

Experimental

Plant material: Okra (*Abelmoschus esculentus*) seeds were collected at Nakornpatom, Thailand, in November 2010. The plant material was identified by the botanist, Mrs Parinyanutch Klinrat, and the voucher specimens (BCU013433) were deposited at the Herbarium of the Department of Botany, Faculty of Science, Chulalongkorn University, Thailand.

Extraction and isolation: The air-dried seeds (62 g) were ground and extracted with methanol (3 × 250 mL) at room temperature. The extract was evaporated under reduced pressure to afford a brown syrup (12 g). The methanolic extract was absorbed on silica gel (20 g) and subjected to chromatography on silica gel, eluting (500 mL each fraction) with dichloromethane, methanol-dichloromethane (1:9), methanol-dichloromethane (2:8) and methanol-dichloromethane (1:1). The active fraction (Fr2), which was mainly eluted with methanol-dichloromethane (2:8), was dissolved in ethyl acetate and centrifuged. The precipitates, which are soluble in methanol, were further purified on a Sephadex LH-20 column (methanol), yielding quercetin-3-*O*-β-glucopyranoside or isoquercetin (**2**, 490 mg). In addition, the other active fractions, which were mainly eluted with methanol-dichloromethane (1:1) were subsequently purified by Sephadex LH-20 CC (methanol), affording quercetin-3-*O*-β-glucopyranosyl-(1‴→6″)-glucoside (**3**, 189 mg).

Preparation of quercetin: Rutin (100 mg) was dissolved in 3M methanolic HCl (10 mL) and refluxed at 60-70°C for 6 h. The reaction mixture was diluted with water (2 mL) and centrifuged. The precipitate obtained after centrifugation was washed with water until the supernatant was neutral to universal indicator paper, and then oven dried (80-85°C) to afford quercetin (**1**, 47 mg).

α-Glucosidase inhibition assay: The inhibitory effect against α-glucosidase from baker's yeast was tested using our previously reported protocol [16,17]. Briefly, the α-glucosidase (0.1 U/mL) and substrate (1 mM *p*-nitrophenyl-α-D-glucopyranoside) were dissolved in 0.1 M phosphate buffer, pH 6.9. Ten μL of test compound (1 mg/mL in DMSO) was incubated with 40 μL of α-glucosidase at 37ºC for 10 min. Fifty μL substrate solution was then added to the reaction mixture and incubated at 37ºC for an additional 20 min. After the reaction had been terminated by adding 100 μL of 1 M Na_2CO_3, enzymatic activity was quantified by measuring the absorbance at 405 nm (Bio-Red microplate reader model 3550 UV). The percentage inhibition was calculated by $[(A_0-A_1)/A_0] \times 100$, where A_0 is the absorbance without the sample, and A_1 is the absorbance with it. The IC_{50} value was determined from a plot of the percentage inhibition versus the sample concentration. Acarbose was used as the standard control and the experiment was performed in triplicate.

In addition, inhibitory activity against α-glucosidase from rat intestine was determined using our developed method [16,17]. The crude enzyme solution prepared from rat intestinal acetone powder was used as a source of maltase and sucrase. Rat intestinal acetone powder (1 g) was homogenized in 30 mL of 0.9% NaCl solution. After centrifugation (12,000 *g* × 30 min), the aliquot was subjected to assay. Ten μL of test compound was added to a substrate solution (10 mM maltose and 100 mM sucrose, each 20 μL), 0.1 M phosphate buffer (pH 6.9, 30 μL), glucose oxidase solution (80 μL) and enzyme solution (20 μL). The reaction mixture was incubated at 37°C (10 min for maltase and 40 min for sucrose) and its absorbance determined at 500 nm. Percentage inhibition and IC_{50} values were obtained using the aforementioned methodology.

Kinetic study of α-glucosidase inhibitory effect: The mechanism underlying the inhibitory effect was investigated by analyzing the enzyme kinetic data using the above reaction. Maltase activity was maintained at 0.45 U/mg protein in the presence of quercetin (from 0.1–1.0 mg/mL) at various concentrations of maltose (2, 6, 10, 16, 20 mM). A series of V_{max} and K_m values were obtained from the Y intercepts and calculated by slope × V_{max}, respectively. A similar method was also applied for sucrase, in which its activity was kept at 0.07 U/mg protein**.**

Acknowledgments - This work was supported by the Thailand Research Fund (DBG5380037) and National Research University Project of CHE and Ratchadaphiseksomphot Endowment Fund (FW645A).

References

[1] Chiasson JL, Josse RG, Gomis R, Hanefeld M., Karasik A, Laakso M. (**2002**) Acarbose for prevention of type 2 diabetes mellitus: The STOP-NIDDM randomised trial. *Lancet*, ***359***, 2072-2077.

[2] Hung HY, Qian K, Morris-Natschke SL, Hsu CS, Lee KH. (**2012**) Recent discovery of plant-derived anti-diabetic natural products. *Natural Product Reports*, ***29***, 580-606.

[3] Phuwapraisirisan P, Puksasook T, Kokpol U, Suwanborirux K. (**2009**) Corchorusides A and B, new flavonol glycosides as α-glucosidase inhibitors from the leaves of *Corchorus olitorius*. *Tetrahedron Letters*, ***50***, 5864-5867.

[4] Tomoda M, Shimizu N, Gonda R, Kanari M, Hikino H. (1989) Anticomplementary and hypoglycemic activity of okra and *Hibiscus* mucilages. *Carbohydrate Research, 190*, 323-328.

[5] El-Mahdy AR, El-Sebaiy LA. (**1984**) Preliminary studies on the mucilages extracted from okra fruits, taro tubers, Jew's mellow leaves and fenugreek seeds. *Food Chemistry*, ***14***, 237-249.

[6] Ramadas Bhat U, Tharanathan RN. (**1986**) Fractionation of okra mucilage and structural investigation of an acidic polysaccharide. *Carbohydrate Research*, ***148***, 143-147.

[7] Palanuvej C, Hokputsa S, Tunsaringkarn T, Ruangrungsi N. (**2009**) *In vitro* glucose entrapment and alpha-glucosidase inhibition of mucilaginous substances from selected Thai medicinal plants. *Scientia Pharmaceutica*, ***77***, 837-849.

[8] Aslan M, Sezik E, Yeşilada E. (**2003**) Effect of *Hibiscus esculentus* L. seeds on blood glucose levels in normoglycaemic, glucose-hyperglycaemic and streptozotocin-induced diabetic rats**.** *Gazi Universitesi Eczacilik Fakultesi Dergisi*, ***20***, 1-7.

[9] Shui G, Peng LL. (**2004**) An improved method for the analysis of major antioxidants of *Hibiscus esculantus* Linn. *Journal of Chromatography A*, ***1048***, 17-24.

[10] Markham KR, Geiger H. (**1994**) ^{1}H Nuclear magnetic resonance spectroscopy of flavonoids and their glycosides in hexadeuterodimethylsulfoxide. In *The Flavonoids, Advances in Research Since 1986*. Harborne JB. (Ed.). Chapman & Hall, London, UK, 448-463.

[11] Oki T, Matsui T, Osajima Y. (**1999**) Inhibitory effect of α-glucosidase inhibitors varies according to its origin. *Journal of Agricultural and Food Chemistry*, ***47***, 550-553.

[12] Lee DS, Jong GK, Lee SH. (**2006**) Inhibition of α-glucosidase activity by quercetin. *Korean Journal of Microbiology and Biotechnology*, ***34***, 368-372.

[13] Li YQ, Zhou FC, Gao F, Bian JS, Shan F. (**2009**) Comparative evaluation of quercetin, isoquercetin and rutin as inhibitors of α-glucosidase. *Journal of Agricultural and Food Chemistry*, ***57***, 11463-11468.

[14] Sesink ALA, Arts ICW, Faassen-Peters M, Hollman PCH. (**2003**) Intestinal uptake of quercetin-3-glucoside in rats involves hydrolysis by lactase phlorizin hydrolase. *Journal of Nutrition*, ***133***, 773-776.

[15] Day AJ, Gee JM, DuPont MS, Johnson IT, Williamson G. (**2003**) Absorption of quercetin-3-glucoside and quercetin-4′-glucoside in the rat small intestine: The role of lactase phlorizin hydrolase and the sodium-dependent glucose transporter. *Biochemical Pharmacology*, ***65***, 1199-1206.

[16] Wikul A, Damsud T, Kataoka K, Phuwapraisirisan P. (**2012**) (+)-Pinoresinol is a putative hypoglycemic agent in defatted sesame (*Sesamum indicum*) seeds though inhibiting α-glucosidase**.** *Bioorganic & Medicinal Chemistry Letters*, ***22***, 5215-5217.

[17] Worawalai W, Wacharasindhu S, Phuwapraisirisan P. (**2012**) Synthesis of new *N*-substituted aminoquercitols from naturally available (+)-*proto*-quercitol and their α-glucosidase inhibitory activity. *Medicinal Chemistry Communications*, ***3***, 1466-1470.

Phytochemistry Letters 6 (2013) 350–354

Contents lists available at SciVerse ScienceDirect

Phytochemistry Letters

journal homepage: www.elsevier.com/locate/phytol

Three new phenylpropanoyl amides from the leaves of *Piper sarmentosum* and their α-glucosidase inhibitory activities

Thanakorn Damsud [a,b], Sirichai Adisakwattana [c], Preecha Phuwapraisirisan [a,*]

[a] Natural Products Research Unit, Department of Chemistry, Faculty of Science, Chulalongkorn University, Bangkok 10330, Thailand
[b] Program of Biotechnology, Faculty of Science, Chulalongkorn University, Bangkok 10330, Thailand
[c] Department of Nutrition and Dietetics, Faculty of Allied Health Science, Chulalongkorn University, Bangkok 10330, Thailand

ARTICLE INFO

Article history:
Received 1 February 2013
Received in revised form 28 March 2013
Accepted 14 April 2013
Available online 9 May 2013

Keywords:
Piper sarmentosum
Phenylpropanoyl amide
Glucosidase inhibitor
Pyrrolidone

ABSTRACT

Piper sarmentosum is pungent climber that is a widely used vegetable in Southeast Asia. In screening for α-glucosidase inhibitors from edible plants, an inhibitory activity in the leaf extract of *P. sarmentosum* was observed. Bioassay-guided fractionation resulted in the isolation of three new phenylpropanoyl amides, named chaplupyrrolidones A (**1**) and B (**2**) and deacetylsarmentamide B (**7**). Chaplupyrrolidones A and B contained a 5-oxygenated-Δ^3-2-pyrrolidone moiety, which is the first report of their natural encounter. Of these all isolated compounds, **2** revealed most potent inhibition against α-glucosidase, which is 18-fold more active than its demethylated congener, **1**. Kinetic evaluation of **2** indicated that it acts as a noncompetitive inhibitor.

1. Introduction

Piper sarmentosum Roxb. (Piperales: Piperaceae), commonly known in Thai as Chaplu, is a climbing or erect herb with a characteristic pungent odor within the family Piperaceae, which is comprised of over 700 known species worldwide (Parmar et al., 1997). Several promising bioactivities of *P. sarmentosum*, such as inducing apoptosis through mitochondrial transmembrane disruption (Pan et al., 2011), modulating HIF-2 transcription (Bokesch et al., 2011), *in vivo* antioxidant (Hussain et al., 2010) and allelopathy (Piyatida et al., 2012), have recently been reported.

Members of the *Piper* genus have a high economical, commercial and medicinal importance. Predominant secondary metabolites encountered in the genus include the phenylpropanoid (C6–C3) derived compounds, such as lignans, propenylphenols and kawapyrones, in addition to phenylpropanoyl amides, which are rather unique to fewer genera. To date, over 30 phenylpropanoyl amides have been isolated from *P. sarmentosum*, and phytochemical investigation of this species remains attractive due to the unprecedented array of different chemical structures that vary with different cultivars/geographical cultivation areas. In the search for α-glucosidase inhibitors from edible plants (Phuwapraisirisan et al., 2008, 2009) and synthesis of glycomimics from cyclitols (Worawalai et al., 2012a,b), *P. sarmentosum* became of interest due to its inhibitory activity against α-glucosidase in our preliminary screening and the previous report of its antidiabetic activity (Peungvicha et al., 1999; Zar et al., 2012). α-Glucosidase inhibitory guided fractionation led to the isolation of three new phenylpropanoyl amides, named chaplupyrrolidones A (**1**) and B (**2**) and deacetylsarmentamide B (**7**), in addition to four known phenylpropanoids (**3**–**6**) (Fig. 1).

2. Results and discussion

The active CH_2Cl_2 extract obtained from the dried leaves of *P. sarmentosum* was bioassay-guided fractionated to yield seven main fractions. The active fractions were further purified by chromatography techniques to afford new compounds **1**, **2** and **7**, whose structures were characterized based on spectroscopic data and chemical analysis.

Chaplupyrrolidone A (**1**) was obtained as yellow powder. The molecular formula $C_{13}H_{13}NO_3$ was determined by HRESIMS of pseudomolecular ion $(M+H)^+$ at *m*/*z* 232.0975 (calcd 232.0974), in conjunction with NMR data analysis. The ^{13}C NMR spectrum showed ten carbon signals that were ascribable to two methylene (δ_C 29.9 and 38.0), eight methine (δ_C 81.9, 126.3 (2×), 128.5 (3×), 128.6 and 147.4) and three quaternary carbons (δ_C 140.5, 167.7 and 173.6), based on the HSQC data analysis. In addition, **1** revealed ^1H NMR signals in three distinct regions: phenyl protons [δ_H 7.13–7.24 (m, 5H)], olefinic protons [δ_H 6.12 and 7.07 (each 1H)] and downfield methylene protons [δ_H 3.20 and 2.93 (each 2H)]. The COSY spectrum also showed three separate spin systems (Fig. 2a) that were comprised of monosubstituted benzene, two contiguous

* Corresponding author. Tel.: +66 2 218 7624; fax: +66 2 218 7598.
E-mail address: preecha.p@chula.ac.th (P. Phuwapraisirisan).

1874-3900/$ – see front matter
http://dx.doi.org/10.1016/j.phytol.2013.04.001

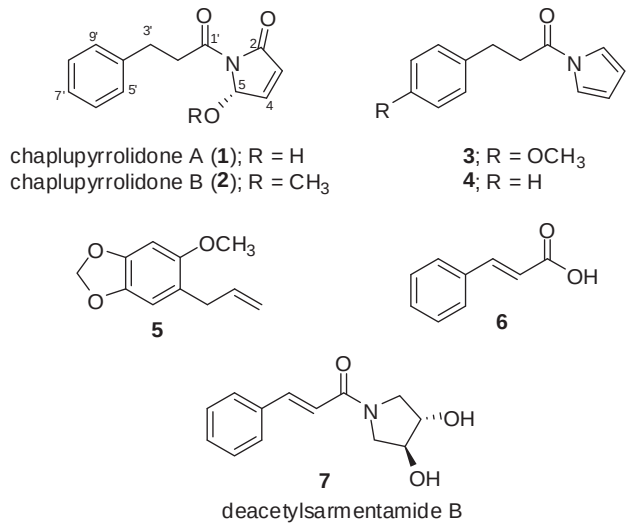

Fig. 1. Structures of isolated compounds.

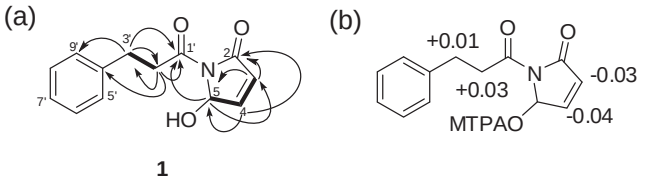

Fig. 2. (a) Selected HMBC (arrow curves) and COSY (bold lines) correlations of chaplupyrrolidone A (**1**); (b) the $\Delta\delta H_{SR}$ distribution of MTPA esters of **1**.

methylenes as well as olefinic methines linked with oxygenated proton at δ_H 6.07. Each established residue was assembled using the HMBC data analysis. The left end of the two contiguous methylenes was connected with a benzene ring, as evident by the cross peaks of H-3′/C-9′ and H-2′/C-4′, while the right terminal was linked to C-1′ (δ_C 173.6), as indicated by the HMBC correlations of H-2′ and H-3′ to C-1′, thereby establishing the phenylpropanoyl motif. The remaining portion ($C_4H_4NO_2$) contained an α,β-unsaturated amide, as deduced by the presence of the quaternary carbon at δ_C 167.7 and the olefinic signals [δ_H 6.12 (d, J = 6.0 Hz) and δ_C 128.5, and δ_H 7.07 (dd, J = 4.4, 6.0 Hz) and δ_C 147.4]. This portion was similar to the Δ^3-2-pyrrolidone moiety of sarmentamide A (Tuntiwachwuttikul et al., 2006), except for the presence of unusual downfield shifts of the methine signal (δ_H 6.07 and δ_C 81.9). The aforementioned data indicated that the methylene group in the Δ^3-2-pyrrolidone moiety of sarmentamide A was replaced by an oxygenated methine in **1**, thereby establishing the 5-hydroxy-Δ^3-2-pyrrolidone portion. The diagnostic HMBC cross peak of H-5/C-1′ indicated the connectivity of phenylpropanoyl and 5-hydroxy-Δ^3-2-pyrrolidone moieties through a nitrogen atom, thus constructing the overall structure of **1**. The absolute configuration of the secondary alcohol group at C-5 was addressed using Mosher's method (Ohtani et al., 1991). MTPA esters of **1** were prepared and the differences in chemical shifts ($\Delta\delta H_{SR}$) between *S*-(−)-MTPA and *R*-(+)-MTPA esters were deduced as shown in Fig. 2b. The $\Delta\delta H_{SR}$ distribution around C-5 indicated its absolute configuration to be *S*.

Chaplupyrrolidone B (**2**) was obtained as yellow powder. The molecular formula was deduced from the HRESIMS analysis of pseudomolecular ion $(M+H)^+$ at m/z 246.1121 (calcd 246.1130), which accounted for the $C_{14}H_{15}NO_3$ formulae. It displayed ^1H and ^{13}C NMR resonances nearly identical to those of **1**, except for subtle difference in signals of the H-5 (δ_H 5.93) and C-5 (δ_C 88.9). Careful examination of the NMR spectra together with additional 14 amu and one methoxy signal (δ_H 3.32 and δ_C 55.4) in **2** pointed out the presence of the methoxy group, which was positioned at C-5 by the discernable HMBC cross peaks of 5-OCH_3 (δ_H 3.32) to C-5 and H-5 to 5-OCH_3 (δ_C 55.4). Although **2** has one chiral center at C-5, the absolute configuration could not be readily addressed by applying Moscher's method. However, the closely related NMR spectra of **1** and **2** along with the negative specific rotation of **2** allowed us to propose the *S* configuration for **2**.

Deacetylsarmentamide B (**7**) was obtained as yellow solid. The molecular formula $C_{13}H_{15}NO_3$ was established by the HRESIMS analysis of the pseudomolecular ion $(M+Na)^+$ at m/z 256.0944 (calcd 256.0950). **7** showed ^1H and ^{13}C NMR spectra that only resembled those of **1** and **2** in the aromatic region. Although signals of olefinic protons (H-2′ and H-3′) were also observed in **7**, a large coupling constant of 15.6 Hz indicated their *trans*-orientation. The HMBC cross peaks of H-2′/C-4′, H-3′/C-1′, H-3′/C-2′ and H-3′/C-9′ suggested that *trans*-olefinic protons were located between the benzene ring and the quaternary carbonyl (δ_C 167.7), which was relatively upfield compared to those observed in **1** and **2**, which together established the *trans*-cinnamoyl moiety. The remaining residue of $C_4H_8NO_2$ was assigned to be a dioxygenated pyrrole based on the COSY and HMBC data analysis (Fig. 3b). The COSY spectrum showed contiguous correlations of H-2 (δ_H 3.68 and 3.71), H-3 (δ_H 4.20), H-4 (δ_H 4.13) and H-5 (δ_H 3.60 and 3.95), suggesting a spin system of –N–CH_2–CH(O)–CH(O)–CH_2–N–. The ^1H and ^{13}C NMR chemical shifts of this residue were related to those of the deoxygenated pyrrole group in sarmentamide B, except for the striking upfield shifts of C-3 and C-4. This information indicated that the two acetoxy groups in sarmentamide B were both replaced by hydroxy groups in **7**. The dioxygenated pyrrole moiety was connected to the cinnamoyl residue through an amide bond, supported by the HMBC

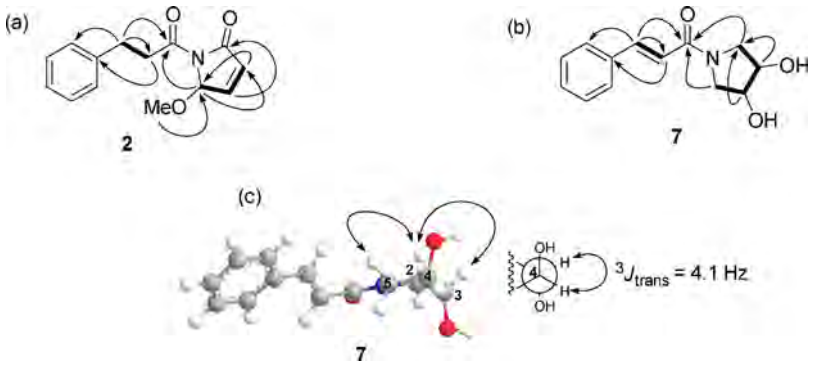

Fig. 3. (a and b) Selected HMBC (arrow curves) and COSY (bold lines) correlations of **2** and **7**, respectively; (c) diagnostic NOESY correlations and Newman projection showing dihedral angle of H-3 and H-4 on deoxygenated pyrrole of **7**.

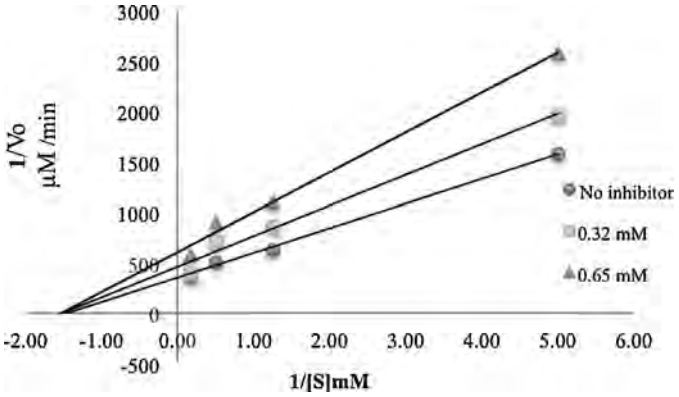

Fig. 4. Lineweaver–Burk plot of chaplupyrrolidone B (**2**) against α-glucosidase.

correlations of H-2/C-1′ and H-5/C-1′. Once the overall structure of **7** was established, the relative configuration of C-3 and C-4 were addressed by NOESY and coupling constant analysis. The observed NOESY correlations of H-2β/H-5β and H-2β/H-3 (Fig. 3c) indicated that they occupied the same phase, whilst the small coupling constant (4.1 Hz) of H-3 and H-4 suggested their *trans*-orientation to the vicinal protons in the dihydroxy pyrrolidine ring (Clerc and Simon, 1989).

1 and **2** were both found to inhibit α-glucosidase *in vitro* with IC_{50} values of 7820 and 430 μM, respectively, while **3**–**7** showed no detectable inhibition (Table 2). Interestingly, compound **2** was 18-fold more potent than that of **1** and was comparable to the antidiabetic drug acarbose (IC_{50} value of 404 μM). To gain insight into the mechanism underlying the inhibitory effect of **2**, a kinetic study was also conducted. The Lineweaver–Burk plots (Fig. 4) revealed a linear relationship at each tested concentration of **2**, all of which intersected the *x*-axis at a single negative value. The analysis demonstrated that V_{max} decreased with increasing concentrations of **2** while K_m remained constant, supporting that **2** inhibits α-glucosidase in a noncompetitive manner (K_i of 1.04 mM) by equally forming enzyme-inhibitor and substrate–enzyme-inhibitor complexes

In summary, three new phenylpropanoyl amides (**1**, **2** and **7**) were isolated, of which **1** and **2** act as α-glucosidase inhibitors. Regardless of sarmentamide A, which encompasses a Δ^3-2-pyrrolidone moiety, **1** and **2** are the first reported natural 5-oxygenated-Δ^3-2-pyrrolidones products. Acyl and alkyl 5-oxygenated-Δ^3-2-pyrrolidones have been employed as versatile building blocks (Kiren et al., 2009) for the synthesis of unusual γ-amino acids and particular alkaloids, such as gelsemine (Cooper et al., 1995). In addition, the striking difference in α-glucosidase inhibitory activity between **1** and **2** suggested that the 5-OMe group was possibly associated with the observed α-glucosidase inhibition.

3. Experimental

3.1. General experimental procedures

UV spectra were measured with a UV-7504 spectrophotometer. Optical rotations were determined using a Perkin-Elmer 341 polarimeter using a cell with a 2-mL capacity and a 10 cm path length. High resolution mass spectra were recorded on a Bruker micrOTOF mass spectrometer, equipped with an electrospray ionization (ESI) ion source. The ^1H and ^{13}C NMR spectra were acquired by Varian Mercury+ 400 and Bruker AVANCE 400 spectrometers. Chemical shifts were reported in δ (ppm) relative to deuterated solvent residues (7.25 and 77.0 ppm for $CDCl_3$ and 3.30 and 49.0 ppm for CD_3OD). TLC was performed on precoated Merck silica gel 60 F_{254} plates (0.25 mm thick layer), and spots were visualized under UV or dipped in 3% (v/v) anisaldehyde, 9.7% (v/v) H_2SO_4, 87.3% (v/v) MeOH followed by heating. α-Glucosidase (EC 3.2.1.20) from *Saccharomyces cerevisiae* and 4-nitrophenyl-α-D-glucopyranoside (PNPG) were obtained from Sigma–Aldrich (St. Louis, MO, USA). Acarbose was obtained from Bayer Vitol Leverkusen, Germany. Spectrophotometric measurements for the α-glucosidase inhibition and kinetic study were taken on a Sunrise microplate reader.

3.2. Plant material

The leaves of *P. samentosum* were collected from Samutprakan, in February 2011. Plant authentication was performed Mrs. Parinyanutch Klinrat, Department of Botany, Faculty of Science, Chulalongkorn University. A voucher specimen (BCU013525) has deposited at the Department of Botany, Faculty of Science, Chulalongkorn University (Bangkok, Thailand).

3.3. Extraction and isolation

The dried leaves of *P. sarmentosum* (812 g) were sequentially extracted at room temperature with hexane (3× 4 L) and MeOH (3× 5 L), respectively. The MeOH extract was suspended in water and partitioned with CH_2Cl_2 (3× 1 L) to afford the active CH_2Cl_2 extract, which was chromatographed by Vacuum column chromatography (silica gel 60G Merck) column (120 mm ID × 7 cm length) and eluted with a six step gradient mobile phase of 0:1, 1:9, 3:7, 1:1, 4:1 and 1:1 (v/v) ratio EtOAc:hexane, to afford seven major fractions. Fraction 3 was preliminarily chromatographed on Sephadex LH-20 with a 1:9 (v/v) MeOH:CH_2Cl_2 mobile phase to remove the residual chlorophylls, which eluted in the early fractions. The fractions that eluted after the chlorophylls were combined, concentrated and subsequently purified by silica gel centrifugal chromatography using mixtures of EtOAc:hexane as the eluting mobile phase. Two major bands eluted in the 3:7 (v/v) EtOAc:hexane fractions and were collected separately to yield **1** (24 mg) and **2** (20 mg). *N*-(3-(4′-Methoxyphenyl)propanoyl)pyrrole (**3**, 12 mg), *N*-(3-phenylpropanoyl)pyrrole (**4**, 9 mg) and asaricin (**5**, 18 mg) were subsequently obtained in the fractions eluted with 4:6 (v/v) EtOAc:hexane. Fraction 5 was chromatographed on Sephadex LH-20 (1:9 MeOH–CH_2Cl_2) followed by crystallization (MeOH) to afford cinnamic acid (**6**, 380 mg). Fraction 7 was chromatographed on Sephadex LH-20 (1:9 MeOH–CH_2Cl_2) to remove the chlorophylls, and the combined fractions eluted after the chlorophylls were further purified by silica gel centrifugal chromatography and eluted with a 2:8 (v/v) MeOH:CH_2Cl_2 mobile phase to give deacetylsarmentamide B (**7**, 40 mg).

3.3.1. Chaplupyrrolidone A (*1*)

Yellow powder; $[\alpha]_D^{20}$ −2.4° (*c* 0.335, CH_2Cl_2); UV (CH_2Cl_2) λ_{max} (log ε) 266 (6.46) nm; HRESIMS *m*/*z* $[M+H]^+$ 232.0975 (calcd for $C_{13}H_{14}NO_3$, 232.0974); ^1H NMR ($CDCl_3$, 400 MHz) and ^{13}C NMR ($CDCl_3$, 100 MHz) spectral data are given in Table 1.

3.3.2. Chaplupyrrolidone B (*2*)

Yellow powder; $[\alpha]_D^{20}$ −3.5° (*c* 0.425, CH_2Cl_2); UV (CH_2Cl_2) λ_{max} (log ε) 266 (7.31) nm; HRESIMS *m*/*z* $[M+H]^+$ 246.1121 (calcd for $C_{14}H_{16}NO_3$, 246.1130); ^1H NMR ($CDCl_3$, 400 MHz) and ^{13}C NMR ($CDCl_3$ 100 MHz) spectral data are given in Table 1.

3.3.3. Deacetylsarmentamide B (*7*)

Yellow solid; $[\alpha]_D^{20}$ +5.1° (*c* 0.180, CH_3OH); UV (CH_3OH) λ_{max} (log ε) 277 (1.71) nm; HRESIMS *m*/*z* $[M+Na]^+$ 256.0944 (calcd for $C_{13}H_{15}NO_3Na$, 256.0950); ^1H NMR (CD_3OD, 400 MHz) and ^{13}C NMR (CD_3OD, 100 MHz) spectral data are given in Table 1.

Table 1
^{1}H (400 MHz) and ^{13}C (100 MHz) NMR data of chaplupyrrolidones A (**1**), B (**2**) recorded in $CDCl_3$ and deacetylsarmentamide B (**7**) recorded in CD_3OD.

Position	**1**		**2**		**7**	
	δ_C	δ_H, mult, *J* in Hz	δ_C	δ_H, mult, *J* in Hz	δ_C	δ_H, mult, *J* in Hz
2	167.7		168.5		53.7	α 3.71, dd, 4.1, 11.2 β 3.68, d, 11.2
3	128.5	6.12, d, 6.0	128.5	6.08, d, 5.9	75.1	4.20, brd, 4.1
4	147.4	7.07, dd, 4.4, 6.0	146.7	7.00, dd, 4.8, 5.9	77.9	4.13, brd, 4.1
5	81.9	6.07, brd, 4.4	88.9	5.93, brd, 4.8	55.3	α 3.60, d, 13.2 β 3.95, dd, 4.4, 13.2
5-OH		4.34, brs[a]				
5-OCH_3			55.4	3.32, s		
1′	173.6		173.1		167.7	
2′	38.0	3.20, m	38.5	3.20, m	119.4	6.94, d, 15.6
3′	29.9	2.93, t, 7.6	30.2	2.94, t, 7.6	143.6	7.63, d, 15.6
4′	140.5		140.7		136.4	
5′, 9′	128.5	7.24, m	128.7	7.22, m	129.1	7.64, m
6′, 8′	126.3	7.13, m	126.6	7.12, m	129.9	7.40, m
7′	128.6	7.13, m	128.8	7.12, m	131.0	7.40, m

[a] The signal underwent deuterium exchange completely soon before acquiring 2D NMR experiment.

3.3.4. Modified Mosher analysis of *1*

To a solution of **1** (5 mg) in dried pyridine (50 μL) was added (−)-MTPA chloride (10 μL). The reaction mixture was kept at room temperature for 30 min and subsequently quenched with 2 mL of 2 M $NaHCO_3$. The mixture was extracted twice with an equal volume of EtOAc, and the organic layer was washed with 1.0 M NaCl and dried over anhydrous Na_2SO_4. The residue was subject to silica gel Pasteur pipette column chromatography and eluted with a 1:9 (v/v) EtOAc: hexane mobile phase, yielding the *S*-(−)-MTPA ester of **1**. The *R*-(+)-MTPA ester was also prepared by the same method. The $\Delta\delta H_{SR}$ distribution is depicted in Fig. 2b.

3.4. Glucosidase inhibition assay

α-Glucosidase inhibitory activity was assayed using the method previously described (Worawalai et al., 2012a). Briefly, 10 μL of the test sample was mixed with α-glucosidase (0.1 U/mL, 40 μL) in 1 mM phosphate buffer (pH 6.9) and incubated at 37 °C for 10 min. Then 40 μL of 0.1 mM *p*-nitrophenyl-α-D-glycopyranoside (PNPG) was added and the mixture was then incubated for 30 min prior to being quenched with the addition of 100 μL 0.1 M Na_2CO_3. The enzymatic activity was monitored by following the concentration of released *p*-nitrophenol, evaluated *via* monitoring the absorbance at 415 nm. The percent inhibition was determined according to the equation: % inhibition = $(A_{blank} - A_{sample})/A_{blank} \times 100$; in which A_{sample} and A_{blank} are the absorbance of solution containing PNPG and α-glucosidase with and without sample, respectively. The IC_{50} value was determined from a plot of percentage inhibition on the *y*-axis against the sample concentration on the *x*-axis. Acarbose was used as the positive control.

Table 2
α-Glucosidase inhibitory effect of **1**–**7**.

Compounds	α-Glucosidase inhibition IC_{50} (μM)
1	7820 ± 6.0
2	430 ± 1.2
3	NI[a]
4	NI
5	NI
6	NI
7	NI
Acarbose	404 ± 0.4

[a] Inhibitory effect less than 30% at concentration of 10 mg/mL.

3.5. Kinetic study

The enzyme kinetic analysis was performed according to the above reaction except that the quantity of α-glucosidase was maintained at 0.3 U/mL while the concentration of each tested inhibitor was varied at 0, 0.32 and 0.65 mM. The type of inhibition was determined from Lineweaver–Burk plots, where the K_i values were determined from the secondary plots of slope *vs.* [I] and the interception *vs.* [I] of the Lineweaver–Burk plot.

Acknowledgments

This work was financially supported by the Thailand Research Fund (DBG5380037) and Chulalongkorn University (FW645A). T.D. is grateful to Office of the Higher Education Commission, Thailand, under the Strategic Scholarships Fellowships Frontier Research Networks (Specific for Southern region) for the Join Ph.D. Program Thai Doctoral Degree Program; a CHE-SSR-Ph.D. SW Scholarship. We thank Dr. Robert Douglas John Butcher, Faculty of Science Publication Counseling Unit, for editing this manuscript.

Appendix A. Supplementary data

Supplementary data associated with this article can be found, in the online version, at http://dx.doi.org/10.1016/j.phytol.2013.04.001.

References

Bokesch, H.R., Gardella, R.S., Rabe, D.C., Bottaro, D.P., Linehan, W.M., McMahon, J.B., McKee, T.C., 2011. A new hypoxia inducible factor-2 inhibitory pyrrolinone alkaloid from roots and stems of *Piper sarmentosum*. Chem. Pharm. Bull. 59, 1178–1179.

Clerc, P., Simon, S., 1989. Tables of Spectral Data for Structure Determination of Organic Compounds, 2nd ed. Springer-Verlag, Berlin.

Cooper, D.M., Grigg, R., Hargreaves, S., Kennewell, P., Redpath, J., 1995. X = y-ZH compounds as potential 1,3-dipoles. Part 44: asymmetric 1,3-dipolar cycloaddition reactions of imines and chiral cyclic dipolarophiles. Tetrahedron 51, 7791–7808.

Hussain, K., Ismail, Z., Sadikun, A., Ibrahim, P., 2010. Standardization and in vivo antioxidant activity of ethanol extracts of fruit and leaf of *Piper sarmentosum*. Planta Med. 76, 418–425.

Kiren, S., Hong, X., Leverett, C.A., Padwa, A., 2009. A facile synthesis of 5-alkoxypyrrol-2(5H)-ones using a modified aza-Achmatowicz oxidation. Tetrahedron 65, 6720–6729.

Ohtani, I., Kusumi, T., Kashman, Y., Kakisawa, H., 1991. High-field FT NMR application of Mosher's method: the absolute configurations of marine terpenoids. J. Am. Chem. Soc. 113, 4092–4096.

Pan, L., Matthew, S., Lantvit, D.D., Zhang, X., Ninh, T.N., Chai, H., Carcache De Blanco, E.J., Soejarto, D.D., Swanson, S.M., Kinghorn, A.D., 2011. Bioassay-guided isola-

tion of constituents of *Piper sarmentosum* using a mitochondrial transmembrane potential assay. J. Nat. Prod. 74, 2193–2199.
Parmar, V.S., Jain, S.C., Bisht, K.S., Jain, R., Taneja, P., Jha, A., Tyagi, O.D., Prasad, A.K., Wengel, J., Olsen, C.E., Boll, P.M., 1997. Phytochemistry of the genus *Piper*. Phytochemistry 46, 591–673.
Peungvicha, P., Thirawarapan, S.S., Temsiririrkkul, R., Watanabe, H., Prasain, J.K., Kadota, S., 1999. Hypoglycemic effect of the water extract of *Piper sarmentosum* in rats. J. Ethnopharmacol. 60, 27–32.
Phuwapraisirisan, P., Puksasook, T., Jong-aramruang, J., Kokpol, U., 2008. Phenylethyl cinnamides: a new series of α-glucosidase inhibitors from the leaves of *Aegle marmelos*. Bioorg. Med. Chem. Lett. 18, 4956–4958.
Phuwapraisirisan, P., Puksasook, T., Kokpol, U., Suwanborirux, K., 2009. Corchorusides A and B, new flavonol glycosides as α-glucosidase inhibitors from the leaves of *Corchorus olitorius*. Tetrahedron Lett. 50, 5864–5867.
Piyatida, P., Suenaga, K., Ohno, O., Kato-Noguchi, H., 2012. Isolation of allelopathic substance from *Piper sarmentosum* Roxb. Allelopathy J. 30, 93–102.
Tuntiwachwuttikul, P., Phansa, P., Pootaeng-on, Y., Taylor, W.C., 2006. Chemical constituents of the roots of *Piper sarmentosum*. Chem. Pharm. Bull. 54, 149–151.
Worawalai, W., Wacharasindhu, S., Phuwapraisirisan, P., 2012a. Synthesis of new *N*-substituted aminoquercitols from naturally available (+)-*proto*-quercitol and their α-glucosidase inhibitory activity. Med. Chem. Commun. 3, 1466–1470.
Worawalai, W., Rattanangkool, E., Vanitcha, A., Phuwapraisirisan, P., Wacharasindhu, S., 2012b. Concise synthesis of (+)-conduritol F and inositol analogues from naturally available (+)-*proto*-quercitol and their glucosidase inhibitory activity. Bioorg. Med. Chem. Lett. 22, 1538–1540.
Zar, C.T., Teoh, S.L., Das, S., Zaiton, Z., Farihah, H.S., 2012. Use *Piper sarmentosum* as an effective antidiabetic supplement in South East Asia: a review. Clin. Ter. 163, 505–510.